

NOT TO BE CITED WITHOUT PRIOR  
REFERENCE TO THE AUTHOR(S)

Northwest Atlantic



Fisheries Organization

Serial No. N7513

NAFO SCR Doc. 24/010

**SCIENTIFIC COUNCIL MEETING – JUNE 2024**

**Environmental and Physical Oceanographic Conditions on the Eastern Canadian shelves  
(NAFO Sub-areas 2, 3 and 4) during 2023.**

by

F. Cyr<sup>1</sup>, J. Coyne<sup>1</sup>, P. S. Galbraith<sup>2</sup>, C. Layton<sup>3</sup> D. Hebert<sup>3</sup>

<sup>1</sup>Northwest Atlantic Fisheries Centre, Fisheries and Oceans Canada, St. John's (NL)

<sup>2</sup>Maurice-Lamontagne Institute, Fisheries and Oceans Canada, Mont-Joli (QC)

<sup>3</sup>Bedford Institute of Oceanography, Fisheries and Oceans Canada, Dartmouth (NS)

**Abstract**

Oceanographic and meteorological observations in NAFO Sub-areas 2, 3 and 4 during 2023 are presented and referenced to their long-term averages. The winter North Atlantic Oscillation (NAO) index, a key indicator of the direction and intensity of the winter wind field patterns over the Northwest (NW) Atlantic was near neutral (+0.2) in 2023. Since 2014, all years except 2021 were positive (normally indicative of colder conditions). The vast majority of parameters and indices presented in this report ranged from normal to warmer than normal in 2023 (normal being defined as the average over the 1991–2020 climatological period). The air temperatures across the NW Atlantic were above normal in 2023 at all sites reported except St. John's. The sea-ice season volume and area across the Newfoundland and Labrador shelf were about normal (-0.5 SD) for a second year in a row. Sea surface temperatures averaged over the ice-free months were at their second warmest level since the 1980s. The last three years were the warmest years recorded, including the record warm in 2022. The transport on the Scotian Slope was above normal for the first time in a decade (+1.4 SD), potentially contributing to a return the normal conditions observed in many areas of the Scotian Shelf after a record warm year in 2022.



## Introduction

This report presents an overview of the 2021 environmental and physical oceanographic conditions in NAFO sub-areas 2, 3 and 4 on eastern Canadian shelves (see Figure 1). It complements similar reviews of environmental conditions on the Northeast US Shelf, the Labrador Sea and West Greenland Waters as part of the Scientific Council's annual review of environmental conditions in the NAFO Convention Area. The information presented for 2023 is derived from various sources:

1. Ice data are from the Canadian Ice Service and meteorological data are from Environment Canada and other sources cited in the text;
2. Air temperature data from Canadian sites are from the second generation of Adjusted and Homogenized Canadian Climate Data (AHCCD), which accounts for shifts in station location and changes in observation methods (Vincent et al., 2012);
3. Sea Surface Temperatures (SSTs) (Galbraith et al., 2021). These correspond to a blend of Advanced Very High Resolution Radiometer (AVHRR) data from Pathfinder version 5.3 (1982–2014), the Maurice Lamontagne Institute (1985–2013) and the GHRSST NOAA/STAR L3S-LEO-Daily (2007–present). See (Galbraith et al., 2021 , 2023) for a description;
4. Observations made throughout the year at historical monitoring stations 27 (near St. John's, NL), Prince-5 (Bay of Fundy) and Halifax-2 (Scotian Shelf);
5. Measurements made during the summer along standard NAFO and Atlantic Zone Monitoring Program (AZMP) (Therriault et al., 1998) cross-shelf sections (see Figure 1);
6. Oceanographic observations made during multi-species and ground fish resource assessment surveys (NAFO sub-areas 2 to 4);
7. Other multi-source historical data (ships of opportunity, international campaign, other DFO regions surveys, Argo program, etc.).

All vertical profiles of temperature and salinity used in this report (e.g. points 4-7 above) are available at <https://doi.org/10.20383/102.0739> [consulted 2024-05-30] (Coyne et al., 2023).

Time series of temperature and salinity anomalies as well as other derived climate indices were constructed by removing the annual cycle computed over a standard climatological. According to the World Meteorological Organization, (2017). The “Normal” is defined here as the average over this period. Annual or seasonal anomalies were sometimes normalized by dividing the values by the standard deviation (SD) of the data time series over the climatological period. A value of 2, for example, indicates that the index was 2 SD higher than its long-term average. As a general guide, anomalies within  $\pm 0.5$  SD are considered to be normal.

The normalized values of water properties and derived climate indices presented in this document are color-coded in “scorecards” with gradations of 0.5 SD (Figure 2). Shades of blue represent cold-fresh environmental conditions and reds warm-salty conditions. In some instances (NAO, ice and cold water areas or volumes, for example) negative anomalies may indicate warm conditions and hence are colored red. Most of the colormaps used in this report are taken from the *cmocean* colormaps package for oceanography (Thyng et al., 2016).

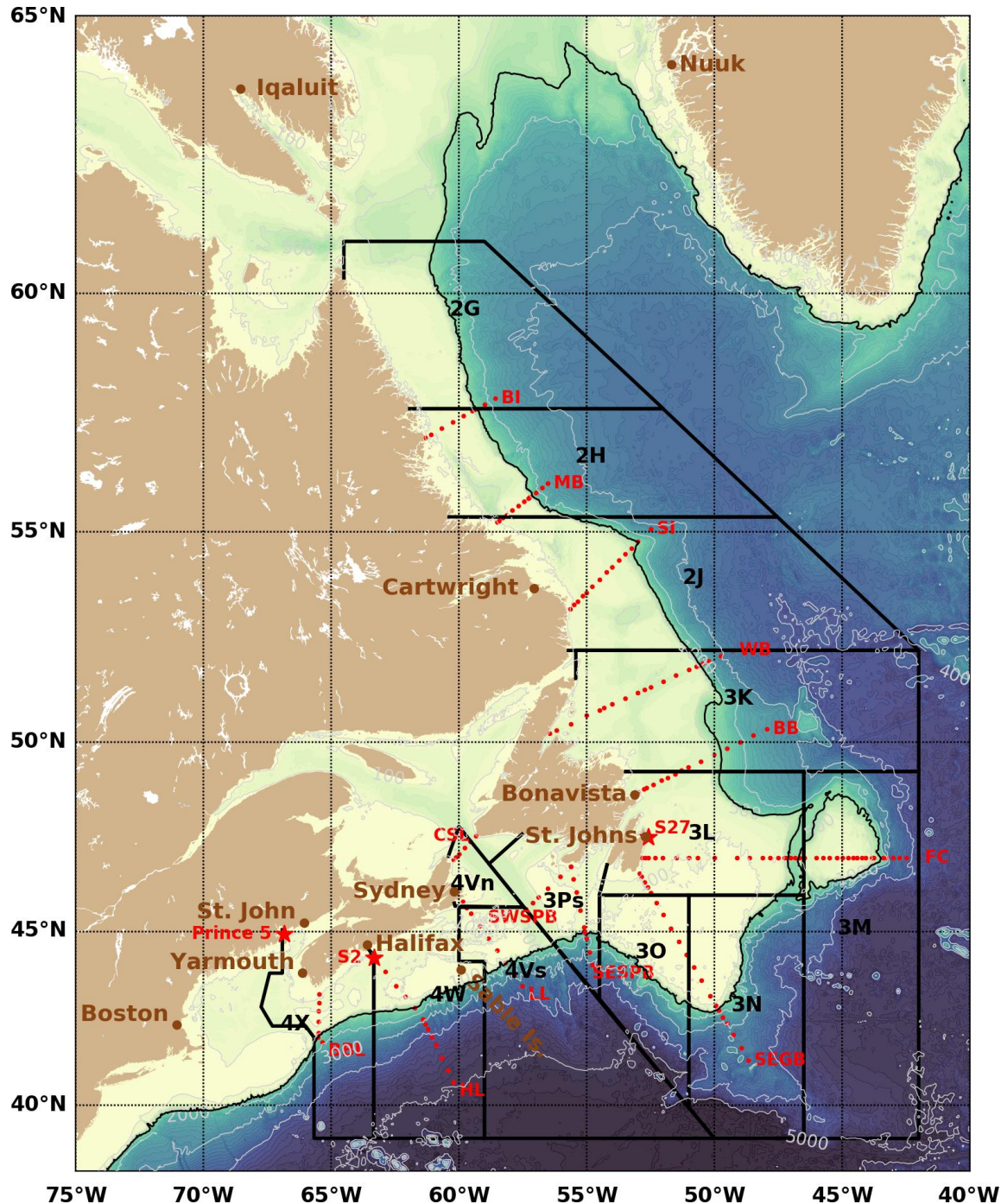


**Figure 1.** Map showing NAFO Divisions and main bathymetric features of the Northwest Atlantic. The hydrographic sections reported here are shown with red dots and the fixed stations by red stars. The stations used for air temperature time series and in brown. The black contour is the isobath 1000m that is used here to delimit the continental shelf.

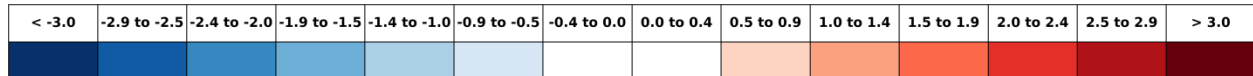


**Figure 2.** Color scale used for the presentation of normalized anomalies. Color levels are incremented by 0.5 standard deviations (SD), where blue is below normal and red above normal. Values between 0 and  $\pm 0.5$  SD remain white indicating normal conditions.

### Meteorological Conditions

The winter North Atlantic Oscillation (NAO) is defined as anomaly in the sea-level pressure (SLP) difference between the sub-tropical high (average location near the Azores) and the sub-polar low (average location near Iceland). Several definitions of the NAO exists and the definition used here is the one from the National Center for Environmental Information of the National Oceanic and Atmospheric Administration (NOAA) and available [online](#). The winter NAO (defined here as the average of monthly values from December to March) is considered a measure of the strength of the winter westerly and north westerly winds over the Northwest Atlantic. A high NAO index (positive phase) occurs during an intensification of the Icelandic Low and Azores High. Except for some years for which the SLP patterns are spatially shifted (e.g. 1999, 2000 and 2018 where the location of high and low SLP were reversed in March), positive winter NAO years favor strong northwesterly winds, cold air and sea surface temperatures, and heavy ice conditions on the NL shelves (Colbourne et al., 1994; Drinkwater, 1996; Petrie et al., 2007). The winter NAO was neutral in 2023 (+0.2; first row in Figure 3) for the second time in 3 years (2021 was also neutral). While the lowest winter NAO index value was reached in 2010, all years between 2012 and 2020 (except 2013) were positive, including the record high of +1.6 in 2015.

The Arctic Oscillation (AO) is a larger scale index intimately linked with the NAO. During a positive phase, the arctic air outflow to the Northwest Atlantic increases, resulting in colder winter air temperatures over much of the NL and adjacent shelf regions. Similar to the NAO, the AO was neutral in 2023 at 0.0 (Figure 3), indicative of warmer than usual air temperatures above the region. In 2015, the AO was at its highest value since 1990 at +1.6. A record low was reached in 2010 when it was below normal at -1.5 (warm air temperatures).

The Atlantic Multidecadal Oscillation (AMO) is also provided in Figure 3. This index, based on the Sea Surface Temperature of the Atlantic Ocean, evolves as part of a 65-80 year cycle that influences the regional climate and has consequences on the ocean circulation in the North Atlantic (e.g., Kerr, 2000). The AMO has been in a positive phase since the late 1990s.

Air temperature anomalies (winter and annual values) from five coastal communities around the Northwest Atlantic (Nuuk Greenland, Iqaluit Baffin Island, Cartwright Labrador, Bonavista and St. John's Newfoundland) are shown in Figure 3 as normalized anomalies (referenced to the 1991-2020 period) between 1980 and 2021, and in Figure 4 and Figure 5 as cumulative annual and monthly anomalies, respectively. Except for Nuuk for which data are obtained from the Danish Meteorological Institute, the air temperature data from Canadian sites are from the second

generation of Adjusted and Homogenized Canadian Climate Data (AHCCD), which accounts for shifts in station location and changes in observation methods (Vincent et al., 2012). Because the AHCCD product was not ready for the year 2023, historical data from the Government of Canada [Monthly Climate Summaries](#) have been used for that year.

Overall, the air temperature was above normal for all sites in 2023, except for St. John's (normal) (Figure 3 and Table 1). Temperatures were especially warm for the southern sites, with normalized anomalies  $>1$  SD on the Scotian shelf and Gulf of Maine (Table 1). compared to  $<1$  SD the eastern Arctic and NL shelf (Figure 3).

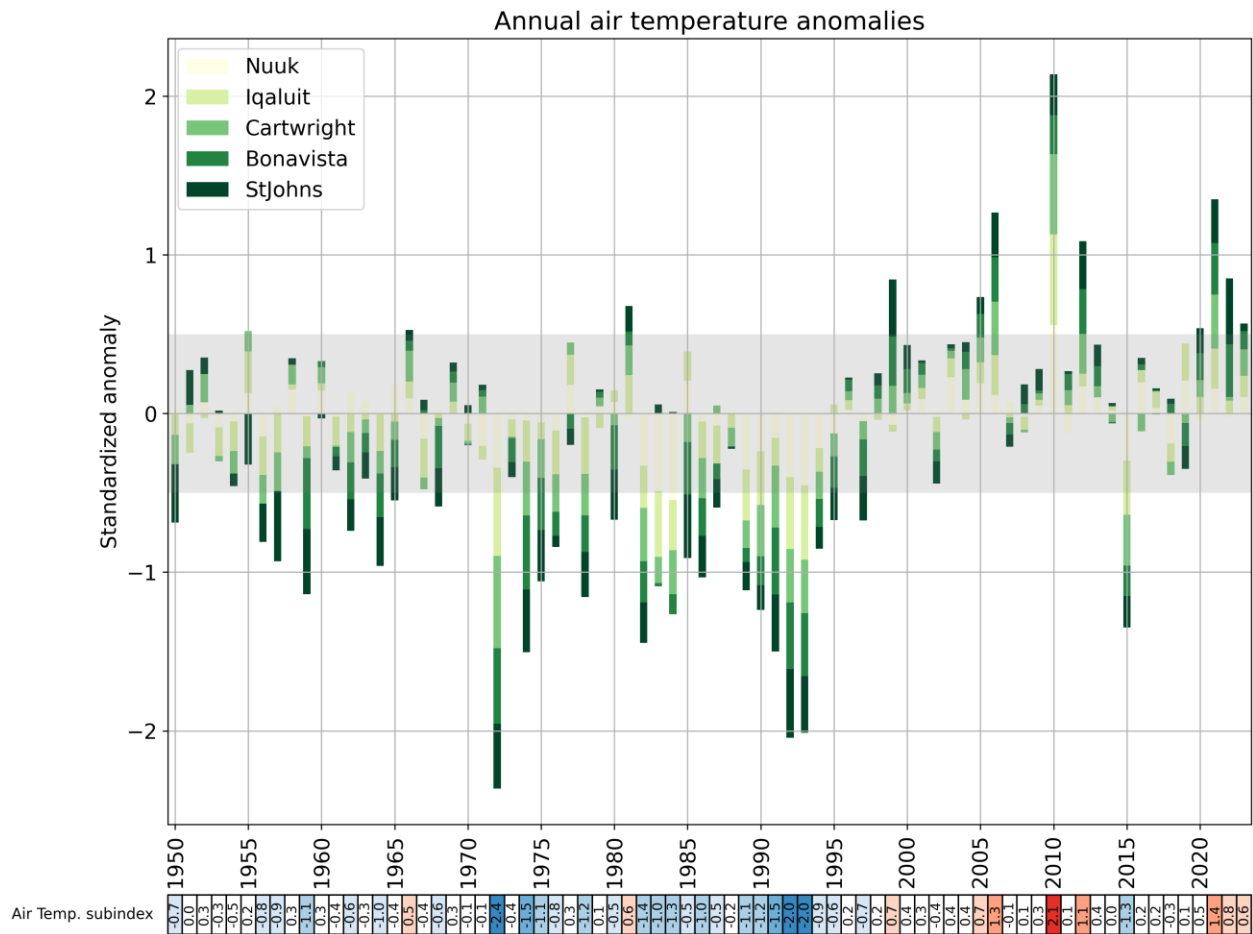
In the Arctic and on the NL shelf the air temperature exhibited large intra-annual fluctuations generally coherent between all sites (Figure 5). Temperatures were especially cold in February and warm in March, July and during the late fall. Averaged over the year, the air temperatures were above normal, making 2023 the 9th warmest year since 1950 at +0.6 SD (Figure 4). 2010 was the warmest year at +2.1 SD, and all of the warmest 5 years have happened since 2005.

Annual air temperature anomalies for six sites in the Scotian Shelf-Gulf of Maine region (location in Figure 1) are shown in in Figure 6 and in Table 1. In 2023, the mean annual air temperature anomalies were well above normal at all sites with anomalies ranging from +1.0 to +1.9 SD. The time series of annual anomalies indicates that all sites have increasing temperatures over the long term with decadal scale variability superimposed. Over shorter periods, there are times when there is no trend or a decreasing trend in the temperature. Linear trends from 1900 to present for Sydney, Sable Island, Halifax, Yarmouth, Saint John and Boston correspond to changes (and 95% confidence limits) per century of +1.3°C (+0.9°C, +1.6°C), +1.4°C (+1.1°C, +1.7°C), +2.0°C (+1.7°C, +2.4°C), +1.3°C (+1.0°C, +1.6°C), +1.3°C (+1.0°C, +1.7°C) and +2.8°C (+2.5°C, +3.2°C), respectively.

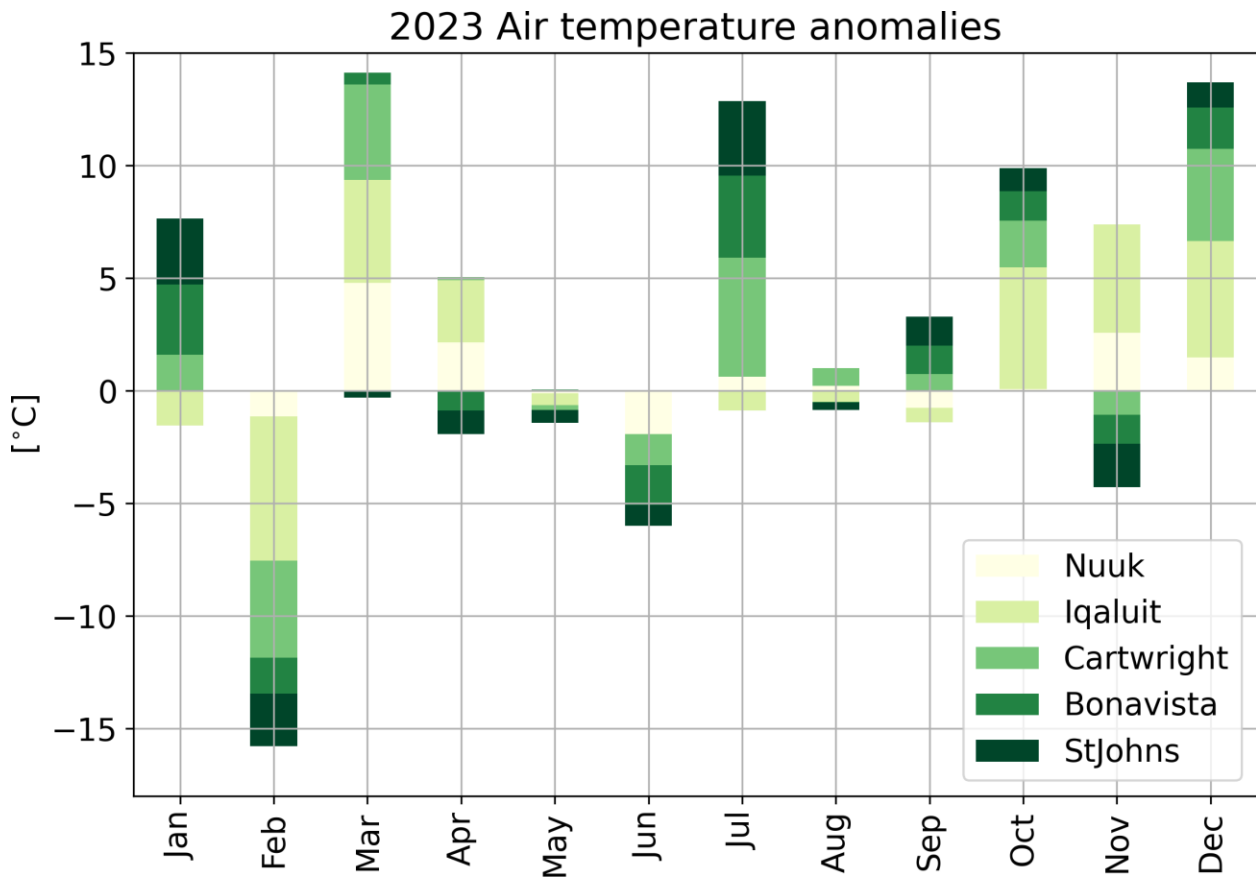
The anomalies for all 6 sites are displayed in

Figure 7 as a composite sum. For most years the anomalies have the same sign. Since 1900, for the 114 years when all sites were operating, 100 had five or more stations with the annual anomalies having the same signs; for 93 years, all six stations had anomalies with the same sign. This indicates that the spatial scale of the air temperature patterns is greater than the largest spacing among sites.

**Figure 3.** Scorecard of large-scale indices (winter NAO, AO and AMO) and normalized air temperature anomalies (winter and annual) for five cities between 1980 and 2023. Means and standard deviations for the air temperatures during the 1991-2020 period are provided in the last column (in °C). No means or standard deviations are provided for the large-scale indices (grayed boxes).



**Figure 4.** Normalized annual air temperature anomalies for Nuuk, Iqaluit, Cartwright, Bonavista and St. John's. This figure shows the average of the five stations, in which the length of each bar corresponds to the relative contribution of the individual station to the average. The shaded area corresponds to the 1991–2020 average  $\pm 0.5$  SD, a range considered normal. The numerical values of this time series are reported in a color-coded scorecard at the bottom of the figure.



**Figure 5.** Cumulative monthly air temperature anomalies at Nuuk, Iqaluit, Cartwright, Bonavista and St. John's for 2023.

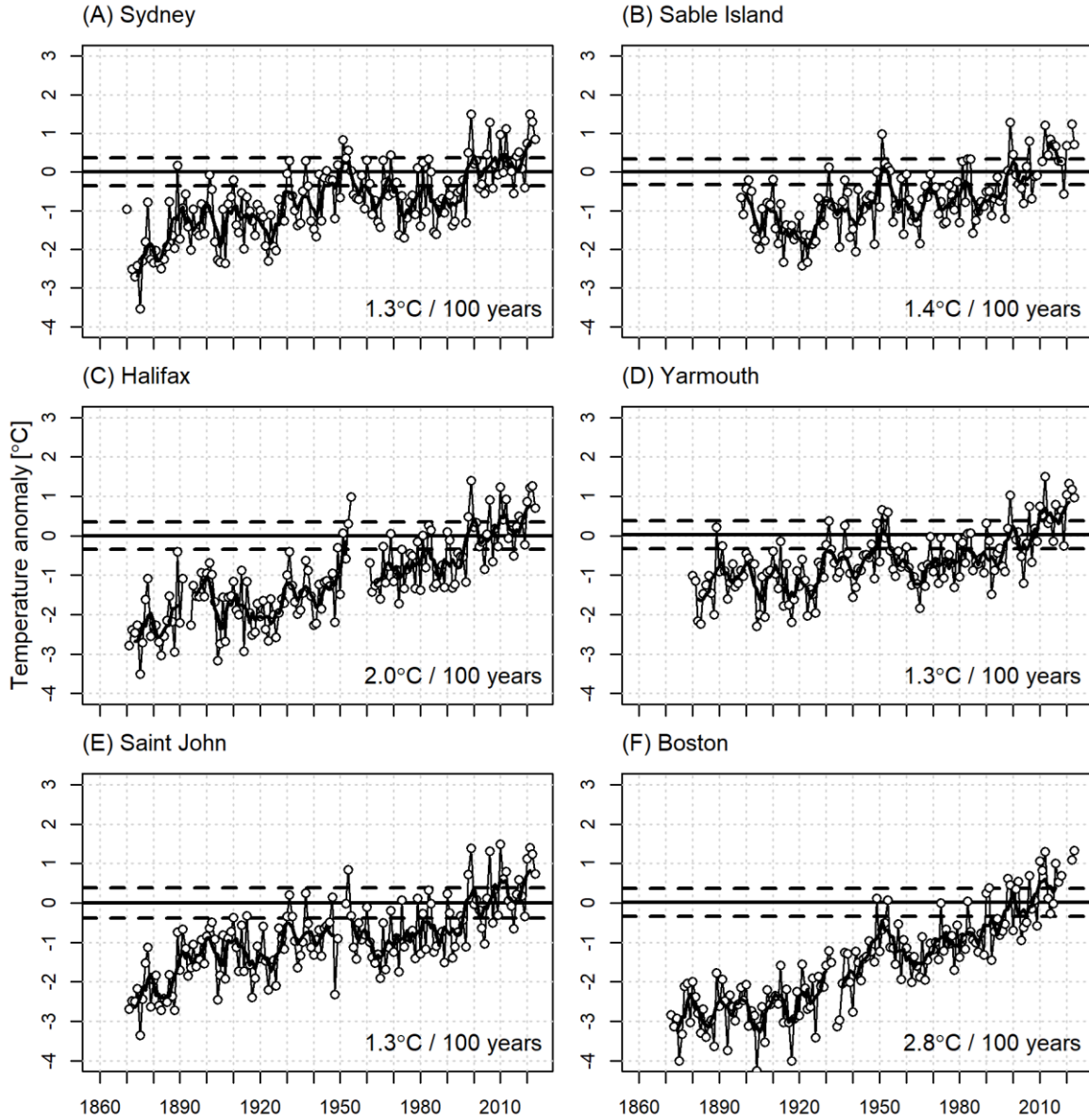


**Figure 6.** Annual air temperature anomalies in °C (dashed line) and five year running means (solid line) at selected sites (Sydney, Sable Island, Shearwater, Yarmouth, Saint John and Boston) in Scotian Shelf-Gulf of Maine region (years 1860 to 2023). Horizontal dashed lines represent the 1991-2020 climatological average  $\pm 0.5$  SD.

**Table 1.** The 2023 annual mean air temperature anomaly in degrees and standardize anomaly (relative to the 1991-2020 climatology) for Scotian Shelf and Gulf of Maine.

Site	Annual Anomaly		1991-2020 Climatology	
	Observed (°C)	Normalized	Mean (°C)	SD (°C)
Sydney	+0.8	+1.2	6.45	0.72
Sable Island	+0.7	+1.1	8.35	0.67
Shearwater (Halifax)	+0.7	+1.0	7.16	0.70
Yarmouth	+1.0	+1.4	7.69	0.71
Saint John	+0.7	+1.0	5.71	0.77
Boston	+1.3	+1.9	10.98	0.71

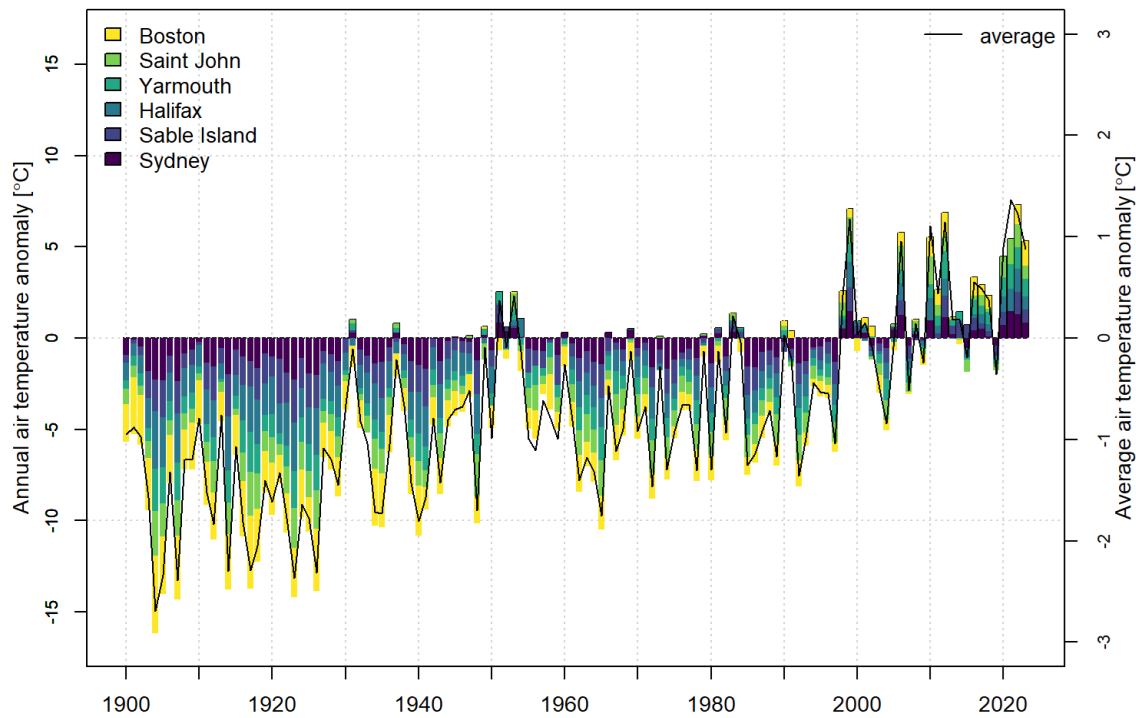


**Figure 7.** The contributions of each of the annual temperature anomalies for 6 Scotian Shelf-Gulf of Maine sites (Boston, Saint John, Yarmouth, Shearwater, Sable Island and Sydney) are shown as a stacked bar. Anomalies are referenced to the 1991-2020 period.

## Sea-Ice Conditions

Ice cover area, volume and seasonal duration are estimated from ice cover products obtained from the Canadian Ice Service (CIS). These products consist of Geographic Information System (GIS) charts covering the East Coast and Hudson Bay system, the latter providing coverage of the Northern Labrador Shelf. The East Coast region has weekly charts available for 1969–2023 and daily charts for 2009–2023 while only weekly charts are available for the Hudson Bay system for 1980–2023. All vector charts were further converted into regular  $0.01^{\circ}$  latitude by  $0.015^{\circ}$  longitude grids (approximately 1 km resolution), with ice concentrations and growth stages attributed to each grid point. Average thicknesses (and therefore regional volumes) are estimated from standard thicknesses attributed to each stage of ice growth from new ice and nilas (5 cm), grey ice (12.5 cm), grey-white ice (22.5 cm), thin first year ice (50 cm), medium first year ice (95 cm) and thick first year ice (160 cm). Prior to 1983, the CIS reported ice categories with fewer classifications, where a single category of first year ice ( $\geq 30$  cm) was used with a suggested average thickness of 65 cm. We have found this value to lead to underestimates of the seasonal maximum thickness and volume based on high interannual correlations between the estimated volume of the weekly seasonal maximums and its area or sea-ice season duration. The comparisons of the slope of these correlations pre- and post-1983 provided estimates of first-year ice thickness of 85 cm in the Gulf of St. Lawrence and 95 cm on the Newfoundland and Labrador Shelf for this single first year ice category, which were used instead of the suggested 65 cm.

Several products were computed to describe the sea-ice cover inter-annual variability. The day of first and last occurrence, ice season duration (Figure 8) and distribution of ice thickness during the week of maximum volume (Figure 9) are presented as maps. These two figures combine information from the East Coast sea ice charts and Hudson Bay system charts, leading to a slight jump in the climatology maps of first occurrence and duration. This occurs because there are often missing weeks in the Hudson Bay charts around the period of first occurrence on the northern Labrador Shelf. Therefore, anomalies of these two parameters have more uncertainty than the rest. Regional scorecards of anomalies in the first and last day of ice, duration of the sea ice season and maximum ice volume are presented in Figure 10 for the Labrador and Newfoundland shelves. Here, the areas defined as Northern and Southern Labrador shelves and Newfoundland Shelf are shown in Figure 9, with the Newfoundland Shelf and Gulf of St. Lawrence delimited at the Eastern end of the Strait of Belle Isle. Evolution of the ice volume during the 2023 ice season is presented in Figure 11 for the three regions in relation to the climatology and historical extremes. The Northern Labrador Shelf progression is shown using weekly data extracted from Hudson Bay charts and the others are shown using daily data extracted from East Coast charts. Time series of seasonal maximum ice volume, area (excluding thin new ice) and ice season duration are presented for the Northern (top left) and Southern (top right) Labrador Shelf and for the Newfoundland Shelf (bottom) in Figure 12. The December-to-April air temperature anomaly at Cartwright showed the best correlation with sea ice properties to the South on the Newfoundland Shelf ( $R^2 = 0.62\text{--}0.78$ ) and is included with reversed scale in the Newfoundland Shelf panel; this is indicative of the advective nature of sea ice on the Newfoundland Shelf with strong ice cover associated with cold air temperatures in the

source area. The durations shown in Figure 10 and Figure 12 are different products. The first corresponds to the number of weeks where the volume of ice anywhere within the region exceeded 5% of the climatological maximum, while the second is the average duration at every pixel of Figure 8, which is much shorter than the first.

Ice typically starts forming in December along the Labrador coast and only by late February at the southern extent of sea-ice presence (Figure 8). Last occurrence is typically in late June to early July on the Labrador coast, leading to sea-ice season durations of 23 weeks or more. There has been a declining trend in ice cover severity since the early 1990s reaching the lowest values in 2011 and 2010, with a rebound in 2014 third lowest value in 2021 (Figure 10 and Figure 12). On the Newfoundland Shelf, the sea ice metrics of annual maximum ice area, volume, and ice cover duration are well correlated with each other ( $R^2 = 0.70$  to  $0.74$ ; Figure 12). Sensitivity of the Newfoundland Shelf ice cover to air temperature increase (e.g. through anthropogenic climate change) can thus be estimated using 1969-2023 co-variations between winter air temperature and sea-ice parameters, which indicate losses of  $14 \text{ km}^3$ ,  $26\,000 \text{ km}^2$  and 8 days of sea-ice season for each  $1^\circ\text{C}$  increase in winter air temperature.

In 2023, the sea-ice cover first appeared at generally later than normal dates (Figure 8), leading to regional thresholds marking the beginning and end of the season that were crossed later than normal (Figure 10). The last occurrence on the northern Labrador Shelf was a mix of earlier than normal inshore and later than normal offshore, with the opposite on the Newfoundland and Southern Labrador Shelves (Figure 8). Sea ice volumes progressed below normal on the Labrador Shelf until April, closer to normal in May and well above normal in June before ending very abruptly (Figure 11). The volume progression on the Newfoundland Shelf was well below normal with three pulse events of advection from the Labrador Shelf (Figure 11). The maximum ice volumes reached during the season were near normal on the Labrador Shelf, at  $106 \text{ km}^3$  (-0.1 SD) and  $83 \text{ km}^3$  (-0.45 SD) on the northern and southern parts respectively, but below normal on the Newfoundland Shelf at  $44 \text{ km}^3$  (-0.7 SD). The December-to-June seasonal averages followed the same pattern of near normal at  $51 \text{ km}^3$  (-0.2 SD) and  $33 \text{ km}^3$  (-0.48 SD) on the Northern and Southern Labrador Shelves and below normal at  $9 \text{ km}^3$  (-0.8 SD) on the Newfoundland Shelf (Figure 10). From North to South, the pixel average durations were below normal at 113 (-0.7 SD), 83 (-0.6 SD) and 29 days (-0.8 SD), respectively (Figure 8 and Figure 12). The maximum area reached within each region (excluding ice less than 15 cm thick) was near normal at  $97\,000 \text{ km}^2$  (-0.2 SD),  $113\,000 \text{ km}^2$  (-0.35 SD) and  $120\,000 \text{ km}^2$ , -0.05 SD). An overview of sea ice conditions (volume and season duration) for NL since 1969 is presented in Figure 13 as the average of normalized anomalies. In 2023, this index was near normal at -0.5 SD.

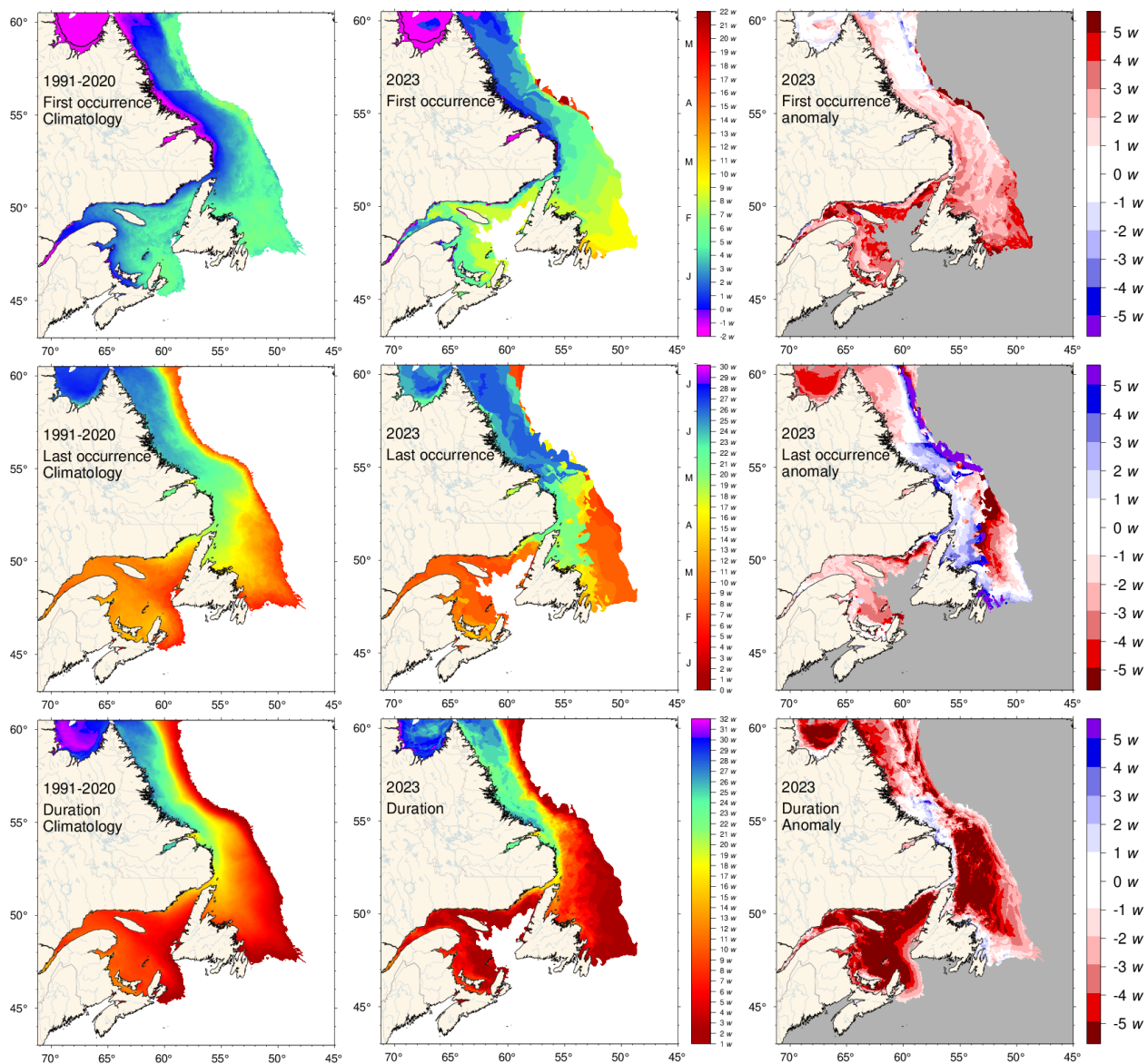


**Figure 8.** First (top) and last (middle) occurrence of ice and ice season duration (bottom) based on weekly data. The 1991-2020 climatologies are shown (left) as well as the 2023 values (middle) and anomalies (right). First and last occurrences are defined here as the first and last weekly chart in which any amount of ice is recorded for each pixel and are illustrated as day-of-year. Ice duration sums the number of weeks with ice cover for each pixel. Climatologies are shown for pixels that had at least 15 years out of 30 with occurrence of sea-ice, and therefore also show the area with 50% likelihood of having some sea-ice at any time during any given year. The duration anomaly map includes pixels with no ice cover where some was expected based on the climatology.

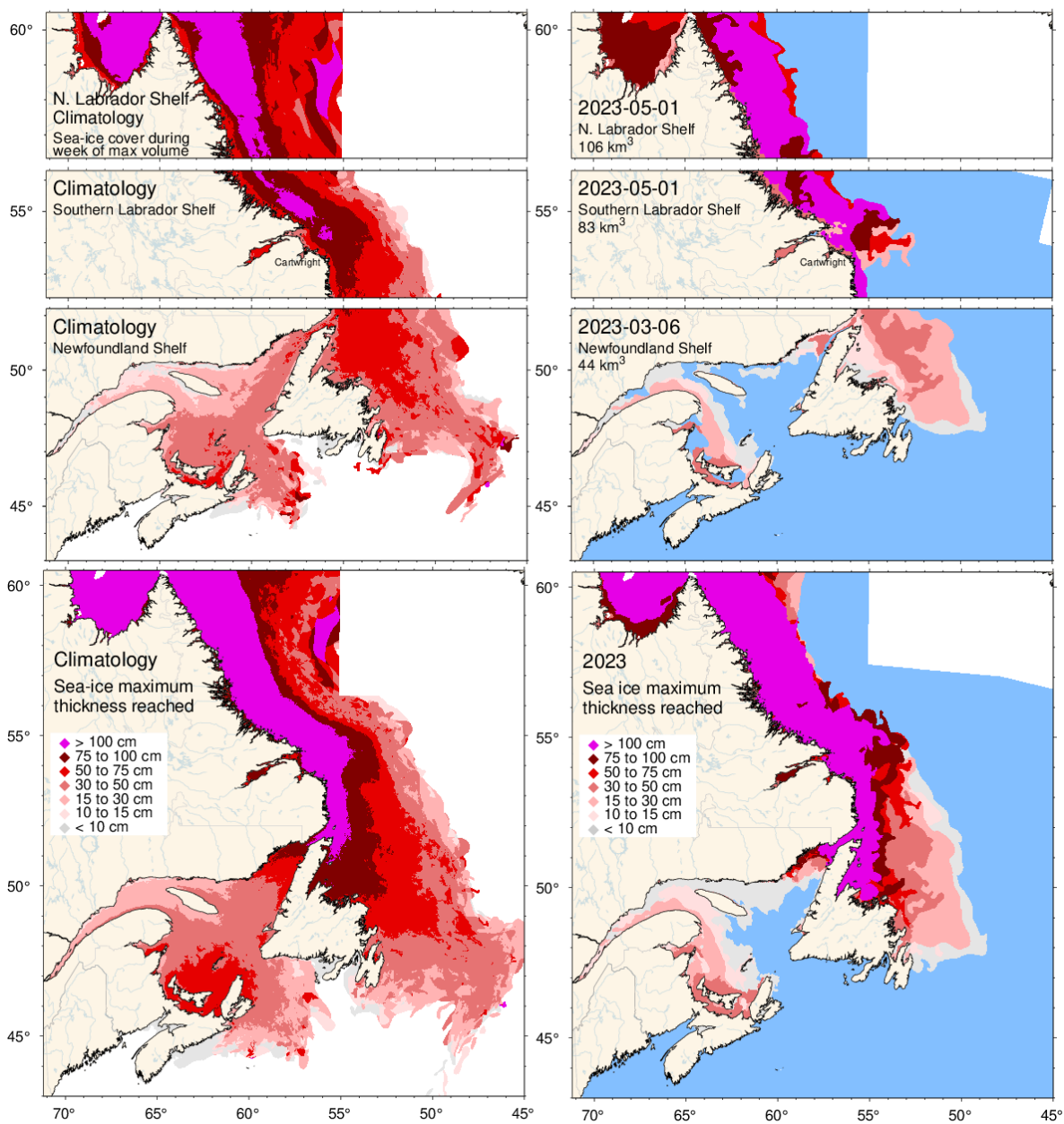


**Figure 9.** Ice thickness map for 2023 for the week with the maximum annual volume on the Newfoundland and Labrador Shelf (three upper right panel) and similarly for the 1991-2020 climatology of the weekly maximum (three upper left panel). Note that these maps reflect the ice thickness distribution on that week. The maximum ice thickness observed at any given location during the year is presented in the lower panels, showing the 1991-2020 climatology and 2023 distribution of the thickest ice recorded during the season at any location.

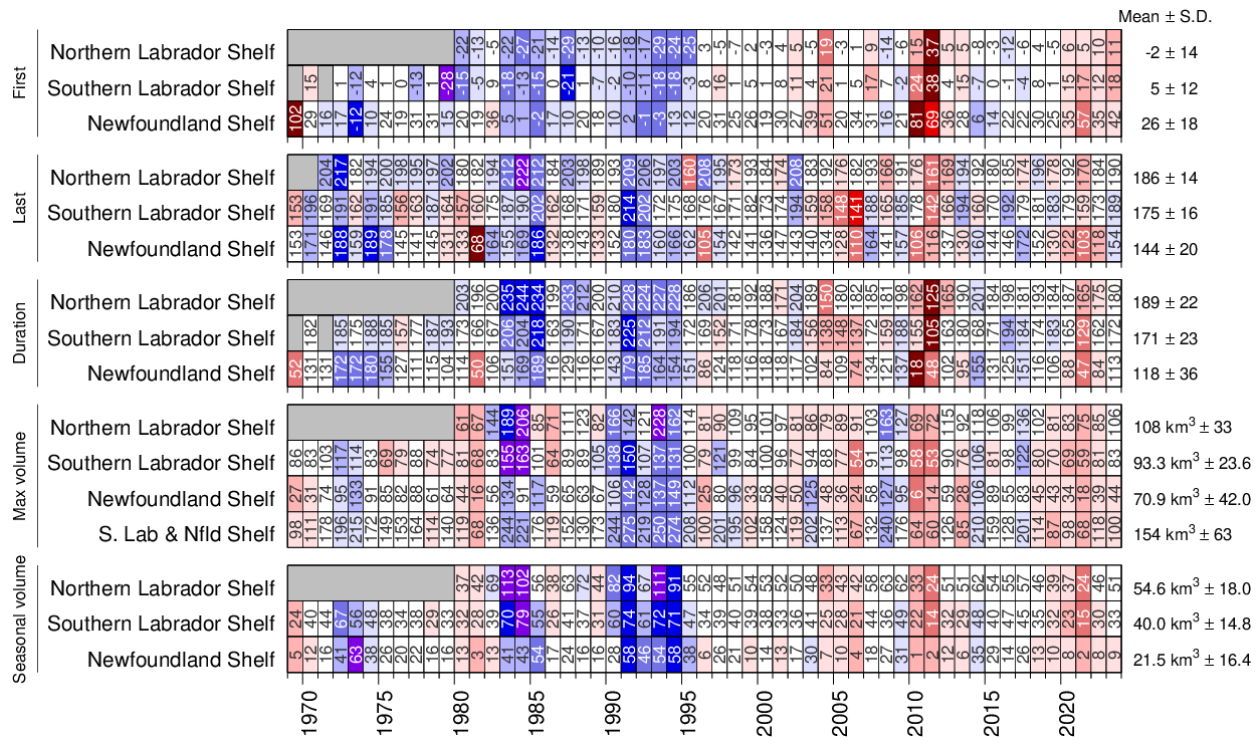


**Figure 10.** First and last day of ice occurrence, ice duration, maximum seasonal ice volume and average seasonal (DJFMAMJ) ice volume by region. The moment when ice was first and last observed in days from the beginning of each year is indicated for each region, and the color code expresses the anomaly based on the 1991–2020 climatology, with blue (cold) representing earlier first occurrence and later last occurrence. The threshold is 5% of the climatological average of the seasonal maximum ice volume. Numbers in the table are the actual day of the year or volume, but the color coding is according to normalized anomalies based on the climatology of each region. Duration is the numbers of days that the threshold was exceeded. Seasonal average volumes (last block of lines) are reported in the ICES Report on Ocean Climate (Cyr & Galbraith, 2022).

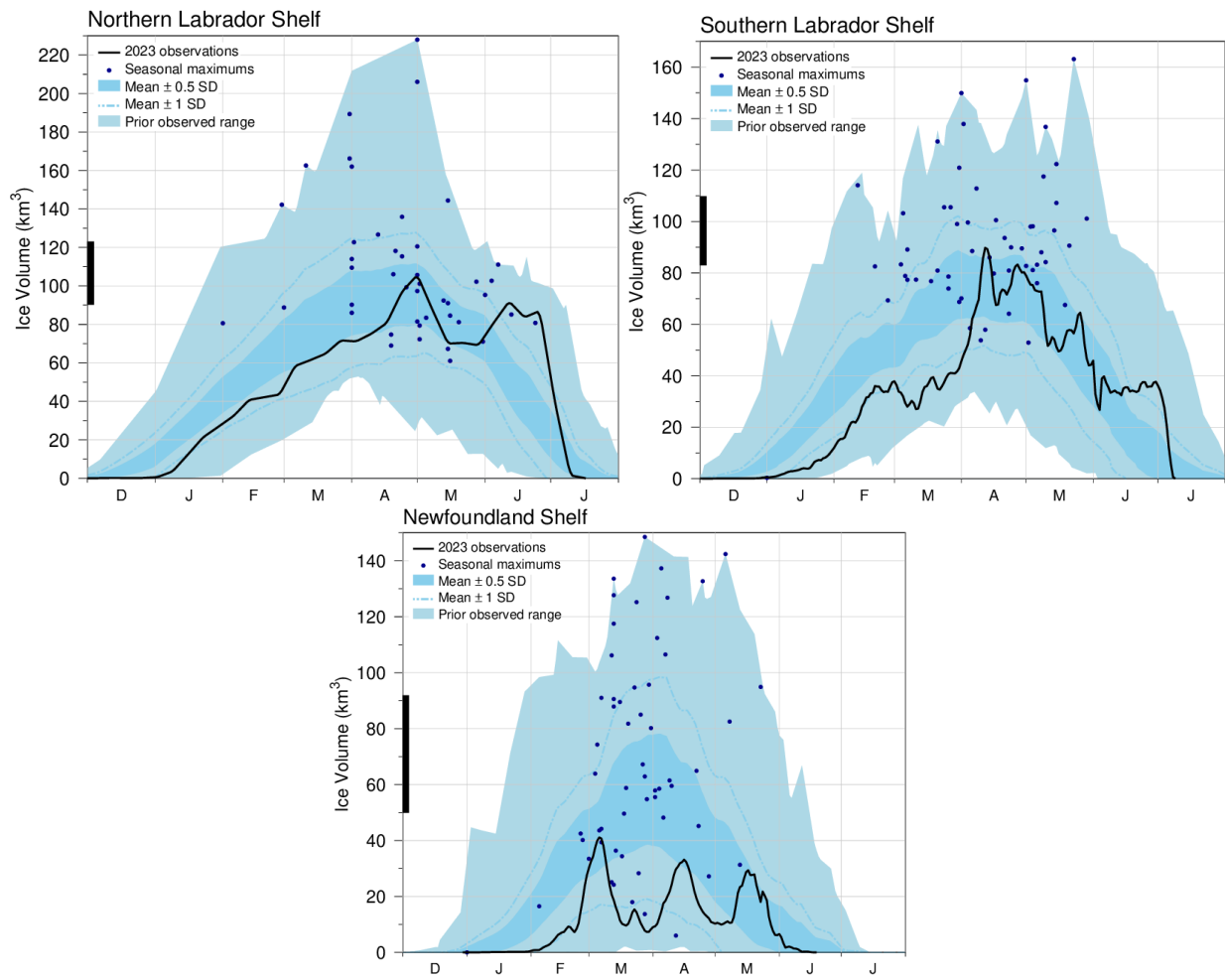


**Figure 11.** Time series of the 2022-2023 mean ice volume (black lines) for the Northern Labrador Shelf (top left), Southern Labrador Shelf (top right), and Newfoundland Shelf (bottom), the 1991-2020 climatological mean volume  $\pm 0.5$  and  $\pm 1$  SD (dark blue area and dashed line respectively), the minimum and maximum span of 1969-2022 observations (light blue), and the date and volumes of 1969-2023 seasonal maximums (blue dots). The black thick line on the left indicates the mean volume  $\pm 0.5$  SD of the annual maximum ice volume, which is higher than the peak of the mean daily ice volume distribution.

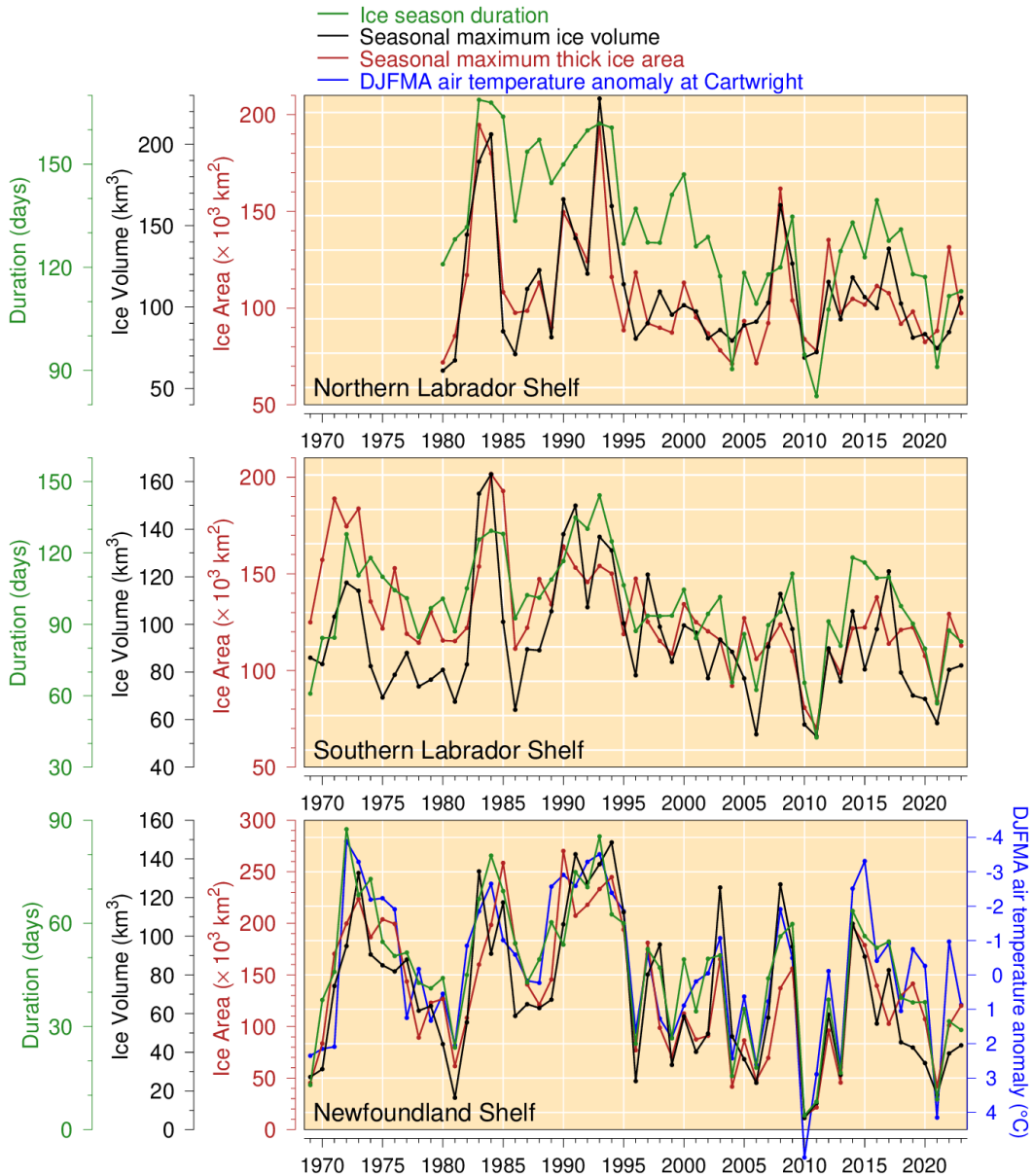


**Figure 12.** Seasonal maximum ice volume and area (excluding ice less than 15 cm thick), and ice season duration for the Northern and Southern Labrador Shelf (top and middle) and Newfoundland Shelf (bottom), and December-to-April air temperature anomaly at Cartwright.

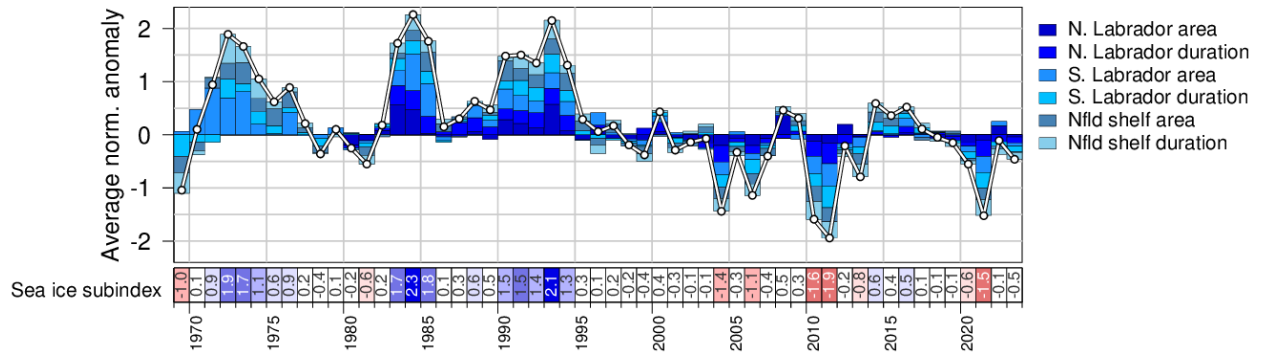


**Figure 13.** Newfoundland and Labrador sea ice index established by averaging the normalized anomalies of volume and duration of sea ice for Newfoundland and Labrador shelves (black and green time series in Figure 12).

### Satellite Sea-Surface Temperature Conditions

Sea Surface Temperatures (SSTs) used here is a blend of data from Pathfinder version 5.3 (1982-2014), Maurice Lamontagne Institute (1985-2013) and GHRSST NOAA/STAR L3S-LEO-Daily “super-collated” product (0.02° resolution for 2007 to present; NOAA/STAR, 2021). This last product has changed since our last published report and has significantly higher temperatures for 2021 than were reported then; it would have been reported as the record high. Monthly temperature composites are based on averaged daily anomalies to which monthly climatological average temperatures are added (see Galbraith et al. 2021, 2023 for details).

Averaged over ice-free periods of the year as short as June to November on the Labrador Shelf, May to November in the Gulf, to the entire year on the Scotian Shelf, air temperature has been found to be a good proxy of sea surface temperature. The warming trend observed in air temperature since the 1870s of about 1°C per century is also expected to have occurred in surface water temperatures across Atlantic Canada (Galbraith et al. 2021). The Zone experienced its warmest surface temperatures in 2022 when all regions had positive anomalies over ice-free months, with records reached in seven regions.

In 2023, monthly average sea surface temperatures were generally normal to above normal in ice-free areas. (Figure 14 to Figure 16). A cool month of June was followed by a marine heat wave that left all regions with July as their warmest on record. The July average anomaly at 4 of the regions (2J, 3K, 3L and 3M) were at or more than +3.0 SD, with the area over Flemish Cap (3M) reaching +5.1°C (+3.7 SD). Temperatures were also at record highs in winter on the Scotian Shelf, in August on the Labrador and northern Newfoundland Shelf, in September in 3P, and in October in 3P/4V regions

Sea surface temperature seasonal averages were above normal across the zone, reaching record highs in regions of the Labrador Shelf (2H, 2J), the northern Newfoundland Shelf (3K) and Flemish Cap (3M). The spatially weighted zonal average was second highest of the time series (Figure 17, scorecard at the bottom).

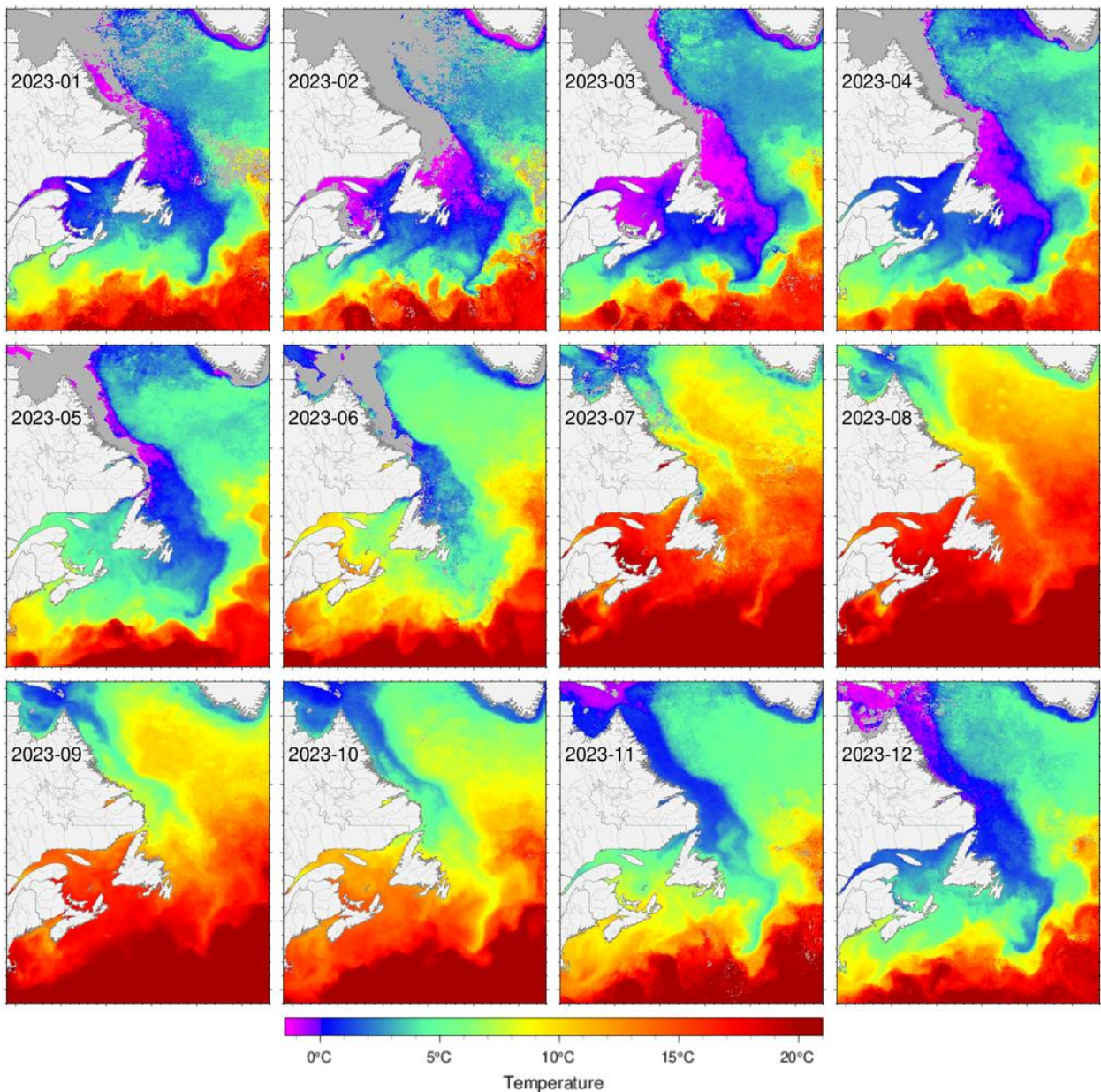


**Figure 14.** Sea-surface temperature monthly averages for 2023 in the Atlantic zone.

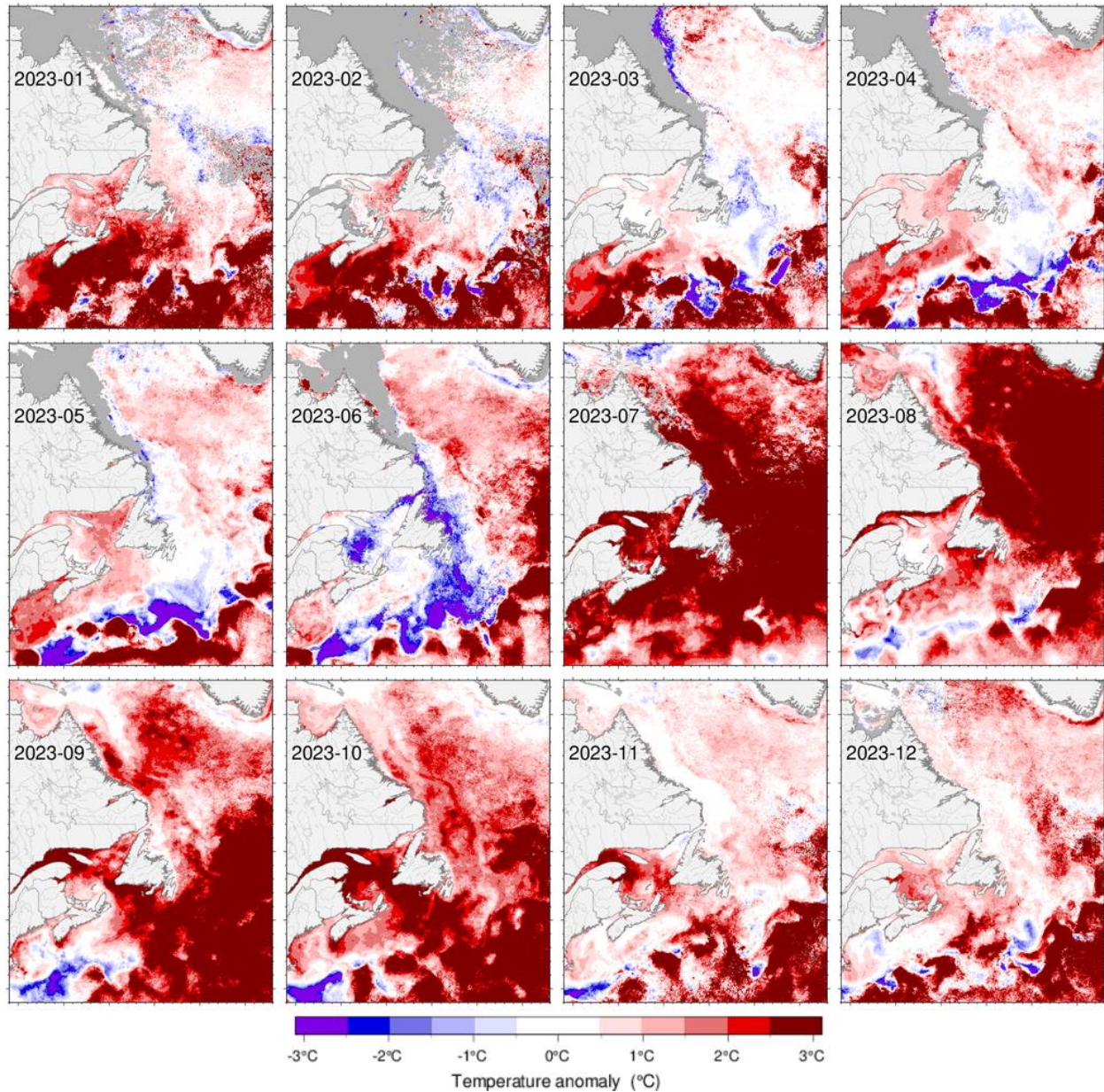


**Figure 15.** Sea-surface temperature monthly anomalies for 2023 in the Atlantic zone. Temperature anomalies are based on a 1985-2010 climatology.

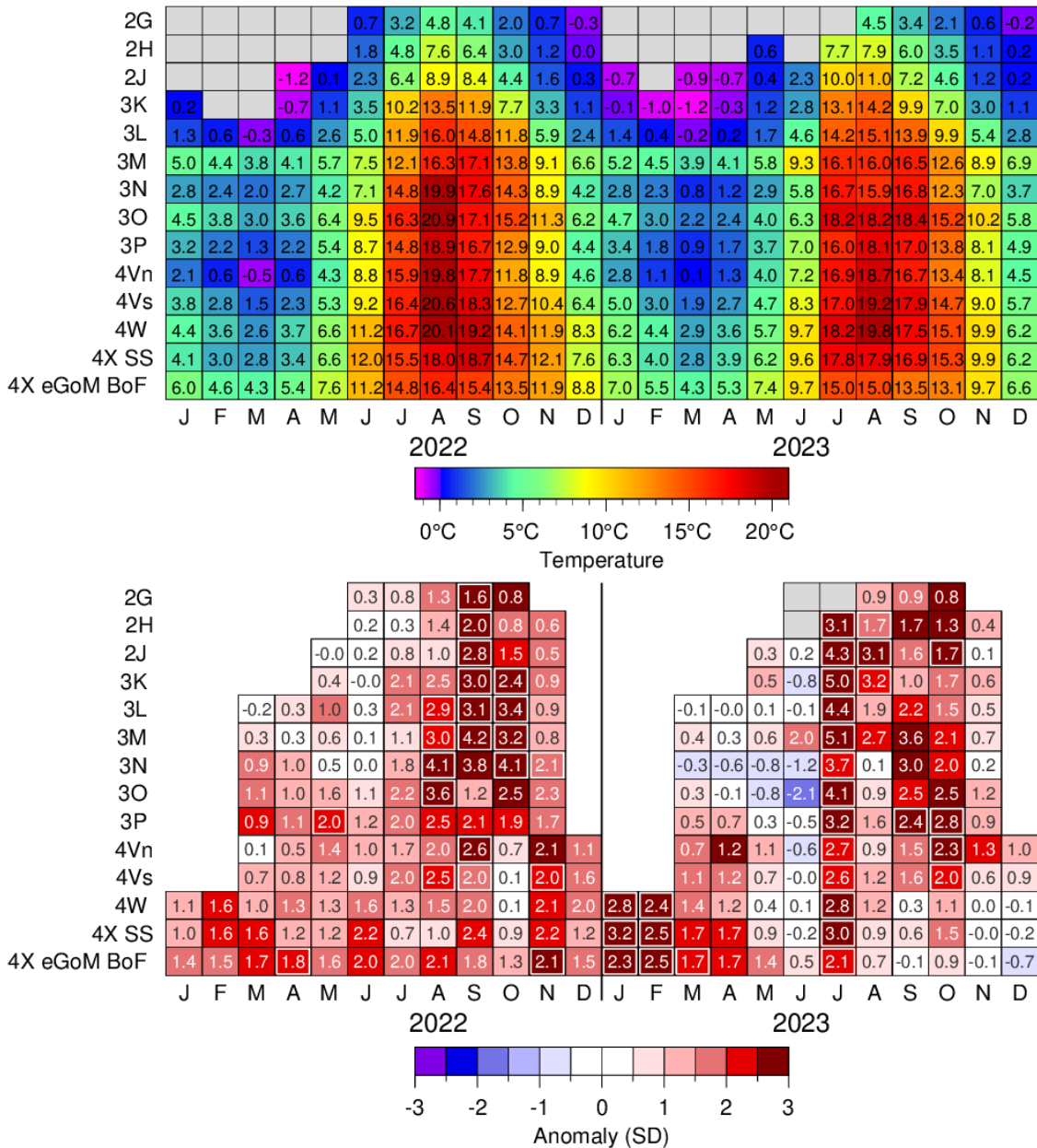


**Figure 16.** Monthly sea surface temperatures (top) and standardized anomalies in °C for NAFO subareas 2, 3 and 4 during 2022 and 2023 based on 1991-2020 climatologies. The area used for each division is limited to the continental shelf (see black contour in Figure 1). Regions and months for which the average temperature was at a record high or low are indicated by white outlines. Grayed boxes represent months ignored either because of missing climatology due to ice cover or because coverage was less than 7%.

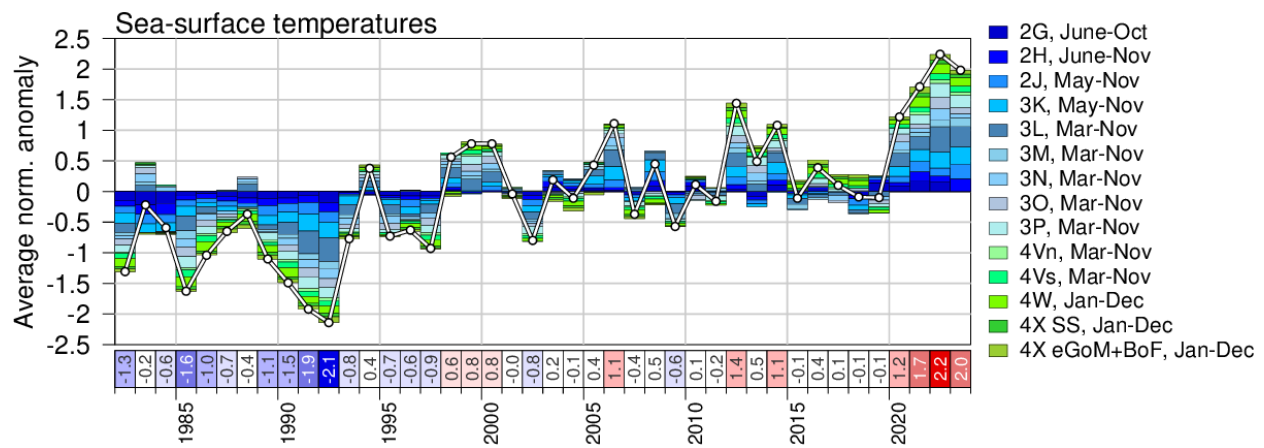


**Figure 17.** Sea Surface Temperature (SST) composite index in NAFO sub-areas 2 (dark blue), 3 (light blue) and 4 (green) since 1982. This index is built by performing a weighted-area average of the seasonal SST normalized anomaly for each NAFO division (divisions and months used are provided on the right-hand side of the figure). The scorecard at the bottom of the figure represents the index.

## Ocean Conditions on the Newfoundland and Labrador Shelf (NAFO Sub-areas 2 and 3)

### Long-term observations at Station 27

Station 27 ( $47^{\circ}32.8'N$ ,  $52^{\circ}35.2'W$ ), is located in the Avalon Channel off Cape Spear, NL (Figure 1). It is one of longest hydrographic time series in Canada with frequent, near-monthly, occupations since 1948. In 2023, the station was occupied 36 times including 16 Conductivity-Temperature-Depth (CTD)-only casts, 18 full AZMP physical-biogeochemical samplings and 2 Expendable Bathythermograph (XBT) measurements.

Since 2017, an automatic profiling system installed on a surface buoy (type Viking) usually provides extended temporal coverage of temperature (T) and salinity (S) at Station 27. The buoy was deployed in June 2023, but unfortunately the mini-winches used to collect CTD profile data were non-operational. Multiple attempts were made to repair the mini-winches at sea but they proved unsuccessful. No CTD profiles were collected in 2023 by the buoy, but all other surface instruments were operational and collected data until late September, after which data collection was impacted by the reduced sunlight affecting the power generation by the solar panels. The buoy was recovered in December.

Station occupations were used to obtain the annual evolution of temperature and salinity at Station 27, as well as the anomaly compared to the 1991–2020 climatology, shown in Figure 18 and Figure 19. These figures demonstrate the seasonal warming of the top layer (~20 m), with temperature peaking in August before being mixed during the fall. The CIL (Petrie et al., 1988), a remnant of the previous winter cold layer and defined by temperatures below  $0^{\circ}C$  (thick black line in Figure 18) is also evident below 100 m throughout the summer. Interestingly, the coldest water body within the CIL (darkest shades of blue in the middle panel of Figure 18) is generally found in the summer between mid-June and mid-August, suggesting advection of cold waters from the Labrador Shelf and the Arctic to the Newfoundland Shelf. The surface layer is generally freshest between early-September and mid-October, with salinities below 31 (Figure 19). These low near-surface salinities are a prominent feature of the salinity cycle on the Newfoundland Shelf and are largely due to the melting of coastal sea-ice. The presence of such a large volume of freshwater late in the summer season also points to advection from northern areas (Labrador and the Arctic).

The water column was warmer and fresher than average during the early months of 2023 (Figure 18 and Figure 19, top and bottom panels). While the fresh conditions continued through the spring and the summer, a cold layer developed in the surface in the spring and in the subsurface in the summer (Figure 18). As a warm anomaly developed in a very thin layer at the surface in July and August (see also Section 6.2), the cold anomaly was significant in August-September, reaching more than  $5^{\circ}C$  below average between about 20-30 m. This cold anomaly is likely driven by the advection of a thick CIL from the north and coherent with the cold month of February on the Labrador shelf (e.g. Figure 5). At depth, the rest of the year was relatively normal. Except for a salty anomaly in August-September consistent with the cold anomaly observed, the water column at Station 27 was fresher than average for most of the year and at all depths (Figure 19).

Over 2023, the annual temperature anomaly (defined as the average of monthly anomalies) for the vertically averaged (0–176 m) temperature was normal (+0.4 SD), while the vertically-averaged salinity was slightly fresh at -1.1 SD (Figure 20 and Figure 21). The fresh anomaly of the early 1970s (Figure 20, bottom panel), commonly referred to as the Great Salinity Anomaly in the North Atlantic (Dickson et al., 1988), now looks very minor compared to the freshening happening at Station 27 since the late 2010s. Normalized anomalies of temperature and salinity for all years since 1980 and for different depth ranges (0–176 m, 0–50 m and 150–176 m) are reported in scorecards in Figure 21.

The summer (May-July) CIL statistics at Station 27 since 1951 are presented in Figure 22. Here the CIL mean temperature corresponds to the average of all temperatures below 0°C. The CIL thickness as well as the CIL core temperature (the minimum temperature of the CIL) and its depth are also presented in Figure 22. In last year's report (Cyr et al., 2024), the discovery in our internal database of a set of problematic casts associated with Mechanical Bathythermographs (MBTs) collected in the 1960s and 1970s, where the negative temperatures were converted into positive values, has slightly reduced the warm anomalies during these decades . This year, we have found and removed more of these problematic data . The new time series suggest that the warm early 1960s to the mid-1970s for the CIL mean and core temperatures remain (top and middle panels, respectively), but that the magnitudes of these anomalies have decreased compared to the assessment prior to the discovery of the problematic MBTs (Cyr et al., 2022). After the prevalence of a warm CIL in the early 2010s (with some of the warmest years since the mid-1970s), there was a cooler period between about 2014 and 2017. The CIL was warmer than normal between 2018 and 2023, except in 2020 when it was normal. The SD of these metrics are reported in a scorecard in Figure 21.

The monthly mean mixed layer depth (MLD) at Station 27 was also estimated from the density profiles as the depth of maximum buoyancy frequency ( $N$ ) calculated from the monthly averaged density profiles ( $\rho(z)$ ) :

$$N^2 = - \frac{g}{\rho_0} \frac{\Delta\rho(z)}{\Delta z},$$

with  $g = 9.8 \text{ ms}^{-2}$  as the gravitational acceleration,  $z$  the depth and  $\rho_0$  as a reference density. Here  $N^2$  is calculated using the Gibbs-SeaWater (GSW) Oceanographic Toolbox (McDougall & Barker, 2011).

Climatological monthly MLD values, as well as monthly MLDs during 2023, are presented in Figure 23. The climatological annual cycle shows a gradual decrease of the MLD between late fall and summer (the mixed layer thickest in December-January and shallowest in July-August). Overall, the MLD was deeper than average in the winter (Jan-Feb; no data for March), close to normal in spring and fall, and shallower than average in June, July and September. The MLD was especially thin in September with values of ~15m, which are as shallow as in July and much shallower than the climatological values of ~35m for this month. Annual mean values of the MLD and its 5-year moving average are shown in Figure 24 (solid gray line and dashed-black line, respectively). In general, there is a strong interannual and decadal oscillation in MLD, but the striking feature is a step-like increase in the 1990s. A scorecard of annual and seasonal MLD anomalies since 1980 can be found in Figure 21.

Stratification is an important characteristic of the water column since it influences, for example, the transfer of solar heat to deeper layers and the vertical exchange of biogeochemical tracers between the deeper layers and the surface. The seasonal development of stratification is also an important process influencing the formation and evolution of the CIL on the shelf regions of Atlantic Canada. It insulates the lower water column from the upper layers, thus slowing the vertical heat flux from the seasonally heated surface layer.

Stratification at Station 27 is calculated from monthly average density profiles using discrete differences between two averaged depth ranges. Unlike in previous reports (Cyr et al., 2022), two definitions of the stratification indices are calculated for Station 27. The first one uses density differences (i.e.  $\Delta\rho/\Delta z$ ) between 0-5 m and 48-53 m (labelled 0-50 m definition) and the second one between 8-13 m and 148-153 m (labelled 10-150 m definition). See bottom two scorecards in Figure 19. Measurements taken from non-bottle instrument types were discarded in the top two depth levels to mitigate the influence of problem surface measurements. The reason for these two definitions is that historical near-surface measurements in the 1950s and 1960s were made at discrete depths of  $z=0, 25$ , and  $50$  m. In the 1970s and 1980s, these discrete depths were changed to  $z=0, 10, 20, 30, 50$  m. Finally, since the widespread use of electronic measurements using CTDs mounted on rosettes started in the 1980s, near-surface ( $z=0$ ) measurements of density are usually discarded, and each high-resolution cast usually starts between 2-5 m depth to avoid electronic noise contamination or damage to the rosette by surface waves or ship motion. There is thus no simple definition that can ensure continuity of the metric from the 1950s to present. Here the definition 0-50 m will mostly focus on the 1950-1990 period, while the definition 10-150 m will be representative of the period 1960-present. Note that the 0-50 m definition is also calculated until present, but it considers the average over 0-5 m as the surface measurement, making it difficult to directly compare with historical data. When reporting annual averages, yearly stratification values are omitted if there is less than 3 months of data available. When reporting seasonal averages, only one measurement must be present.

The 2023 and climatological evolution of the 0-50m stratification throughout the year are shown in Figure 25. The stratification is generally weakest between December and April, before rapidly increasing at the onset of spring until it peaks in August. While the stratification was close to normal for most of the year, a notable observation is the high stratification in September 2023 (Figure 25). This anomalously high stratification value is coherent with the shallow MLD observed that month (Figure 23).

The interannual evolution of the stratification anomaly since 1950 is shown in Figure 26. Strong decadal variations exist in the two different definitions of stratification. For the 0-50m range, an increase in stratification from the 1950s to about 2000 is observed, followed by a slight decrease since then. For the 10-150m definition, no real trends are discernible, but a step-wise increase seems to occur in the early 1990s, especially in the 0-50 definition. We have shown this increase by averaging the stratification between 1950-1990 and 1990-present (Figure 26). In 2023 the annual stratification was about normal relative to the 1991-2020 climatology. A scorecard of annual and seasonal stratification anomalies since 1980 can be found in Figure 21.

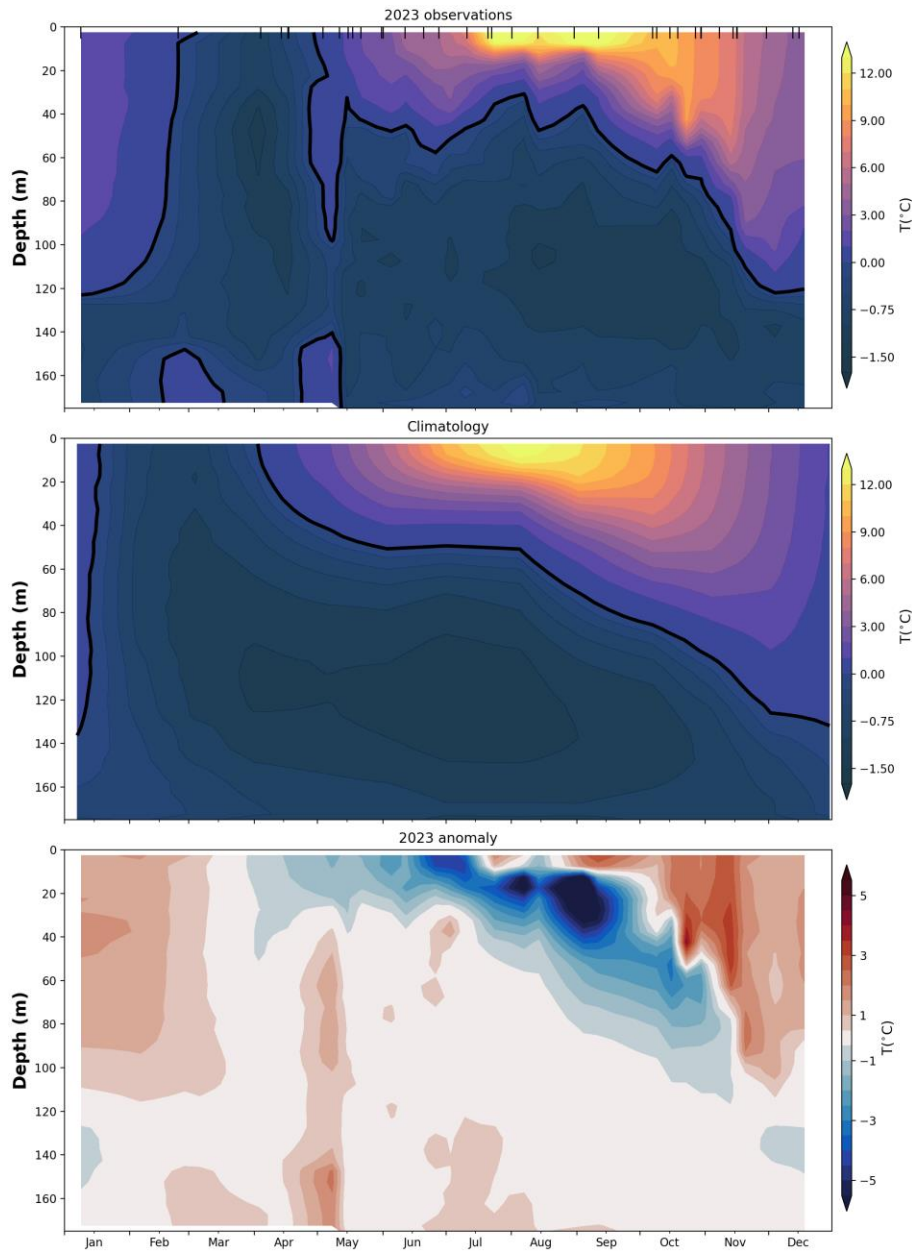


**Figure 18.** Annual evolution of temperature at Station 27. The 2023 contour plot (top panel) is generated from weekly averaged profiles from all available data, including station occupations (indicated by black tick marks on top of panel). The solid black contour delineates the cold intermediate layer (CIL), defined as water below 0°C. The 1991–2020 weekly climatology is plotted in the middle panel. Note the uneven colorbar used in the two first panels: below 0°C, 0.25°C increments are used, while 1°C increments are used above 0°C. The anomaly (bottom panel) is the difference between the 2023 field and the climatology.

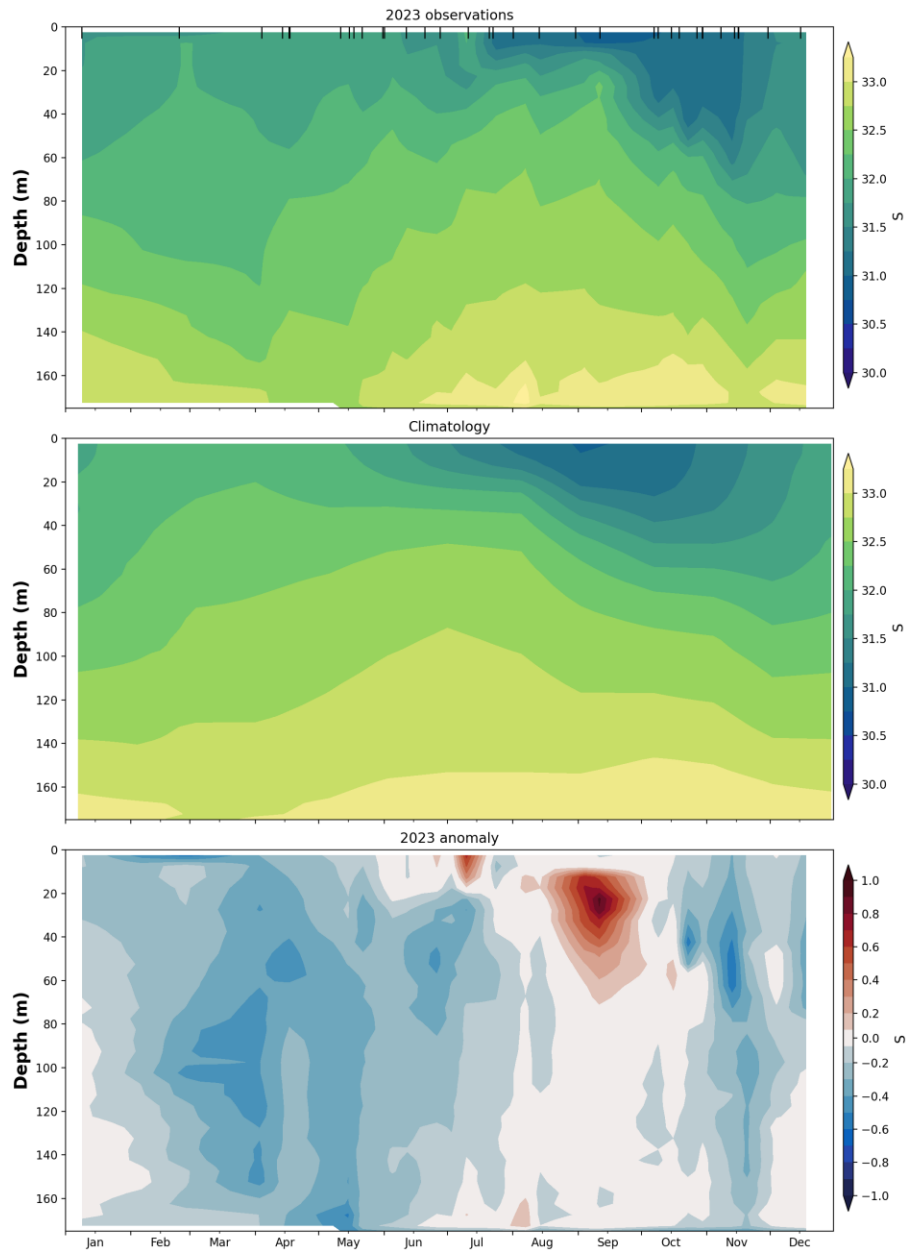


**Figure 19.** Same as in Figure 18, but for salinity.

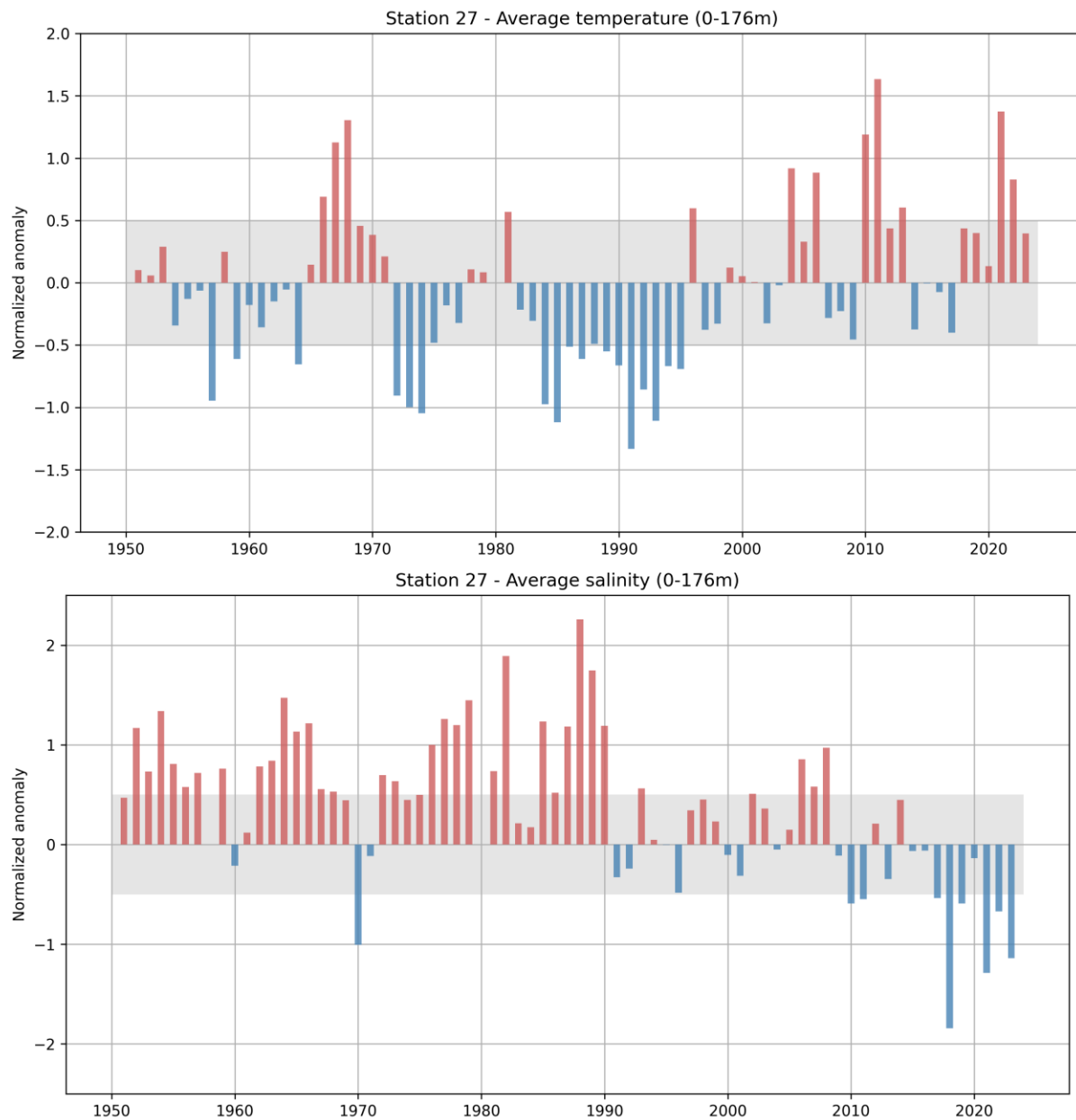


**Figure 20.** Annual normalized anomaly of vertically averaged (0–176 m) temperature (top) and salinity (bottom) at Station 27 calculated from all occupations since 1951. Only years where at least 8 months of the year are sampled are presented. Shaded gray areas represent the climatological (1991–2020) average  $\pm 0.5$  SD range considered “normal”.

-- Vertically averaged temperature --																																													
81	82	83	84	85	86	87	88	89	90	91	92	93	94	95	96	97	98	99	00	01	02	03	04	05	06	07	08	09	10	11	12	13	14	15	16	17	18	19	20	21	22	23	$\bar{x}$	sd	
Temp 0-176m	0.6	-0.2	-0.3	-1.0	-1.1	-0.5	-0.6	-0.5	-0.6	-0.7	-1.3	-0.9	-1.1	-0.7	0.6	-0.4	-0.3	0.1	0.1	0.0	-0.3	0.0	0.9	0.3	0.9	-0.3	-0.2	-0.5	1.2	1.6	0.4	0.6	-0.4	0.0	-0.1	-0.4	0.4	0.4	0.1	1.4	0.8	0.4	0.6	0.6	
Temp 0-50m	0.5	-0.1	-0.1	-1.2	-1.1	-0.5	-0.4	-0.6	-0.4	-0.8	-1.4	-0.7	-0.9	-0.3	-0.6	0.4	-0.5	-0.2	0.2	0.1	0.1	-0.6	0.2	0.5	0.4	1.1	-0.5	0.4	-0.7	0.9	1.0	0.8	0.6	-0.1	0.3	-0.3	0.0	-0.1	0.1	1.9	1.0	0.0	3.5	1.1	
Temp 150-176m	0.5	-0.2	-0.8	-0.9	-1.5	-0.5	-0.5	-0.4	-0.6	-1.0	-1.3	-1.0	-1.3	-1.1	-0.7	0.2	-0.1	0.2	0.3	0.1	0.3	-0.3	-0.3	1.4	0.9	1.0	0.1	-0.1	-0.6	1.1	2.4	0.5	0.6	-0.7	-0.7	-0.6	-0.6	0.4	0.2	0.9	1.9	1.0	0.6	-0.9	0.4
-- Vertically averaged salinity --																																													
Sal 0-176m	0.7	1.9	0.2	0.2	1.2	0.5	1.2	2.3	1.7	1.2	-0.3	-0.2	0.6	0.0	0.0	-0.5	0.3	0.4	0.2	-0.1	-0.3	0.5	0.4	-0.1	0.1	0.9	0.6	1.0	-0.1	-0.6	-0.5	0.2	-0.3	0.4	-0.1	-0.5	-1.8	-0.6	-0.1	-1.3	-0.7	-1.1	32.5	0.1	
Sal 0-50m	0.5	1.8	-0.6	-0.8	1.3	0.5	1.1	2.0	2.0	1.2	-1.3	-0.1	0.1	0.0	-0.7	-0.1	0.0	0.0	-0.4	-0.5	0.9	1.0	0.3	0.3	0.5	0.4	0.7	0.3	-0.8	-0.4	0.2	-0.1	0.1	0.0	0.3	-0.8	-1.1	0.4	0.2	-0.7	-0.4	-0.8	31.9	0.2	
Sal 150-176m	1.6	2.1	0.5	1.0	0.5	0.1	1.0	2.5	0.8	0.8	-0.3	-0.4	0.7	-0.1	0.2	-0.6	0.2	0.6	0.2	0.2	0.0	0.1	-0.4	0.1	0.4	1.2	0.7	0.9	-0.4	0.1	0.1	0.3	-0.6	0.3	-0.4	-0.6	-0.5	-1.6	-1.1	0.0	-1.1	-0.9	-1.1	33.1	0.1
-- Cold intermediate layer (CIL) properties --																																													
CIL temp	0.6	-0.4	-1.0	-0.7	-1.4	-0.9	-0.5	-0.2	-0.1	-0.2	-1.5	-1.1	-1.6	-1.3	-1.0	1.0	-0.5	-0.7	0.3	0.6	0.4	-0.5	-0.4	1.3	0.1	1.2	2.3	1.9	-0.1	1.0	-0.3	-0.5	-0.3	-0.6	1.3	0.7	-0.3	1.4	0.9	1.5	-1.1	0.2			
CIL core T	1.0	-0.9	-1.2	-1.0	-1.5	-1.1	-0.9	-0.1	-0.4	-0.2	-1.4	-0.9	-1.3	-1.5	-1.1	1.3	-0.4	-0.7	0.0	0.7	0.5	-0.4	-0.3	1.1	-0.1	1.5	-0.4	-0.4	-1.2	2.5	2.0	-0.2	1.4	-0.1	-0.2	-0.3	-0.5	0.3	0.4	-0.3	1.2	1.2	1.8	-1.4	0.2
CIL thickness	1.2	-0.6	0.3	1.6	0.3	0.3	-0.1	1.2	-0.6	-0.1	2.0	0.3	-0.1	1.2	0.7	-1.0	0.7	0.7	-0.1	-0.1	-0.1	-0.7	-1.0	-0.1	0.3	-0.3	-0.1	1.2	1.2	0.7	-1.9	-2.3	-1.5	-0.1	0.3	-0.6	0.7	-1.5	-1.0	0.7	0.3	126.7	11.5		
-- Mixed layer depth (MLD) --																																													
MLD winter	-0.8	-0.5	-2.0	-0.3	-1.0	-0.8	-0.8	-0.5	1.4	-0.6	-0.1	-0.7	0.0	-0.4	-0.4	-0.4	-0.7	-1.3	0.0	0.4	-0.1	0.5	0.6	-0.5	-1.8	1.1	0.1	0.0	1.0	-0.4	1.3	-0.1	1.5	-0.8	1.7	55.5	6.2								
MLD spring	-1.0	-1.1	-0.9	-1.3	-1.8	-1.5	-1.8	-0.4	-0.4	0.6	0.2	0.2	-0.4	-0.5	-0.3	-0.8	-0.8	-0.4	0.3	0.0	0.1	-0.5	-0.1	-1.0	-0.7	0.3	-0.3	-0.6	0.2	-0.6	0.9	0.4	0.3	0.9	0.0	0.2	1.3	0.6	-0.3	-0.5	-0.2	35.9	9.0		
MLD summer	-0.1	0.3	0.0	-0.8	-0.1	-0.6	0.7	-0.9	-0.4	-0.2	0.2	1.7	0.1	0.5	0.8	0.3	0.0	-0.6	-0.6	-0.2	0.2	0.4	-0.3	-0.9	0.8	0.0	-0.9	0.7	-0.6	-0.5	0.6	-1.1	-0.2	-0.7	2.3	0.1	-0.6	0.4	0.2	-0.4	1.0	1.1	-0.7	23.9	6.5
MLD fall	0.1	0.1	-2.6	-1.4	-1.4	-1.4	-1.4	-0.2	-0.2	0.5	0.0	0.1	-0.5	-0.4	-0.1	0.1	0.4	-0.9	-1.0	0.9	0.3	0.7	0.4	-0.5	0.2	-0.8	0.1	-1.3	0.6	0.9	0.1	1.2	0.8	-0.8	0.5	0.2	-0.2	1.5	-0.7	0.2	58.9	9.9			
MLD annual	-0.8	-0.5	0.1	-1.3	-0.5	-1.0	-0.7	-1.3	0.2	-0.6	0.1	0.6	-0.1	0.3	-0.2	-0.1	-0.3	-0.4	-0.2	-0.2	0.0	0.1	-0.3	0.0	-0.4	-0.2	0.1	-0.2	-0.7	0.3	0.2	0.2	1.3	-0.2	0.1	0.0	43.6	16.5							
-- Stratification (0-50m) --																																													
strat winter	-0.5	0.9	-0.6	-0.5	-0.7	2.2	0.0	1.0	-1.2	2.2	0.8	0.1	-0.7	1.0	-0.1	0.2	0.5	0.2	-0.3	0.0	-0.4	0.6	0.6	-0.2	-0.1	-0.8	-1.0	-0.7	-0.2	-0.6	0.6	-0.3	-0.3	-0.4	0.3	0.008	0.001								
strat spring	0.9	0.0	2.8	1.3	-1.1	-1.0	-1.5	0.0	0.2	0.6	2.5	-0.9	0.2	1.2	1.1	0.0	0.2	-0.1	0.0	0.3	0.7	0.1	-0.2	1.0	-0.3	0.1	-0.1	-0.4	-0.7	-0.2	-0.6	0.1	-1.2	-1.3	2.3	0.5	-0.5	0.015	0.008						
strat summer	0.1	1.5	-0.5	-0.2	-2.5	-0.8	-0.5	-0.6	-1.0	1.3	0.4	-1.0	-0.1	0.6	1.0	-0.1	0.5	0.1	-0.5	-0.1	0.3	0.2	0.8	0.2	0.1	-0.6	-1.5	0.1	0.7	2.1	-0.9	-0.2	1.1	-1.3	-1.4	0.7	-0.2	0.5	0.7	0.054	0.009				
strat fall	-2.3	-0.9	1.5	-1.4	4.7	-0.3	-0.1	1.7	-0.3	-0.8	-0.5	0.3	0.2	0.4	0.4	0.3	0.7	1.0	-0.9	0.3	-0.6	-0.2	1.0	0.0	1.2	-1.1	0.8	-0.6	-0.9	0.1	-0.4	-1.1	1.0	-0.1	-1.2	0.7	0.4	0.9	1.3	-0.6	0.018	0.011			
strat annual	-0.6	0.4	1.4	-0.7	-0.7	-1.2	-0.8	0.2	-0.2	-0.1	0.0	1.2	-0.3	0.2	0.5	0.8	0.1	0.4	-0.4	-0.2	-0.2	0.0	0.5	0.1	0.4	0.0	-0.1	-0.6	-0.4	0.0	0.2	-0.6	0.0	0.3	-1.2	-1.1	0.6	0.6	0.5	-0.1	0.024	0.02			
-- Stratification (0-150m) --																																													
strat winter	-0.2	-1.4	0.7	-0.4	0.3	-0.6	-1.9	-1.6	0.6	0.2	-0.1	-0.2	-0.1	0.7	0.4	1.1	0.1	-0.4	-0.1	-0.7	0.2	0.2	-0.4	0.7	-0.1	0.4	1.3	0.6	-1.5	1.1	-0.1	1.1	-0.9	-0.7	0.7	0.009	0.001								
strat spring	1.1	-0.7	1.2	1.7	-1.4	-1.4	-1.0	0.5	0.8	2.2	-0.5	0.0	1.0	1.2	0.2	0.3	-1.1	-1.7	-0.4	0.3	1.0	0.2	-0.2	0.7	-0.7	-0.2	0.5	-0.4	-0.8	0.0	1.1	0.3	-0.6	-1.3	2.6	0.7	-0.2	0.011	0.003						
strat summer	1.7	-0.6	0.8	1.1	-0.4	-0.7	-1.2	-0.8	-0.4	-0.9	0.6	0.8	-0.1	0.0	0.9	-0.4	1.0	-0.4	-0.5	-0.4	0.3	0.2	0.0	-0.6	0.6	0.5	-1.4	-0.2	1.2	1.1	-0.4	0.2	1.3	-0.6	-1.5	-0.2	0.2	0.4	-1.0	0.024	0.003				
strat fall	1.4	0.7	0.0	0.5	1.5	-0.8	-0.7	0.3	-0.2	-0.4	0.2	-0.1	0.0	0.8	1.3	-1.6	-0.2	0.0	-0.2	0.8	-0.1	1.1	-1.7	1.1	-0.3	0.0	0.3	0.3	-0.7	-1.1	0.6	-0.3	-0.8	0.9	0.8	1.3	1.8	-0.1	0.018	0.005					
strat annual	1.0	-0.8	1.1	1.1	-0.8	-0.5	-0.5	0.7	-0.9	-0.1	0.2	0.8	-0.3	0.0	0.4	0.7	0.4	0.6	-1.0	-0.7	-0.4	0.1	0.6	-0.1	0.2	-0.3	0.2	0.3	-0.3	0.3	-0.7	-1.2	0.3	1.0	0.5	-0.2	0.016	0.007							



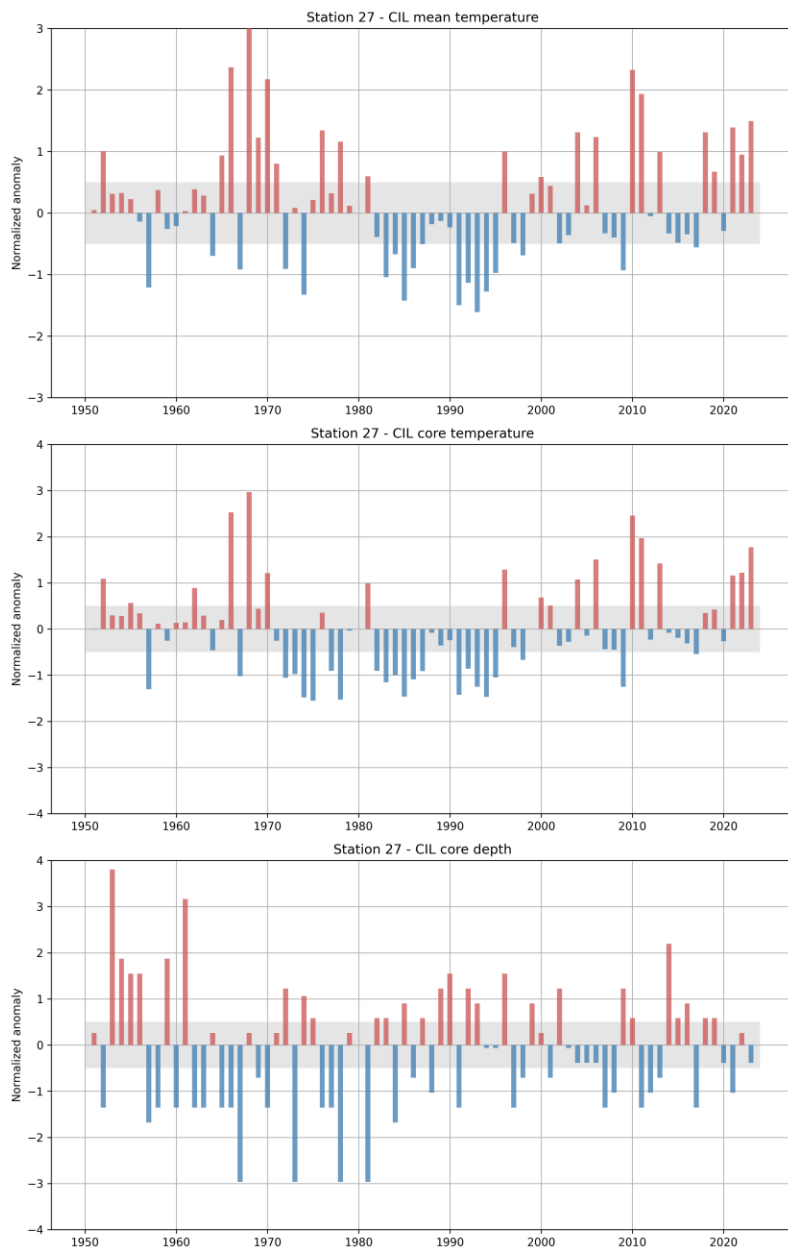


**Figure 22.** Normalized anomalies of summer (May-July) cold intermediate layer (CIL) statistics at Station 27 since 1951. Only years where at least 8 months of the years are sampled are presented. The top panel shows the CIL mean temperature, the middle the CIL core temperature (minimum temperature of the CIL) and the bottom panel the depth of the CIL core. Shaded gray areas represent the climatological (1991–2020) average  $\pm 0.5$  SD range considered “normal”.

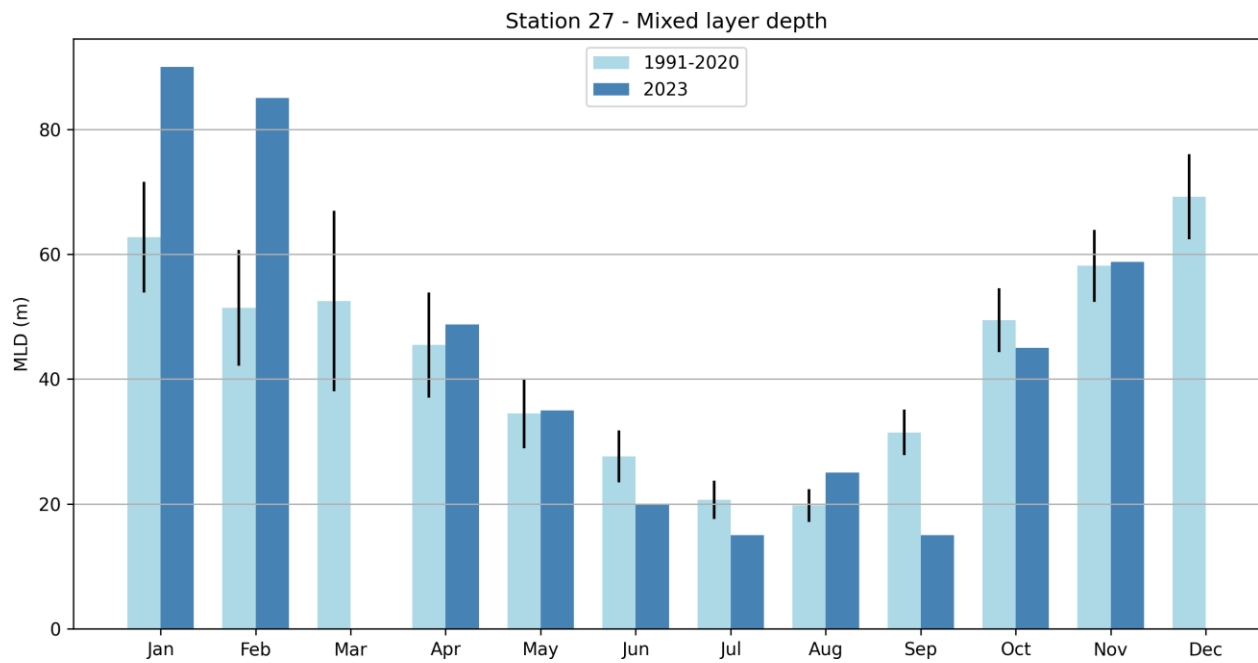


**Figure 23.** Bar plot of the monthly averaged mixed layer depth (MLD) at Station 27. The 1991–2020 climatology is shown in light blue while the update for 2023 is shown in dark blue. The black lines represent 0.5 SD above and below the climatology. No observations were made in March or December.

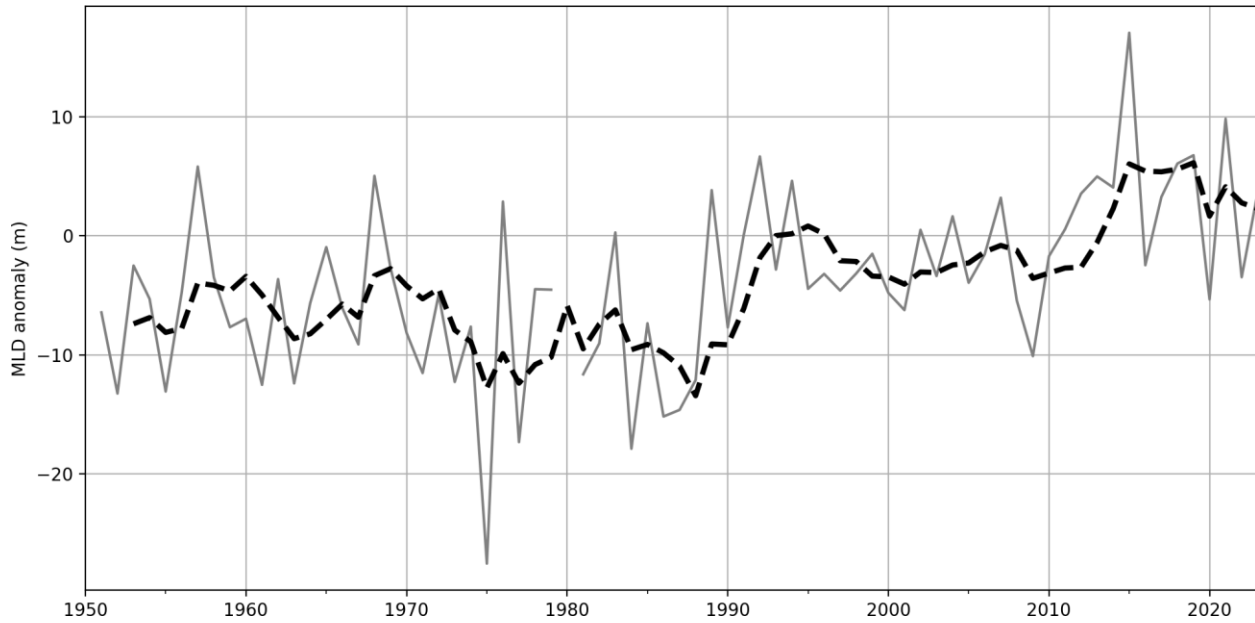


**Figure 24.** Time series of the annual mixed layer depth (MLD) average at Station 27 since 1950 (gray solid line) and its 5-year running mean (dashed-black line).

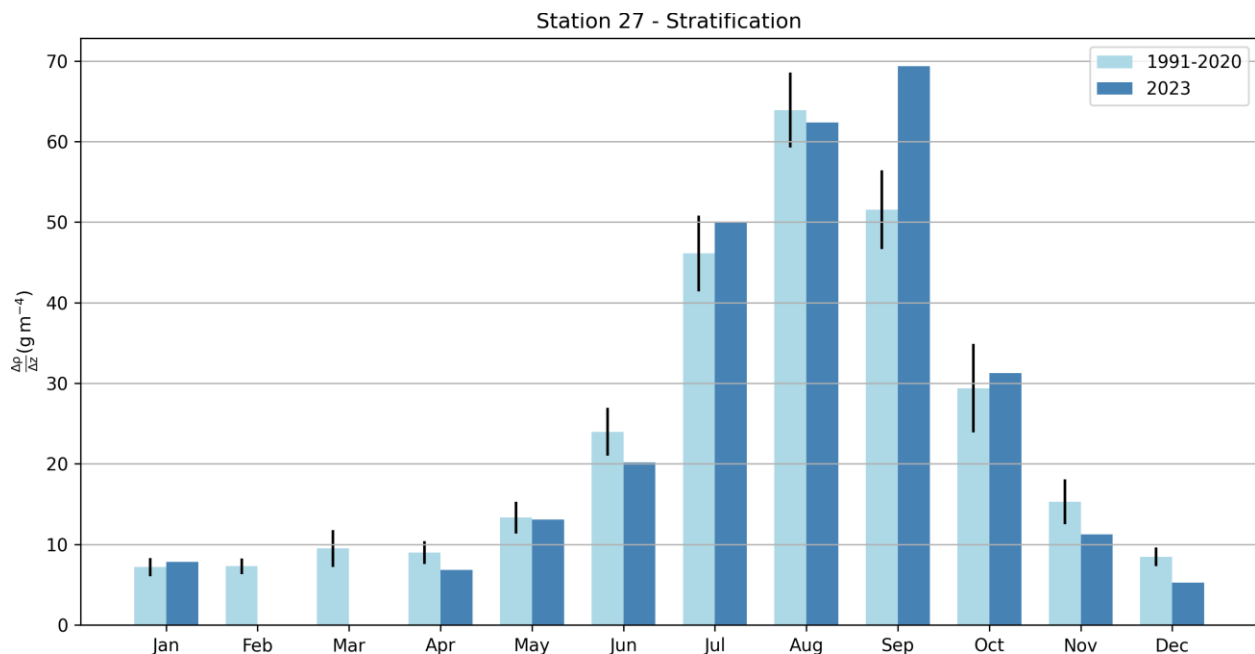


**Figure 25.** Bar plot of the monthly average stratification (defined as the difference in average density between 0-5 and 48-53 m) at Station 27. The 1991–2020 climatology is shown in light blue while the update for 2023 is shown in dark blue. The black lines represent 0.5 SD above and below the climatology. No observations were made in February and March.

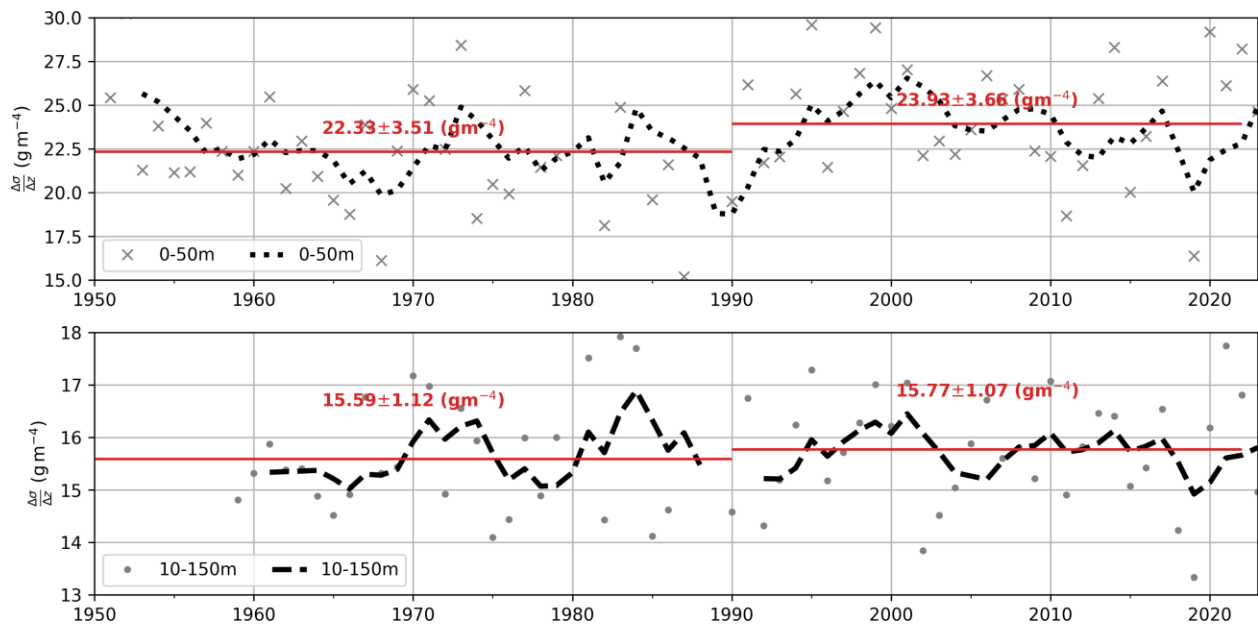


**Figure 26.** Time series of the annual average stratification at Station 27 between 0 and 50m (gray crosses; top) and 10 and 150m (gray dots; bottom) since 1950. For each panel, the 5-year running mean is shown as a dotted/dashed black line. Note the different vertical axis for the two panels.

## Standard Hydrographic Sections

In the early 1950s, several countries under the auspices of the International Commission for the Northwest Atlantic Fisheries (ICNAF) carried out systematic monitoring along hydrographic sections in Newfoundland and Labrador waters. In 1976, ICNAF normalized a suite of oceanographic monitoring stations along sections in the Northwest Atlantic Ocean from Cape Cod (USA) to Egedesminde (West Greenland) (ICNAF 1978). In 1998 under the Atlantic Zone Monitoring Program (AZMP) of Fisheries and Oceans Canada, the Seal Island (SI), Bonavista Bay (BB), Flemish Cap ( $47^{\circ}\text{N}$ ) (FC) and Southeast Grand Bank (SEGB) historical stations were selected as core monitoring sections. The White Bay section (WB) continued to be sampled during the summer as a long time series ICNAF/NAFO section (see Figure 1).

Two ICNAF sections on the mid-Labrador Shelf, the Beachy Island (BI) and the Makkovik Bank (MB) sections, were selected to be sampled during the summer if survey time permitted. Starting in the spring of 2009, a section crossing south-west over St. Pierre Bank (SWSPB) and one crossing south-east over St. Pierre Bank (SESPB) were added to the AZMP surveys.

During the spring 2023 survey (April 3-17 onboard the CCGS Capt. Jacques Cartier), sections SWSPB, SEGB and FC were sampled. The summer 2023 survey (July 20 – August 1 onboard the CCGS John Cabot) sampled sections FC, BB and SI, while the fall 2023 survey (October 6-27 onboard the RRS Discovery) sampled sections SWSPB, SEGB, FC, BB and SI. In this manuscript we present the summer cross-sections of temperature and salinity and their anomalies along the SI, BB and FC sections to represent the vertical temperature and salinity structure across the NL Shelf during 2023.

### *Temperature and Salinity Variability*

The water mass characteristics observed along the standard sections crossing the NL Shelf are typical of Arctic-origin waters with a subsurface temperature range of  $-1.5^{\circ}\text{C}$  to  $2^{\circ}\text{C}$  and salinities from 31.5 to 33.5. Labrador Slope water flows southward along the shelf edge and into the Flemish Pass and Flemish Cap regions. With temperatures in the range of  $3^{\circ}\text{C}$  to  $4^{\circ}\text{C}$  and salinities in the range of 34 to 34.75, this water mass is generally warmer and saltier than the shelf waters. Surface temperatures normally warm to between  $10^{\circ}\text{C}$  and  $12^{\circ}\text{C}$  during late summer, while bottom temperatures remain  $<0^{\circ}\text{C}$  over much of the Grand Banks, increasing to between  $1^{\circ}\text{C}$  and  $3.5^{\circ}\text{C}$  near the shelf edge below 200 m and in the deep troughs between the banks. In the deeper ( $>1,000$  m) waters of the Flemish Pass and across the Flemish Cap, bottom temperatures generally range from  $3^{\circ}\text{C}$  to  $4^{\circ}\text{C}$ . In general, the near-surface water mass characteristics along the standard sections undergo seasonal modification from annual cycles of air-sea heat flux, wind-forced mixing, and the formation and melting of sea ice. These mechanisms cause intense vertical and horizontal temperature and salinity gradients, particularly along the frontal boundaries separating the shelf and slope water masses. The seasonal changes in the temperature and salinity fields along the Bonavista section are presented in Colbourne et al., (2015).

Summer temperature and salinity structures along the SI, BB and FC ( $47^{\circ}\text{N}$ ) are presented in Figure 27 to Figure 29. The dominant thermal feature along these sections is associated with the cold and



relatively fresh CIL overlying the shelf. This water mass is separated from the warmer and denser water of the continental slope region by strong temperature and salinity fronts. The cross-sectional area (or volume) of the CIL is bounded by the 0°C isotherm and highlighted as a thick black contour in the temperature panels. The CIL parameters are regarded as robust indicators of ocean climate conditions on the eastern Canadian Continental Shelf. While the CIL area undergoes significant seasonal variability, the changes are highly coherent from the Labrador Shelf to the Grand Banks. The CIL remains present throughout most of the summer until it gradually decays during the fall as increasing winds and storm episodes deepen the surface mixed layer.

The analysis of summer section observations gives an interesting perspective on the warm SSTs observed in 2023. All sections show the presence of a very thin (<15m) surface layer with temperature anomalies reaching +3.5°C above normal. Below this thin surface layer, a negative anomaly indicates that the top of the CIL was shallower than normal. While the temperature of the CIL was approximately normal, the CIL extended further offshore on the SI section (indicated by a negative anomaly at the shelf break in (Figure 27, bottom left). The CIL remained closer to the shore on the BB section (indicated by a positive anomaly on the offshore part of the shelf in Figure 28, bottom left). The latter anomaly resembles the intrusion of warm and salty slope water on the shelf.

The corresponding salinity cross sections show a relatively fresh (<33) upper water layer over the shelf with sources from Arctic outflow on the Labrador Shelf, in contrast to the saltier Labrador Slope water further offshore with values >34 (Figure 27 to Figure 29, right panels). In 2023, salinities were mostly fresh across all sections, except for a thin surface near-shore lens in the nearshore area of SI section and for the warmer intrusion on the shelf at BB section.

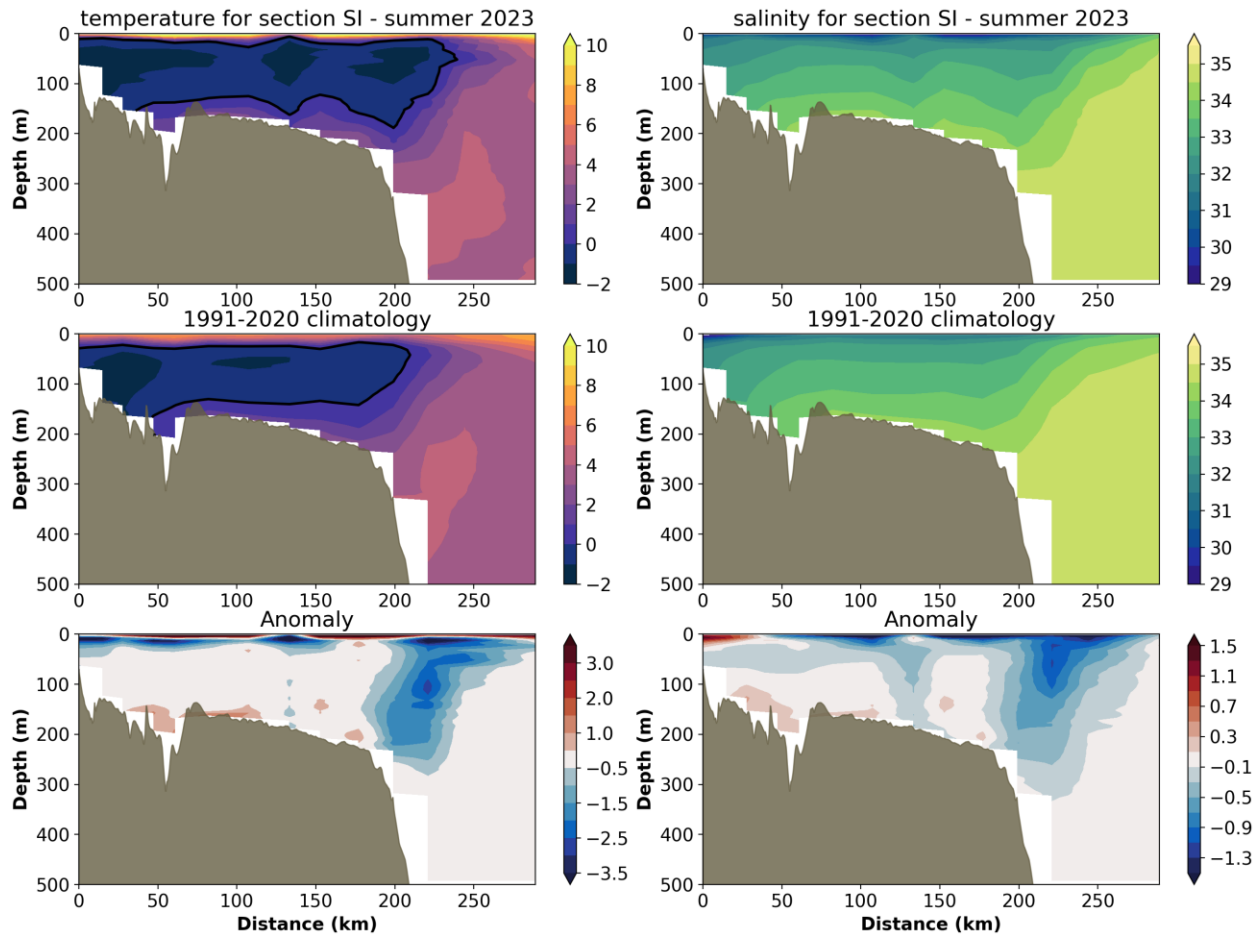


**Figure 27.** Contours of temperature ( $^{\circ}\text{C}$ ) and salinity during summer 2023 (top row) and climatological average (middle row) for Seal Island (SI) hydrographic section (see map Figure 1 for location). Their respective anomalies for 2023 are plotted in the bottom panels.

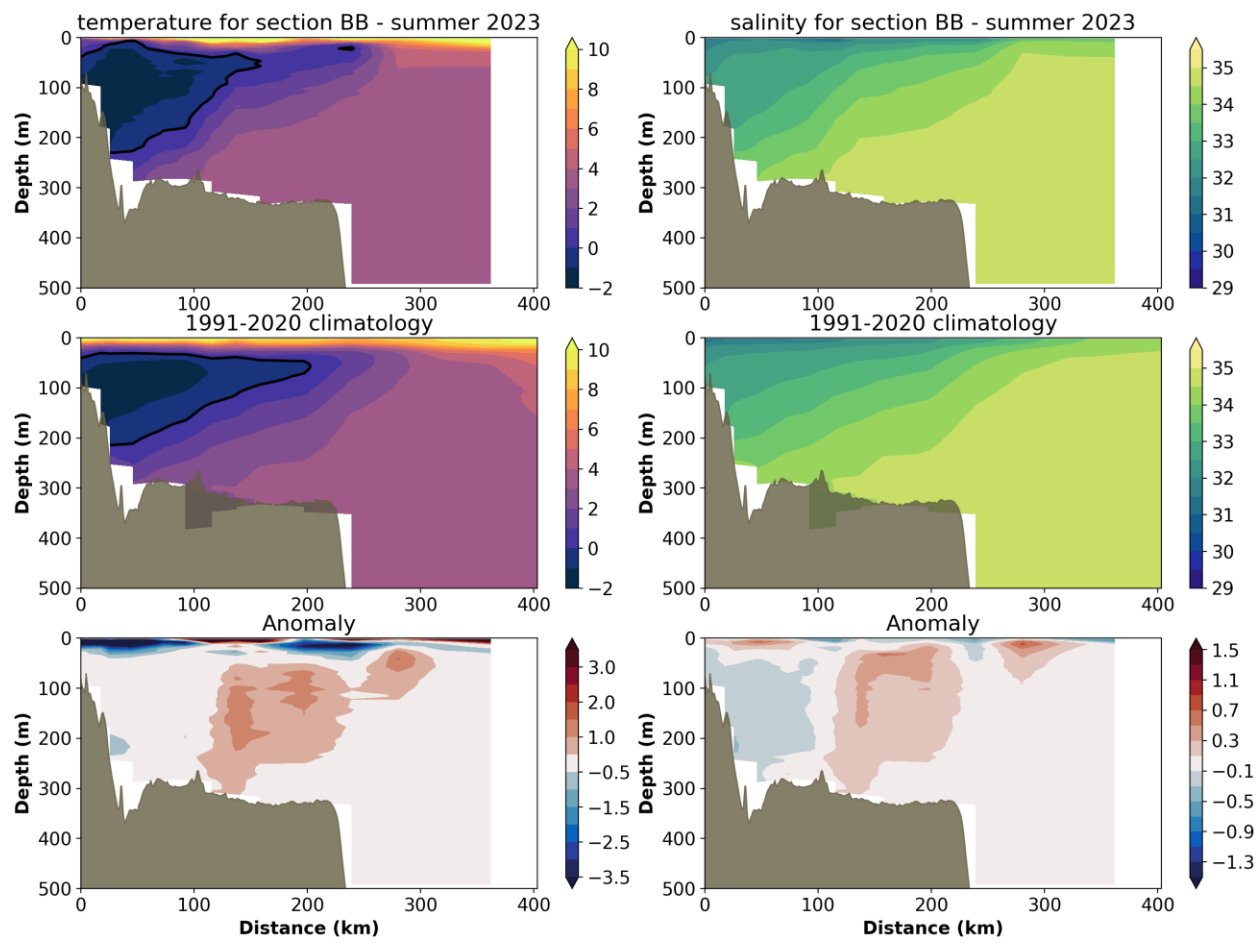


**Figure 28.** Same as in Figure 27, but for Bonavista (BB) hydrographic section (see map Figure 1 for location).

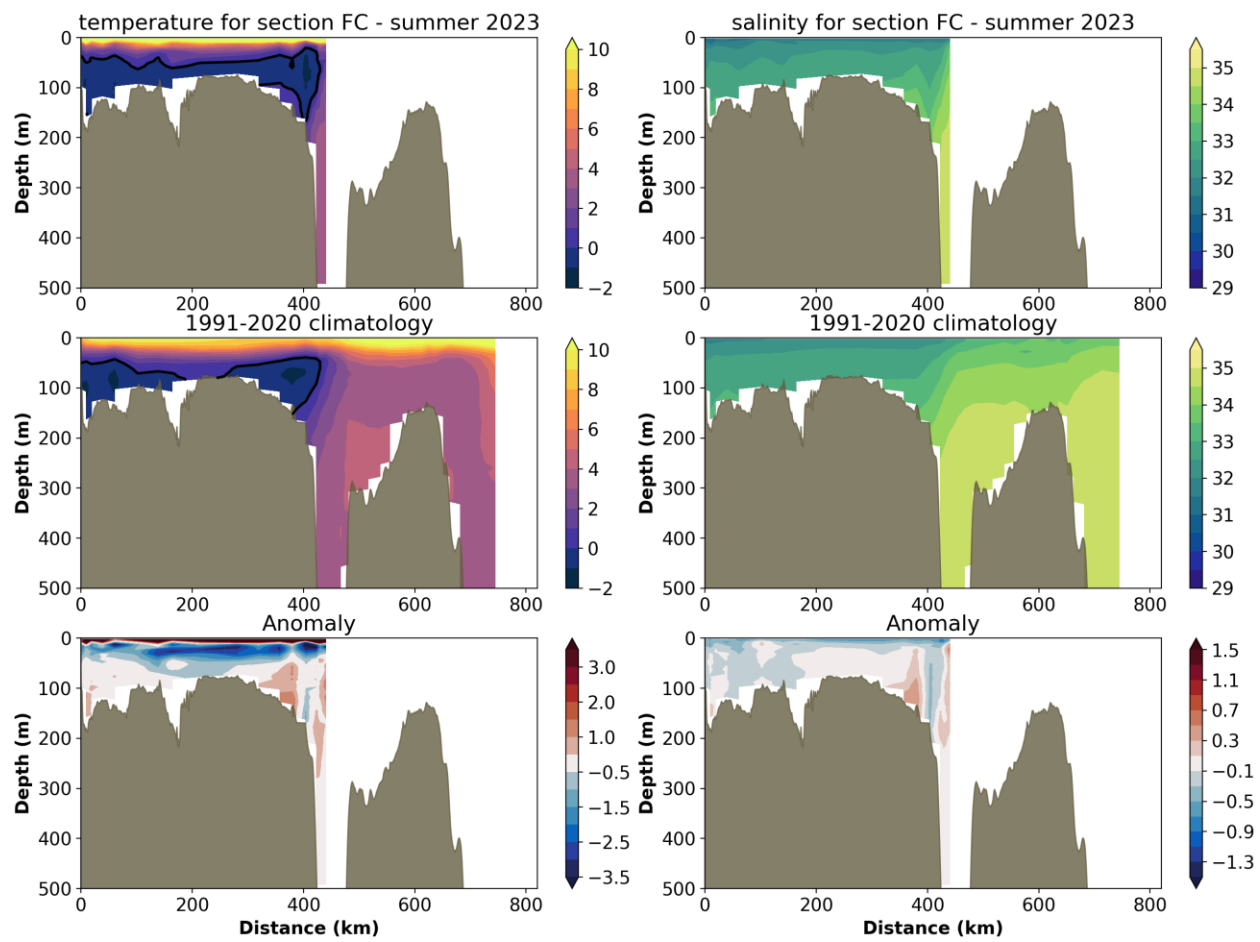


**Figure 29.** Same as in Figure 27, but for Flemish Cap (FC) hydrographic section (see map Figure 1 for location).

### *Cold Intermediate Layer Variability*

Statistics of summer CIL anomalies (CIL area, CIL core temperature and CIL core depth) for the three sections discussed above (SI, BB and FC) are presented in a scorecard in Figure 30. The years where data are re-constructed using profiles collected between June and August are identified in the bottom row of the scorecards with small black dots. Because this method uses the average between June and August, the core CIL temperature is not derived. The climatological average cross-sectional areas of the summer CIL along these sections are  $24\pm6$  km $^2$ ,  $24\pm7$  km $^2$  and  $20\pm5$  km $^2$ , respectively. The averaged anomalies of the CIL cross-sectional area for these three sections are summarized in Figure 31 as a time series going back to 1950. In general, the summer CIL has been predominantly warmer and smaller than average since the mid-1990s, with a cold phase extending from about 2012 or 2014 to 2017. However, the most striking aspect of this long time series is the warm conditions that prevailed in the mid-1960s and mid-1970s, followed by a cold period that lasted from the mid-1980s to the mid-1990s.

In 2023, the CIL area was near-normal (+0.6 SD for SI and FC, and -0.6 SD for BB). Averaged together, this leads to a normal CIL subindex of +0.2 SD for 2023 (Figure 31). The normal CIL is likely the result of the relatively cold winter that occurred in Labrador and in the Eastern Arctic in 2023 and contrasts with near-record warm SSTs. This is because the summer CIL is a remnant of the previous winter's conditions that are advected from the north during the rest of the year, and its properties are isolated from the summer atmospheric warming.

	-- Seal Island section --																																																	
80	81	82	83	84	85	86	87	88	89	90	91	92	93	94	95	96	97	98	99	00	01	02	03	04	05	06	07	08	09	10	11	12	13	14	15	16	17	18	19	20	21	22	23	$\bar{x}$	sd					
CIL area (km <sup>2</sup> )	0.6	-0.4	0.9	0.6	2.0	1.6	-0.3	1.1	-0.3		2.3	1.9	0.9		-0.5	0.3	-0.6	-0.3	0.9	-0.4	-0.2	0.1	-1.0	-0.4	-0.3	-0.3	0.2	1.2	-0.8	-1.2	0.1	-0.4	0.9	1.1	-0.6	1.4	-1.6	-0.8	-1.7	-2.0	0.6	24.1	5.8							
CIL core ('C)															1.1	-0.7	-1.0	0.7	0.7	-1.0				0.8	0.7	0.0	-1.1	-0.7	1.1	1.5	-0.9	1.0	-1.5	-0.2	-0.9	-1.1	1.1	-1.0	1.5	1.5		-0.3	-1.5	0.1						
June-Aug. ave.	*	*	*	*	*	*	*	*	*	*	*	*	*	*	*	*	*	*	*	*	*	*	*	*	*	*	*	*	*	*	*	*	*	*	*	*	*	*												
	-- Bonavista section --																																																	
CIL area (km <sup>2</sup> )	-0.6	-0.5	0.3	1.8	3.1	2.2	-0.3	-0.7	0.7	0.0	2.4	2.2	0.7		-0.4	0.1	-0.5	0.1	-0.4	0.5	-0.9	-0.1	-0.2	0.0	-0.6	-0.8	-0.1	-0.8	0.5	-0.2	-2.2	-0.2	-0.6	1.9	1.0	0.7	0.5	-0.4	-1.0	-1.2	-1.5	-0.5	-0.6	23.4	7.1					
CIL core ('C)																																																		
June-Aug. ave.	*	*	*	*	*	*	*	*	*	*	*	*	*	*	*	*	*	*	*	*	*	*	*	*	*	*	*	*	*	*	*	*	*	*	*	*	*	*	*	*	*	*	*	*	*	*				
	-- Flemish Cap section --																																																	
CIL area (km <sup>2</sup> )	-0.2	-1.2	0.3	1.3	2.4	1.7	1.3	0.2	0.7	0.7	0.7	2.1	1.1		0.1	-0.2	0.9	0.1	-0.5	-0.5	0.3	0.1	-0.2	-0.8	0.2	-1.3	0.5	-0.4	1.4	-2.3	-1.9	1.0	-1.0	1.4	0.6	0.5	0.3	-0.9	-0.3	-1.2	-2.6	-0.7	0.6	20.0	4.8					
CIL core ('C)																																																		
June-Aug. ave.	*	*	*	*	*	*	*	*	*	*	*	*	*	*	*	*	*	*	*	*	*	*	*	*	*	*	*	*	*	*	*	*	*	*	*	*	*	*	*	*	*	*	*	*	*	*	*	*		

**Figure 30.** Scorecards of the cold intermediate layer (CIL) summer statistics along Seal Island, Bonavista and Flemish Cap hydrographic sections. The CIL area is defined as all water below 0°C (see black contours in Figure 27 to Figure 29), and the CIL core temperature and depth are the minimum temperature of the CIL and the depth at which it is encountered respectively. Color codes for the area and depth have been reversed (positive is blue and negative is red) because they represent cold conditions. Grayed cells indicate absence of data. When possible, the AZMP station labeled in the data files are used, but in some instances (indicated here by black dots in the last row of each table) the average June-August profile of all available casts in at 0.25° x 0.25° (lat x lon) box around the nominal station locations are used to reconstruct the section.

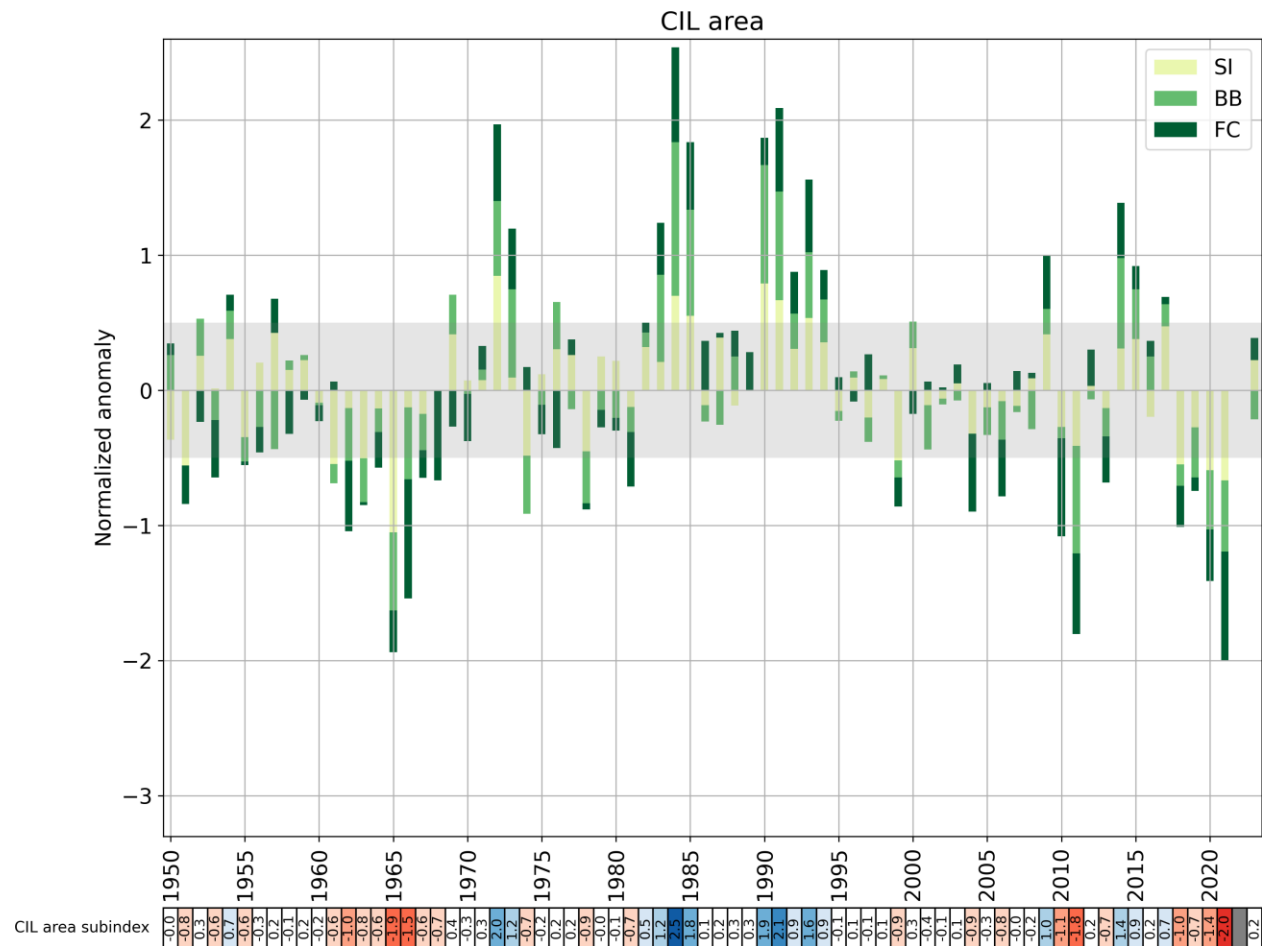


**Figure 31.** Normalized anomalies of the mean CIL area for hydrographic sections Seal Island (SI), Bonavista Bay (BB) and Flemish Cap (FC). This time series corresponds to the average of the three sections, in which the contribution of each section is represented (values for each separate section since 1980 can be found in Figure 30). The shaded area corresponds to the 1991–2020 average  $\pm 0.5$  SD, a range considered “normal”. The numerical values of this time series are reported in a color-coded scorecard at the bottom of the figure. Here negative anomalies (generally corresponding to warmer conditions) are colored red and positive anomalies blue.

## Bottom Observations in NAFO sub-areas

Canada has been conducting stratified random bottom trawl surveys in NAFO Sub-areas 2 and 3 on the NL Shelf since 1971. Areas within each division, with a selected depth range, were divided into strata, and the number of fishing stations in an individual stratum was based on an area-weighted proportional allocation (Doubleday, 1981). Temperature profiles (and salinity profiles since 1990) are available for most fishing sets in each stratum. These surveys provide large spatial-scale oceanographic data sets for the Newfoundland and Labrador Shelf. NAFO Subdivision 3Ps on the Newfoundland south coast and Divisions 3LNO on the Grand Banks are surveyed in the spring, and Divisions 2HJ off Labrador in the north, 3KL off eastern Newfoundland, and 3NO on the southern Grand Bank are surveyed in the fall. The hydrographic data collected on these surveys are routinely used to assess the spatial and temporal variability in the thermal habitat of several fish and invertebrate species. A number of products based on the data are used to characterize the oceanographic bottom habitat. Among these are contour maps of the bottom temperatures and their anomalies, the area of the bottom covered by water in various temperature ranges, etc. In addition, species-specific *thermal habitats* indices are often used in marine resource assessments for snow crab and northern shrimp.

Maps and statistics of bottom temperature and salinity observations, originally introduced by Cyr et al. (2019), are now taken from the Canadian Atlantic Bottom Observations of Temperature-Salinity (CABOTS) data product (Coyne & Cyr, 2024). This methodology is recalled here. . First, all available seasonal (April-June for spring, July-September for summer – not shown in this report –, and October-December for fall) temperature and salinity profiles are taken from the CASTS dataset (Coyne et al., 2023). A 0.05° latitude by 0.05° longitude grid is defined using GEBCO\_2023 gridded bathymetry (GEBCO Compilation Group, 2023). Cycling over each grid cell, all profile measurements taken within 25 m of the recorded depth and less than 2° distance from the point of interpolation were isolated. Profile measurements with land barriers between them and the point of interpolation were not considered. If three or more profile measurements met all of these requirements, inverse distance-weighted interpolation with adaptive power determination (Lu & Wong, 2008) was then used to determine the associated grid cell value. Lastly, bottom observations were restricted between 10m and 1,000m, that is below the surface and shallower than down the continental slope where the data coverage is much lower. This procedure was performed for all years and all seasons between 1980 and 2023, from which the climatological seasonal averages (averages over 1991-2020) were derived.

Before calculating statistics on bottom observations (e.g. mean temperature or salinity, area of the sea floor covered by a certain temperature range, etc.), missing observations on the annual maps (for example when no observations are available for a specific year) are filled with the climatology. This allows us to calculate these metrics on the same seafloor area (especially important for areas covered by a certain temperature range). We note that this method is conservative as it will tend to pull anomalies towards zero. As part of CABOTS, we provide the percentage area of each NAFO division covered so users can assess the confidence of the observations for a certain year and

season. Annual anomalies are calculated as the difference between annual observations and climatology.

### *Spring Conditions*

Maps of spring climatological temperature and salinity, together with 2023 observations and anomalies for NAFO divisions 3LNOPs, are presented in Figure 32 and Figure 33, respectively (with the center panel also showing station occupation coverage). In 2023, the coverage in 3Ps was not sufficient to derive further statistics. Since 2019, we were only capable of deriving spring bottom observations for the entire region in 2022. Due to the COVID-19 pandemic, the area was not surveyed during the spring of 2020, while in 2021 only the division 3Ps was properly sampled.

Bottom temperatures are generally colder in the northern part of the Grand Banks (3L) and warmer in the shallower southern part of the Grand Banks (3NO) and along the slopes (Figure 32, left panel). In 2023, bottom temperatures were slightly warmer than average in 3L and in the eastern part of 3Ps, and colder than average in 3NO. Spring bottom salinities in 3LNO generally range from 32 to 33 over the central Grand Bank, and from 33 to 35 closer to the shelf edge (Figure 33, left panel). In 3Ps, salinities are between 32 and 33 over shallower areas and above 34.5 in the Laurentian Channel. In 2023, salinities were close to normal in most of the Grand Banks, except slightly salty in the northeast part of 3L and slightly fresh in 3Ps and in the southwest part of 3O.

Climate indices based on normalized spring bottom temperature anomalies (mean temperature and temperature in areas shallower than 200 m), as well as the area of the sea floor covered by water above 2°C and below 0°C between 1980 and 2023 are shown in a color-coded scorecard in Figure 34. Overall, the colors visually highlight two contrasting periods of this time series: the cold period of the late 1980s / early 1990s (mostly blue cells) and the warm period of the early 2010s (mostly red cells). This warm period lasted between 2010 and 2013 (2011 being the warmest at 2.2 SD above normal in 3LNO) before returning towards to normal values between 2015 and 2019 (2014 was slightly cold). Between 2016 and 2019 the bottom area that was covered by <0°C water was also normal. While no information was available for 2020, 2021 and 2022 were the third and second warmest years in 3LNO, respectively. Bottom temperatures were however back to normal in 3LNO in 2023.

Division 3Ps bottom temperatures exhibit some similarities to those from 3LNO, with two periods of warm years, 1999–2000 and 2005–06, separated by a colder period (2003 is the coldest year on record since 1991 at -2.1 SD). With the exception of 2017 (which was normal) and 2020 (no data), all years between 2010 and 2022 were warmer than normal. 2021 and 2022 are the warmest years on record since 1980 at +2.5 SD and +2.6 SD, respectively. 2022 also established a new record for the area of the seafloor covered with water >2°C at +2.9 SD, beating the 2021 record of +2.3 SD. While spatial data suggest that the anomalies for 2023 were not as warm as in previous years (Figure 33), bottom statistics were omitted for 3Ps because the coverage was very sparse in the deeper portion of the Division (Figure 34).

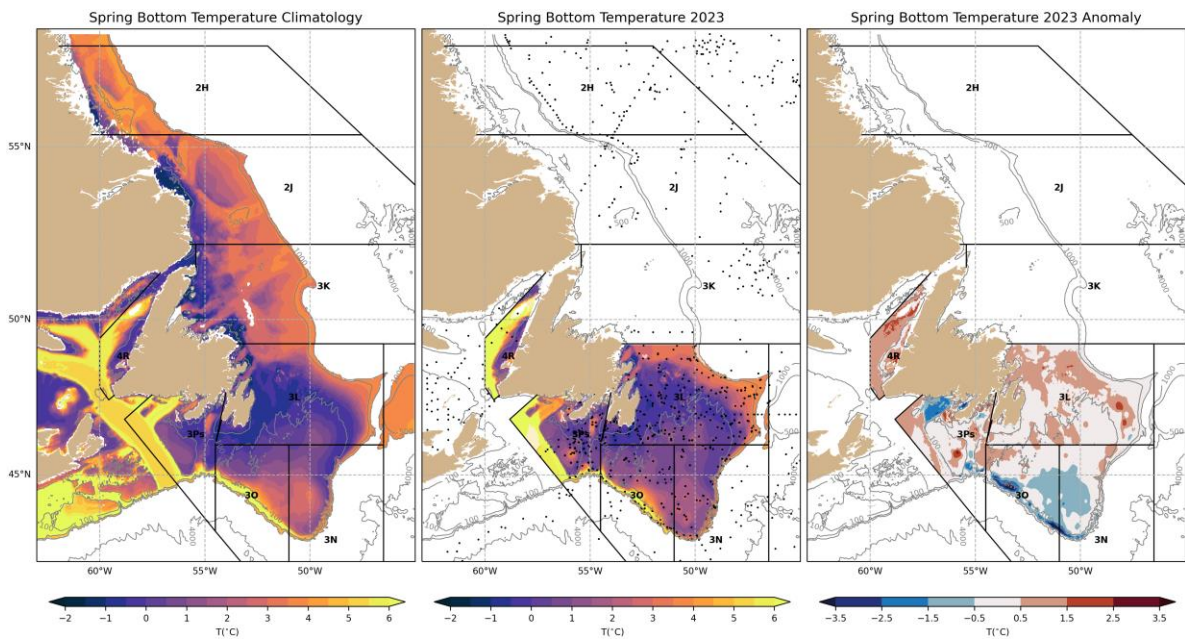


**Figure 32.** Maps of the mean 1991-2020 spring bottom temperature (left), and spring 2023 bottom temperature (center) and anomalies (right) for NAFO Divisions 3LNOPs only. The location of observations used to derive the temperature field is shown as black dots in the center panel. When applicable, the portions of the shelf missing bottom temperatures were filled with the climatology (see methodology) and are left semi-transparent.

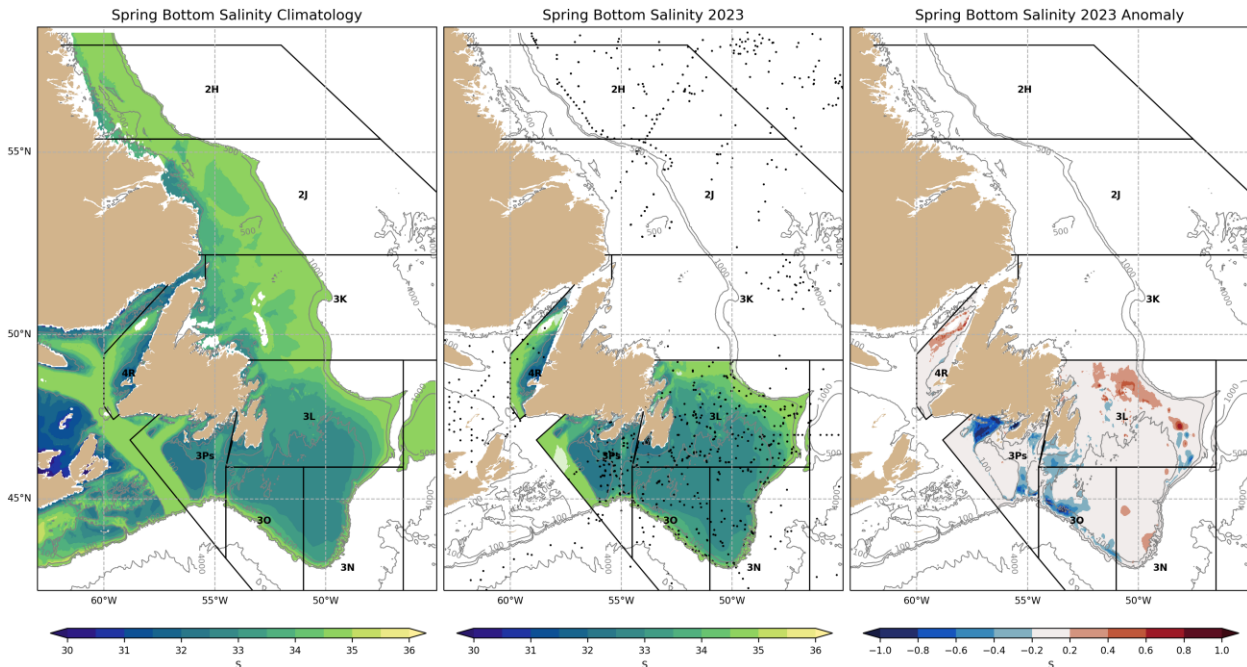


**Figure 33.** Maps of the mean 1991-2020 spring bottom salinity (left), and spring 2023 bottom salinity (center) and anomalies (right) for NAFO Divisions 3LNOPs only. The location of observations used to derive the salinity field is shown as black dots in the center panel. When applicable, the portions of the shelf missing bottom salinities were filled with the climatology (see methodology) and are left semi-transparent.

**Figure 34.** Scorecards of normalized spring bottom temperature anomalies for 3LNO and 3Ps.

### *Fall Conditions*

Maps of fall climatological temperature and salinity, together with 2023 observations and anomalies for NAFO Divisions 2HJ3KLNO, are presented in Figure 35 and Figure 36, respectively (see center panel for station occupation coverage). Bottom temperatures are generally cold ( $<0^{\circ}\text{C}$ ) in shallow areas of 2HJ3KLNO and warmer on the slopes and the different troughs, and on the southern areas of the Grand Banks that lie at depths shallower than the CIL (e.g.  $<50\text{m}$ ). In 2023, anomalies are generally cold along the Labrador coast where the CIL hugs the seafloor, as well as near the tail of the Grand Banks (Division 3N). Scattered areas of warmer anomalies are found near the NL shelf break and in Division 30 of the Grand Banks.

Bottom salinities in divisions 2HJ and 3K generally display an inshore-offshore gradient between  $<33$  close to the coast and 34 to 35 at the shelf edge (Figure 36, left panel). The Grand Banks (3LNO) bottom salinities range from  $<33$  to 35, with the lowest values on the southeast shoal. In 2023 the bottom salinities were close to normal in most of the region, although followed a similar patterns as the temperature with some fresh anomalies near the coast and salty anomalies near the shelf break.

Normalized bottom temperature anomalies (mean temperature and temperature in areas shallower than 200 m), as well as area of the sea floor covered by water above  $2^{\circ}\text{C}$  and below  $1^{\circ}\text{C}$  between 1980 and 2022 are shown in a color-coded scorecard in Figure 37. A clear cold period is visible from the early 1980s to the mid-1990s, with the coldest anomalies reached in NAFO Divisions 2J and 3K. This was followed by a warmer period peaking in 2010 and 2011, the warmest years on records for these divisions. After a slight return to normal-to-cold anomalies between 2012 and 2017, bottom temperatures have been generally above or close to normal since. In 2023, bottom temperatures were above average in 2H with the third warmest anomaly (+1.7 SD) after 2010 and 2011 (tied at +1.8 SD). While slightly above normal in 3K (+0.7 SD), bottom temperatures were normal in 2J and 3LNO.

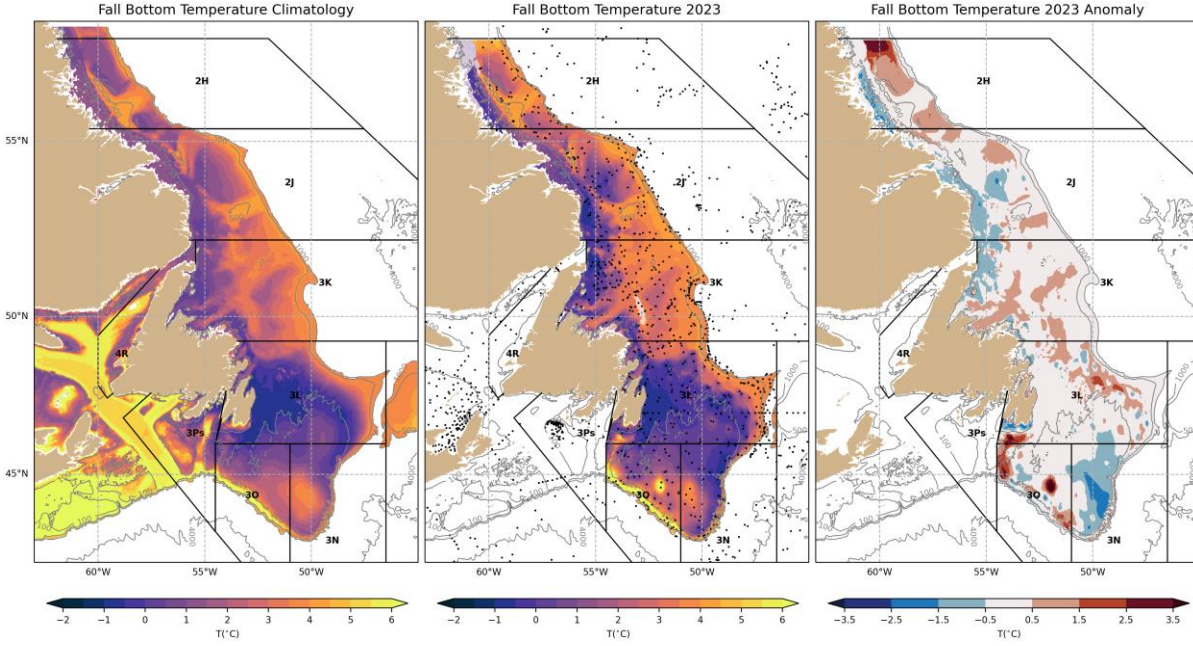


**Figure 35.** Maps of the mean 1991-2020 fall bottom temperature (left), and fall 2023 bottom temperature (center) and anomalies (right) for NAFO Divisions 2HJ3KLNO only. The location of observations used to derive the temperature field is shown as black dots in the center panel. When applicable, the portions of the shelf missing bottom temperatures were filled with the climatology (see methodology) and are left semi-transparent

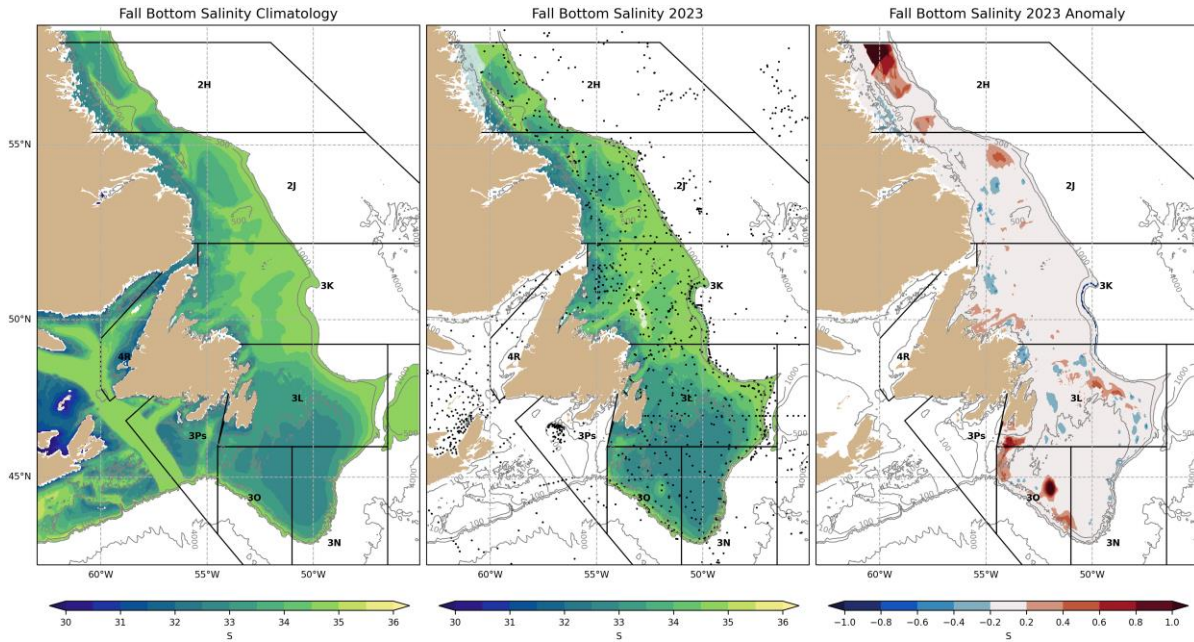


**Figure 36.** Maps of the mean 1991-2020 fall bottom salinity (left), and fall 2023 bottom salinity (center) and anomalies (right) for NAFO Divisions 2HJ3KLNO only. The location of observations used to derive the salinity field is shown as black dots in the center panel. When applicable, the portions of the shelf missing bottom salinities were filled with the climatology (see methodology) and are left semi-transparent

-- NAFO division 2H --																																														
80	81	82	83	84	85	86	87	88	89	90	91	92	93	94	95	96	97	98	99	00	01	02	03	04	05	06	07	08	09	10	11	12	13	14	15	16	17	18	19	20	21	22	23	$\bar{x}$	sd	
T <sub>bot</sub>	-0.5	-0.1	-3.0			-1.8			-2.3					0.1	0.0	0.2	-1.3		1.2		-0.1		0.4	1.8	1.8	0.6	-0.3	-0.6	-0.4	-0.5	-1.3	0.1	0.4	0.4	1.0	0.1	1.7	2.2	0.4							
T <sub>bot&lt;200m</sub>	0.2	0.6	-3.1			-1.0			-2.2					0.3	-0.1	0.1	-1.5		1.0		-0.3		-0.1	1.7	1.8	0.3	-0.7	-0.5	0.0	-0.2	-1.2	0.1	0.9	0.7	1.1	0.7	2.1	1.1	0.5							
Area > 2°C	-1.6	-0.7	-1.7			-1.9			-1.7					0.6	-0.3	0.1	-1.0		1.3		-0.2		-0.3	1.9	2.1	-0.2	-0.5	-0.8	-0.7	-0.7	-0.9	0.1	0.2	1.1	0.8	-1.3	1.2	27.1	7.1							
Area < 1°C	-0.8	1.8	2.3			1.4			2.2					-0.3	0.2	-0.4	2.0		-0.4		0.2		-0.4	-1.2	-1.4	-0.7	0.7	0.2	-0.1	-0.2	1.6	-0.2	-1.3	-0.4	-1.2	1.9	-1.5	15.2	8.2							
% Cov	78	93	64	92	13	80	61	83	52	14	13	91	79	13	15	0	39	98	98	98	17	97	11	16	98	18	98	13	98	20	98	98	98	98	94	91	98	98	98	97	98	93	85			
-- NAFO division 2J --																																														
T <sub>bot</sub>	-1.0	-0.3	1.9	1.9	-2.9	-2.5	-0.4	2.1	-0.5	-1.4	-1.9	1.5	-2.3	-2.3	-1.6	0.3	0.0	0.2	0.4	-0.6	0.3	-0.4	0.6	1.1	1.0	-0.2	1.0	-0.1	0.0	1.8	1.7	0.1	0.0	-0.5	-0.5	0.2	-0.5	0.6	0.9	0.1	1.0	0.1	0.2	2.2	0.5	
T <sub>bot&lt;200m</sub>	-0.7	-0.1	-1.4	-2.1	-2.8	-1.9	-0.2	-1.9	-0.3	-1.0	-1.4	-1.5	-2.1	-2.1	-1.4	0.5	-0.1	0.1	0.4	-0.5	0.3	-0.4	0.5	0.9	1.1	-0.5	0.9	-0.1	-0.1	1.8	1.9	0.0	-0.2	-0.8	-0.5	0.7	-0.5	0.4	1.4	0.1	1.0	0.0	-0.2	1.1	0.6	
Area > 2°C	-0.9	-0.5	-1.9	-1.4	-2.1	-2.2	0.0	-1.9	-0.6	-1.5	-1.9	-1.3	-1.8	-2.0	-1.4	0.8	0.3	0.0	-0.2	-0.7	0.2	-0.6	0.4	1.0	1.4	-0.2	1.3	-0.7	-0.1	1.9	2.0	-0.5	-0.3	-0.6	-0.4	0.3	-0.5	0.5	1.2	0.2	0.9	-0.6	0.2	56.8	14.3	
Area < 1°C	0.7	-0.1	2.1	1.9	2.6	2.0	0.2	2.0	0.2	1.5	2.0	1.8	2.1	2.1	1.5	-0.4	0.2	-0.3	-1.0	0.3	-0.4	0.3	-0.6	-0.9	-1.1	0.4	-0.9	0.2	0.4	-1.4	-1.4	-0.1	0.2	0.9	0.6	-1.0	0.6	-0.6	-1.4	-0.1	0.4	0.1	22.8	16.2		
% Cov	96	92	93	96	93	94	94	93	94	96	95	95	96	71	96	97	97	97	95	97	95	96	97	96	97	96	97	97	97	97	97	97	97	97	97	86	97									
-- NAFO division 3K --																																														
T <sub>bot</sub>	-0.6	-0.4	-1.4	-1.4	-1.8	-2.6	-0.6	-1.5	-0.9	-1.3	-2.2	-1.2	-2.1	-2.1	-2.0	-1.4	-0.3	0.4	0.3	0.6	0.2	-0.3	0.0	0.7	1.2	0.7	0.0	0.7	0.5	-0.1	1.4	2.1	0.2	0.3	-0.4	-0.2	-0.5	-0.8	0.7	0.6	0.6	1.3	0.7	0.7	2.6	0.4
T <sub>bot&lt;200m</sub>	-0.5	-0.1	-1.2	-1.8	-2.3	-2.1	0.0	-1.7	-0.6	-0.8	-1.7	-1.5	-1.8	-1.8	-1.5	-0.4	0.5	-0.2	-0.6	0.2	-0.8	-0.2	0.1	0.4	0.8	0.7	-0.4	1.0	-0.7	-0.3	1.9	2.0	-0.2	-0.3	-1.0	-0.1	0.9	-0.3	1.1	1.3	1.2	1.5	-0.1	-0.7	0.5	0.6
Area > 2°C	-0.6	-0.2	1.8	-1.4	-1.8	-2.6	-0.4	-1.4	-1.3	-1.4	-2.0	-1.0	-1.8	-1.9	-2.1	-1.6	-0.2	0.7	0.6	0.6	0.4	-0.3	-0.1	0.0	0.9	1.0	0.1	0.6	0.5	-0.7	1.6	1.5	0.0	0.3	-0.5	0.0	-0.8	-0.8	1.2	0.9	1.0	1.2	0.6	0.8	78.3	12.8
Area < 1°C	0.4	0.2	0.7	1.4	1.4	2.4	-0.3	0.8	0.0	0.3	2.8	1.3	2.0	2.4	2.1	0.3	-0.6	0.1	0.2	-0.1	0.3	0.0	-0.4	-0.5	-0.9	-0.9	0.5	-1.0	0.2	0.2	-1.2	-1.4	0.4	-0.2	0.5	0.1	-0.7	0.7	-1.1	-1.3	-1.3	-1.2	0.0	0.0	12.9	9.1
% Cov	89	95	83	91	96	93	96	91	92	97	100	99	99	98	96	99	99	99	99	98	98	94	99	99	99	99	99	99	99	99	99	99	99	99	99	99	99	99	99	99	99	99				
-- NAFO division 3LNO --																																														
T <sub>bot</sub>	0.5	-0.5	-1.4	-1.0	-1.8	-2.2	-0.2	-1.1	-0.8	-1.5	-1.3	-1.4	-1.2	-2.2	-1.8	-0.1	-0.5	-0.3	0.8	1.8	-0.2	0.1	0.0	-0.2	0.4	0.3	0.4	-0.1	-0.5	0.8	1.7	2.2	0.4	-0.2	-0.4	0.2	0.1	-0.9	-0.2	-0.4	1.6	0.9	0.3	1.5	0.5	
T <sub>bot&lt;200m</sub>	0.9	-0.2	-1.2	-0.7	-1.6	-1.9	0.2	-0.8	-0.6	-1.2	-1.0	-1.3	-1.0	-2.0	-1.7	0.1	-0.4	-0.3	0.9	1.9	-0.3	0.2	0.0	-0.3	0.2	0.3	0.5	-0.3	-0.8	0.8	1.9	2.2	0.4	-0.3	-0.5	0.1	0.2	-1.0	-0.3	-0.6	1.5	0.8	0.2	1.1	0.5	
Area > 2°C	0.0	-0.7	1.9	-1.0	-2.2	-2.5	0.0	-1.5	-1.0	-2.0	-1.7	-1.2	-1.1	-2.4	-1.9	-0.1	-0.8	-0.1	0.8	2.4	0.2	0.4	0.0	0.0	0.1	0.3	0.2	-0.1	-0.3	0.6	1.6	1.7	0.3	-0.5	-0.3	0.3	0.1	-0.7	-0.5	-0.3	1.5	0.8	0.2	94.5	24.2	
Area < 1°C	0.1	-0.1	0.5	1.1	1.2	1.4	-0.1	0.3	0.5	1.0	0.8	1.6	1.3	1.9	1.9	-0.1	0.3	0.5	-0.4	-0.9	0.7	-0.1	-0.6	0.1	-1.1	-0.7	-1.1	-0.1	0.6	-0.3	-1.4	-2.3	0.0	-0.3	0.5	-0.1	0.3	1.2	-0.7	0.3	-1.3	-1.0	-0.5	76.0	29.5	
% Cov	90	91	78	91	92	93	93	93	94	91	95	96	96	98	97	97	98	98	99	99	99	99	99	99	99	99	99	99	99	99	99	99	99	99	99	99	99	99	99	99	99	99	99	99		

**Figure 37.** Scorecards of normalized fall bottom temperature anomalies for 2H, 2J, 3K and 3LNO.

## **Ocean Conditions on the Scotian Shelf and Gulf of Maine (NAFO Sub-area 4)**

### **Coastal Temperatures and Salinities**

Coastal sea surface temperatures have been collected at Halifax (Nova Scotia) and St. Andrews (New Brunswick) since the 1920s (Figure 38). In 2023 the SST anomaly was +1.6°C (+2.7 SD) for Halifax, an increase of 0.2°C from 2022 and the 3<sup>rd</sup> warmest temperature in the record. In 2023, St. Andrews had an anomaly of +1.2°C (+1.8 SD) and the third warmest temperature in the record, a decrease of 0.3°C from 2022.

Temperature and salinity measurements through the water column, for the most part sampled monthly, have been taken since 1924 at Prince 5, at the entrance to the Bay of Fundy (Figure 38). It is the longest continuously operating hydrographic monitoring site in eastern Canada. Its waters are generally well-mixed from the surface to the bottom (90 m). The depth-averaged (0-90 m) temperature, salinity and density anomaly time series are shown in panels C-E. In 2023, the annual temperature anomaly was +1.2°C (+1.6 SD) and the salinity anomaly was -0.3 (-1.6 SD). These represent changes of -0.2°C and -0.6 from the 2022 values.

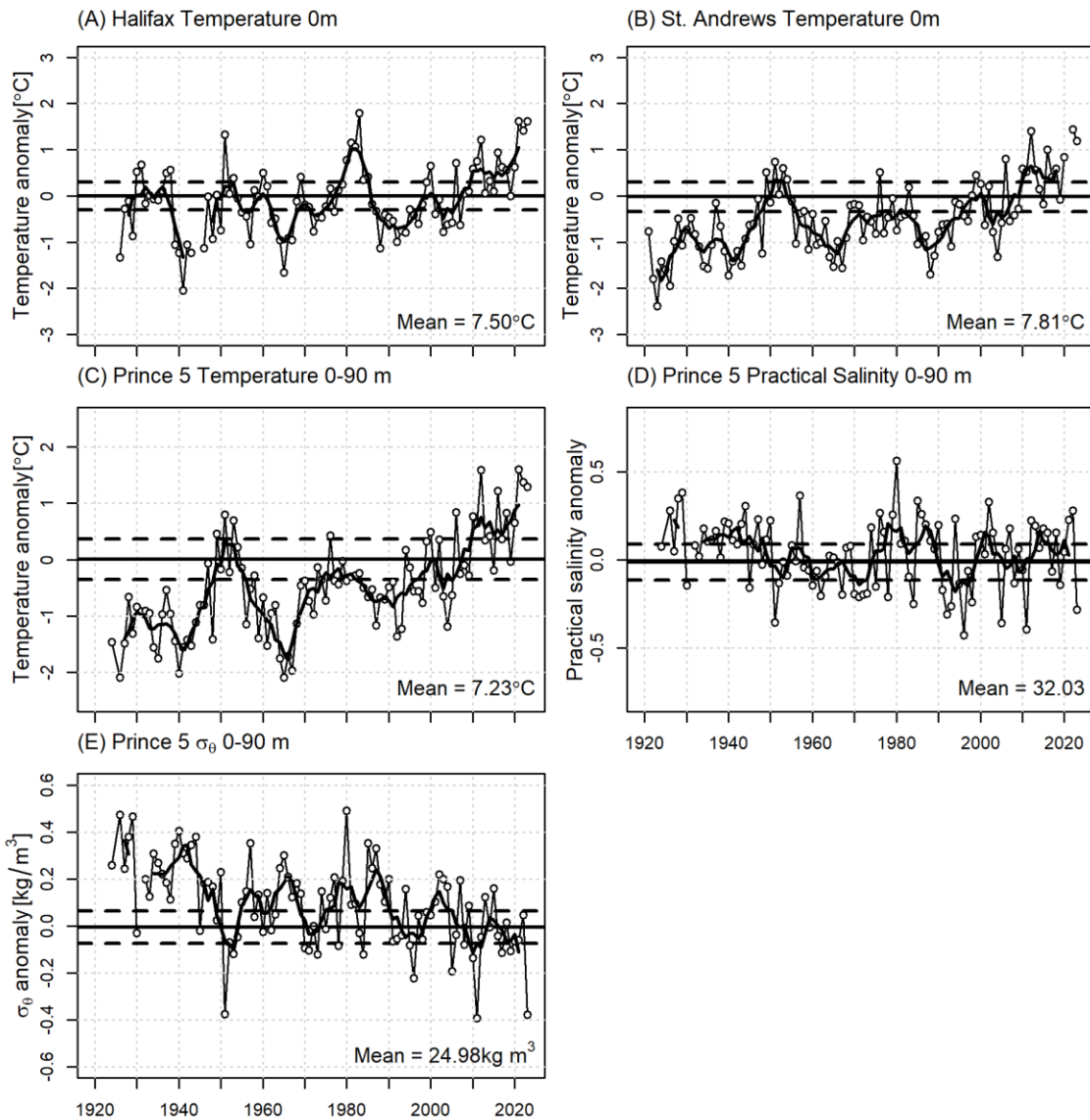


**Figure 38.** The annual surface temperature anomalies (dotted line with circles) and their 5-year running means (heavy black line) for (A) Halifax Harbour and (B) St. Andrews; annual depth-averaged (0-90 m) (C) Temperature, (D) salinity and (E) density anomalies for the Prince 5 monitoring station at the mouth of the Bay of Fundy. Horizontal dashed lines are the 1991-2020 climatological average  $\pm 0.5$  SD.

## Temperatures from Long-term Stations

Drinkwater & Trites (1987) tabulated monthly mean temperatures and salinities from available bottle data for areas on the Scotian Shelf and in the eastern Gulf of Maine that generally correspond to topographic features such as banks and basins. Petrie et al. (1996) updated their report using these same areas and all available hydrographic data. An updated time series of annual mean and filtered (5 year running means) temperature anomalies at selected depths for six areas (see map Figure 39) is presented in Figure 40. The Cabot Strait temperatures represent a mix of Labrador Current Water and Warm Slope Water (e.g., Gilbert et al., 2005) entering the Gulf of St. Lawrence along Laurentian Channel; the Misaine Bank series characterizes the colder near bottom temperatures on the Eastern Scotian Shelf by either inshore Labrador Current water or cold-intermediate layer water from the Gulf of St. Lawrence (Dever et al., 2016); the deep Emerald Basin anomalies represent the Slope Water intrusions onto the Shelf that are subsequently trapped in the deep inner basins (note the large anomaly “events” in Figure 40C , for example, around 1980 and 2009 indicative of pulse of Labrador Slope Water); the Lurcher Shoals observations define the ocean climate on the southwest Scotian Shelf and the shallow waters entering the Gulf of Maine via the Nova Scotia Current; last, the Georges Basin series indicates the slope waters entering the Gulf of Maine through the Northeast Channel. Annual anomalies are based on the averages of monthly values; however, observations may not be available for each month in each area. For Cabot Strait, Misaine Bank, Emerald Basin, Georges Basin, eastern Georges Bank and Lurcher Shoals, 2023 annual anomalies are based on observations from two, three, three, two, four and five months, respectively.

In 2023, the annual anomaly was +1.4°C (+2.2 SD) for Cabot Strait at 200-300 m (the third largest anomaly; the last five years were the warmest). For the shallow Misaine Bank on the eastern Scotian Shelf, the annual anomaly was +0.3°C (+0.5 SD) at 100 m. For the deep basins on the central Scotian Shelf and Gulf of Maine, the 2023 anomalies were +1.3°C (+1.5 SD) for Emerald Basin at 250 m (2<sup>nd</sup> highest value, 2019 was a record high; the last eight years were the warmest in the record) and +0.2°C (+0.3 SD) for Georges Basin at 200 m ( 2018 the warmest in the record). For the shallow banks in western Nova Scotia, the anomalies were +0.4°C (+0.6 SD) for eastern Georges Bank at 50 m and +0.7°C (+0.7 SD) for Lurcher Shoals at 50 m. These values correspond to changes of -0.3°C, -1.5°C, +0.4°C, -0.9°C, -1.0°C, and -2.1°C, from the 2022 values.

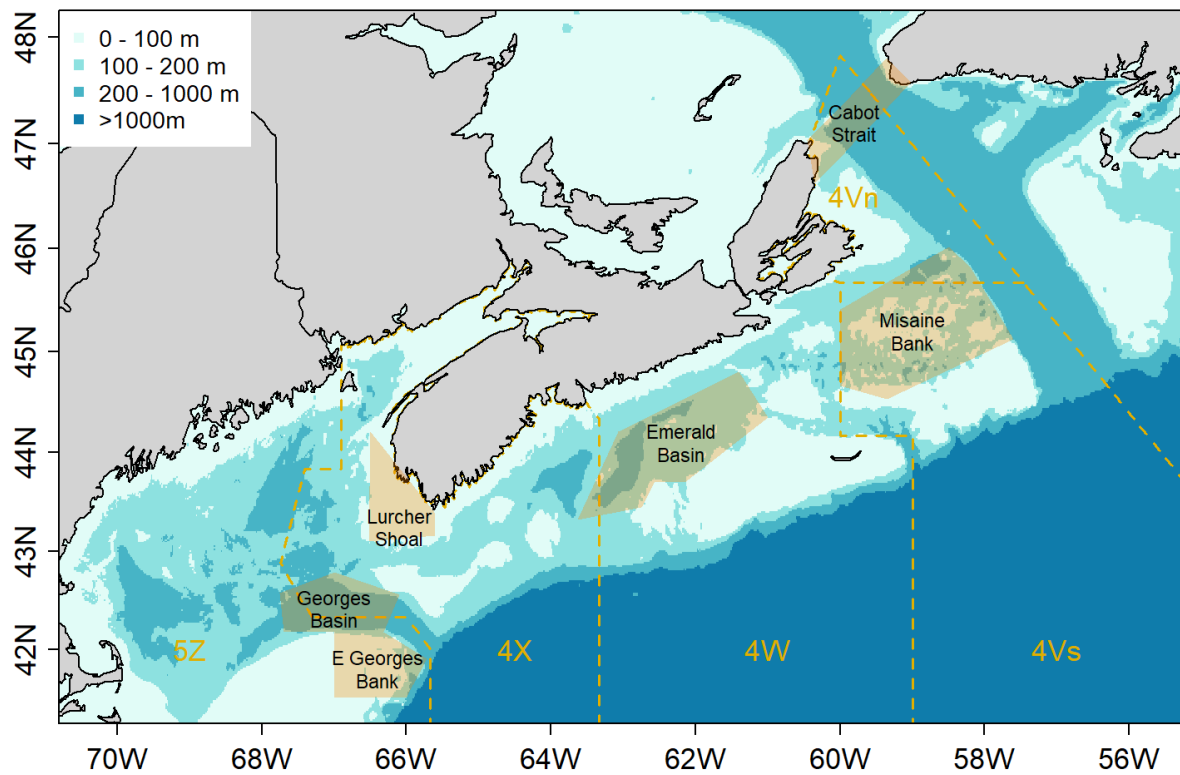


**Figure 39.** Areas on the Scotian Shelf and eastern Gulf of Maine used to characterize the different water masses.

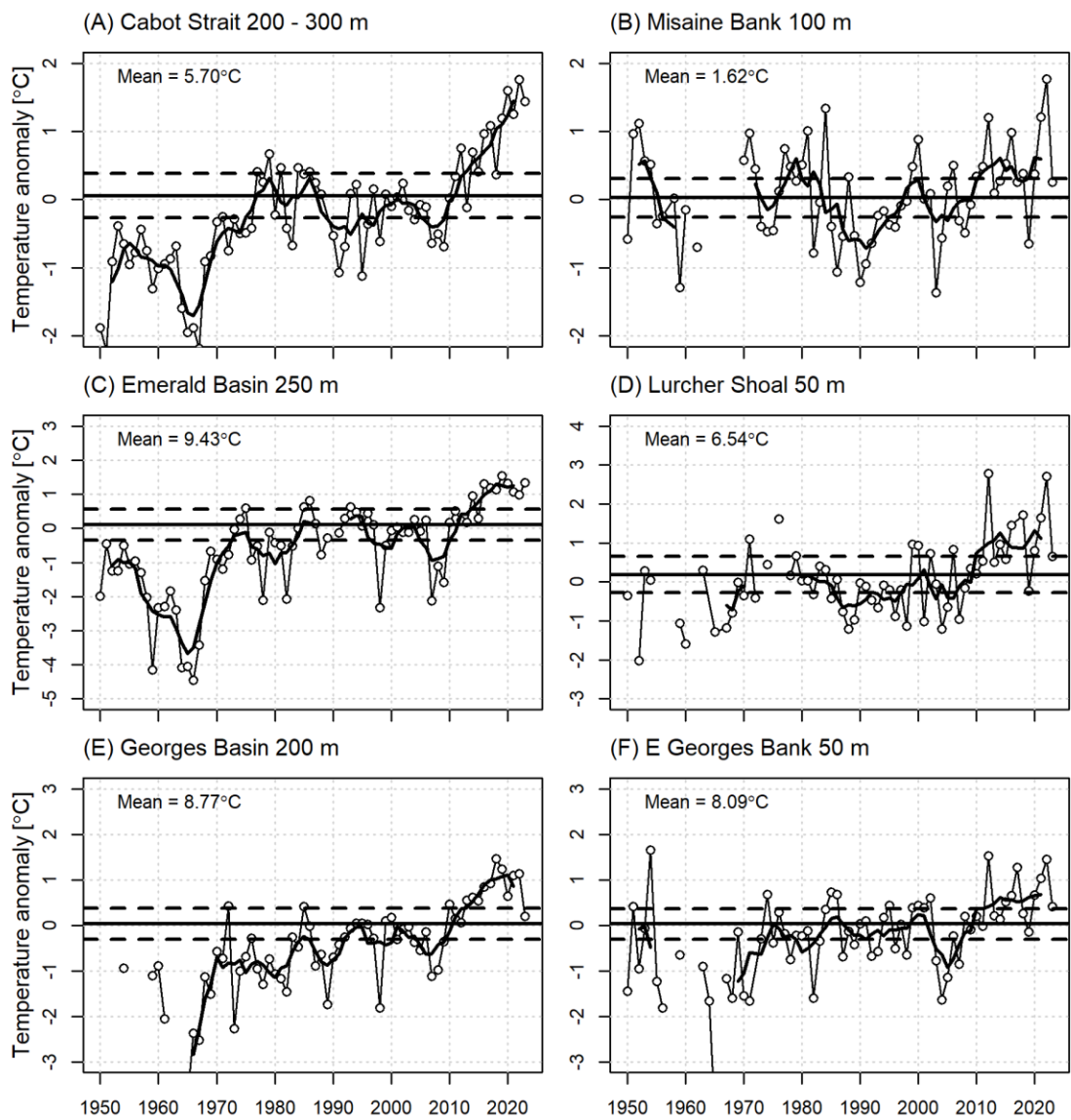


**Figure 40.** The annual mean temperature anomaly time series (dotted line with circles) and the 5 year running mean filtered anomalies (heavy solid line) on the Scotian Shelf and in the Gulf of Maine at (A) Cabot Strait (200-300 m); (B) Misaine Bank (100 m); (C) Emerald Basin (250 m); (D) Lurcher Shoals (50 m); and Georges Basin (200 m) (see Figure 39). Horizontal dashed lines are the climatological average  $\pm 0.5$  SD.

## Temperatures during the Summer Groundfish Surveys

The broadest spatial temperature and salinity coverage of the Scotian Shelf is obtained during DFO's annual summer groundfish survey which covers the Scotian Shelf from Cabot Strait to the Bay of Fundy. The deep water boundary of the survey is marked roughly by the 200 m isobath along the shelf break at the Laurentian Channel, at the outer Scotian Shelf, and at the Northeast Channel into the Gulf of Maine towards the Bay of Fundy. In 2023, the survey covered the mouth of the Bay of Fundy, eastern Georges Bank and east on the Scotian Shelf to Cabot Strait(NAFO Divisions 5Ze, 4X 4W, 4Vs and 4Vn).

The temperatures from the survey were combined and interpolated onto a 0.2° by 0.2° latitude-longitude grid using an objective analysis procedure known as Barnes interpolation. Temperatures were optimally estimated for at the standard depths (e.g. 0 m, 10 m, 20 m, etc.) and for near the bottom. Only the bottom temperatures anomalies averaged over the NAFO Divisions are presented here using the 1991-2020 climatology (Figure 41).

The volume of the Cold Intermediate Layer (CIL), defined as waters with temperatures <4°C, was estimated from the full depth CTD profiles for the region from Cabot Strait to Cape Sable (Figure 39). There is considerable variation in the volume of the CIL from 1998 until 2009 (Figure 42). The smallest volume was in 2022 where , there almost no water less than 4°C. In 2023, the CIL volume was near normal. The low-frequency variability of the area-weighted average minimum temperature mirrors the CIL volume.

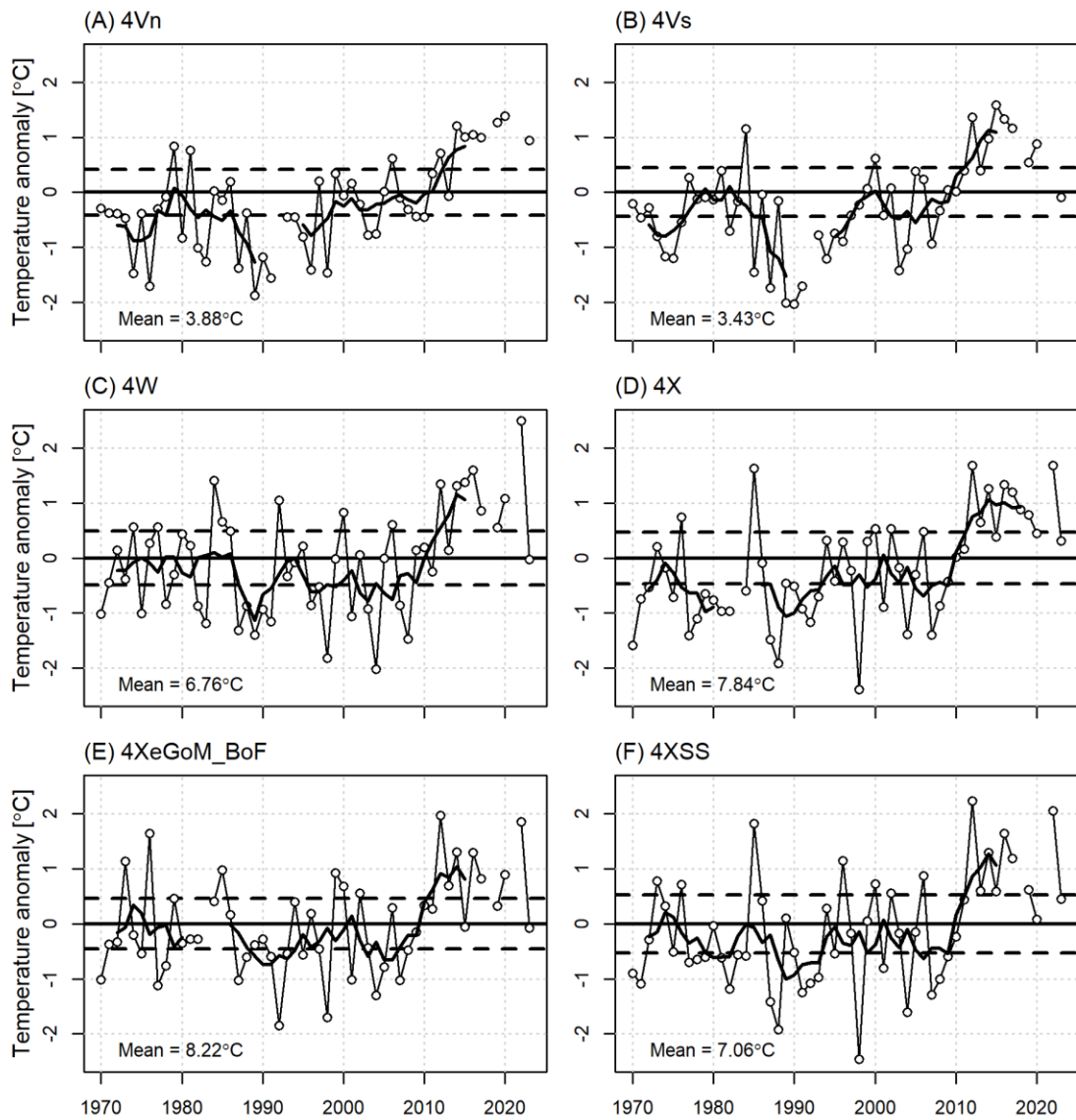


**Figure 41.** Time series of July bottom temperature anomalies (dashed lines with circles) and 5 year running mean filtered series (heavy line) for areas (A) 4Vn, (B) 4Vs, (C) 4W and (D) 4X. The solid horizontal line is the 1991-2020 mean and dashed lines represent  $\pm 0.5$  SD.

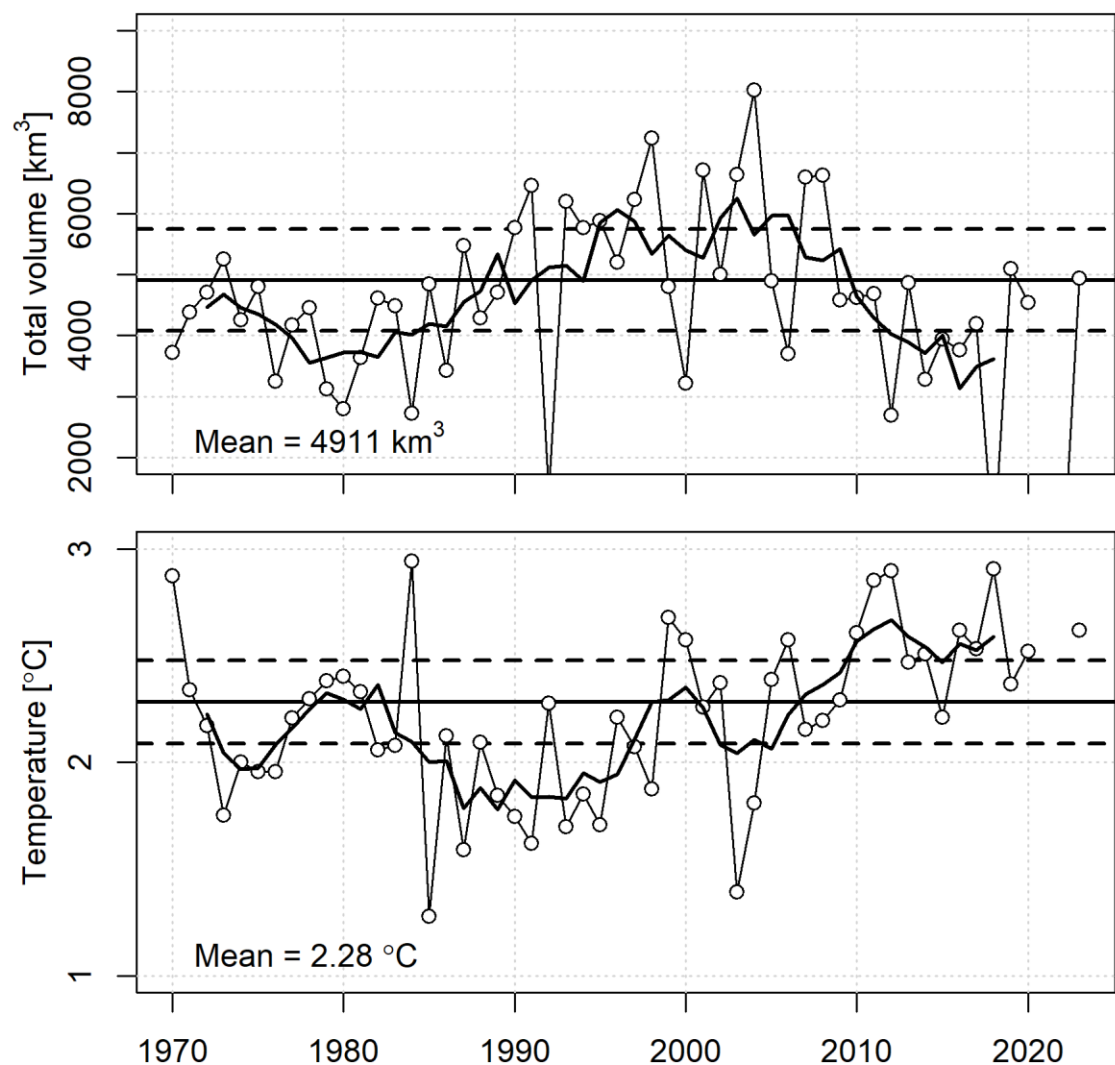


**Figure 42.** Time series of the Cold Intermediate Layer (CIL, defined as waters with  $T < 4^{\circ}\text{C}$ ) volume on the Scotian Shelf based on the July ecosystem survey. The solid horizontal line is the 1991–2010 mean CIL volume and dashed lines represent  $\pm 0.5$  SD.

## Density Stratification

Stratification of the near surface layer influences physical and biological processes in the ocean such as vertical mixing, the ocean's response to wind forcing, the timing of the spring bloom, vertical nutrient fluxes and plankton distribution. Under increased stratification, there is a tendency for more primary production to be recycled within the upper mixed layer and hence less available for the deeper layers. The variability in stratification by calculating the density ( $\sigma_t$ ) difference between the near-surface and 50 m was examined based on monthly mean density profiles on the Scotian Shelf. The long-term monthly mean density gradients for 1991-2020 were estimated; these were subtracted from the individual monthly values to obtain monthly anomalies. Annual anomalies were estimated by averaging all available monthly anomalies within a calendar year. This could be misleading if, in a particular year, most data were collected in months when stratification was weak, while in another year, sampling occurred when stratification was strong. However, initial results, using normalized monthly anomalies, were qualitatively similar to the plots presented here. The annual anomalies and their 5-year running means were for the Scotian Shelf. A value of  $0.01 \text{ kg m}^{-3}/\text{m}$  represents a difference of  $0.5 \text{ kg m}^{-3}$  over 50 m.

The dominant feature is the period from about 1950 to 1990 that featured generally below average stratification in contrast to the past 25 years that is characterized by above normal values (Figure 43). Since 1948, there has been an increase in stratification on the Scotian Shelf, resulting in a change in the 0-50 m density difference of  $0.38 \text{ kg m}^{-3}$  over 50 years. This change in mean stratification is due mainly to a decrease in the surface density, composed of equally of warming and freshening.

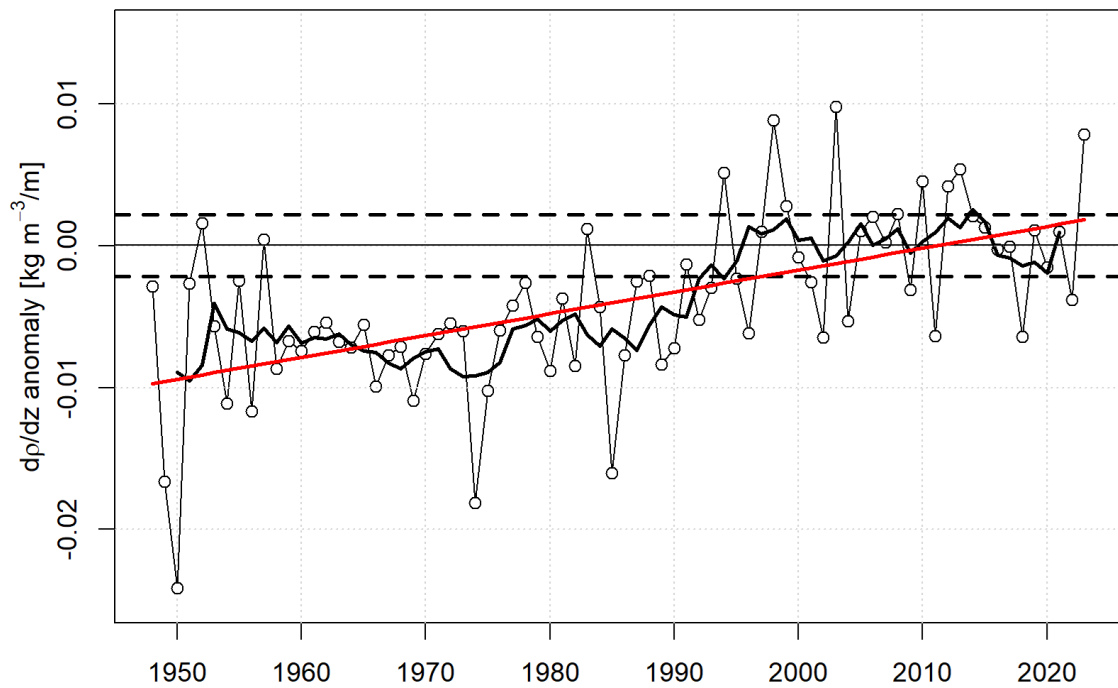


**Figure 43.** The mean annual anomaly (dashed line with circles) and 5-yr running mean (heavy solid line) of the stratification index (0-50 m density gradient) averaged over the Scotian Shelf. The solid horizontal line is the 1991-2020 mean stratification and dashed lines represent  $\pm 0.5$  SD. The linear trend (red line) shows a change in the 0-50 m density difference of  $0.38 \text{ kg m}^{-3}$  over 50 years.

## Labrador Current Variability in NAFO Sub-area 2,3 and 4

The circulation in the NL region is dominated by the south-eastward flowing Labrador Current system, which floods the eastern shelf areas with cold and relatively fresh subpolar waters (Figure 44). This flow can significantly affect physical and biological environments off Atlantic Canada on seasonal and interannual time scales. On the shelf, the Coastal Labrador Current (Florindo-López et al., 2020) originates near the northern tip of Labrador where the outflow from the Hudson Strait combines with the eastern Baffin Island Current and flows southeastward along the Labrador coast. During its southward journey on the on the Labrador shelf, it is strongly influenced by the seabed topography, following the various cross shelf saddles and inshore troughs. A separate offshore branch of the Labrador Current flows southeastward along the western boundary of the Labrador Sea. This current is part of the large-scale Northwest Atlantic circulation consisting of the West Greenland Current that flows northward along the West Coast of Greenland, a branch of which turns westward and crosses the northern Labrador Sea forming the northern section of the Northwest Atlantic subpolar gyre.

Further south, near the northern Grand Banks, the Coastal Labrador Current becomes broader and less defined. In this region, most of the inshore flow combines with the offshore branch and flows eastward, with a portion of the combined flow following the bathymetry southward around the southeast Grand Bank, and the remainder continuing east and southward around the Flemish Cap (Figure 44). A smaller inshore component flows through the Avalon Channel and around the Avalon Peninsula, and then westward along the Newfoundland south coast. Off the southern Grand Bank the offshore branch flows westward along the continental slope, some of which flows into the Laurentian Channel and eventually onto the Scotian shelf. This extension of the Labrador Current on the Scotian shelf is referred to as the Scotian shelf break current. Additionally, there are strong interactions between the offshore branch of the Labrador Current and large-scale circulation. A significant portion of the offshore branch combines with the North Atlantic Current and forms the southern section of the subpolar gyre. Further east, the Flemish Cap is located in the confluence zone of subpolar and subtropical western boundary currents of the North Atlantic. Labrador Current water flows to the east along the northern slopes of the Cap and south around the eastern slopes of the Cap. In the eastern Flemish Pass, warmer high salinity North Atlantic Current water flows northward contributing to a topographically induced anticyclonic gyre over the central portion of the Cap.

Satellite altimetry data are used over a large spatial area to calculate the annual-mean anomalies of the Labrador Current transport (Han et al., 2014). A total of nine cross-slope satellite altimetry tracks are used to cover the Labrador Current on the NL shelf break from approximately 47°N to 58°N latitude (Figure 44). Similarly, five tracks from approximately 55°W to 65°W longitude are used for the Scotian shelf break current. The nominal cross-slope depth ranges used for calculating the transport are from 200 to 3,000 m isobaths over the NL shelf break and from 200 to 2,000 m isobaths over the Scotian shelf break.

An empirical orthogonal function (EOF) analysis of the annual-mean transport anomalies was carried out. An index was developed from the time series of the first EOF mode and normalized by dividing the time series by its SD. The mean transport values are provided based on ocean circulation model output along the NL shelf break (Han et al., 2008) and over the Scotian shelf break (Han et al., 1997). The mean transport of the Labrador Current along the NL shelf break is 13 Sv (1 Sv = 106 m<sup>3</sup> s<sup>-1</sup>) with a SD of 1.4 Sv, and the mean transport of the Scotian shelf break current is 0.6 Sv with a SD of 0.3 Sv. The mean transport values will be updated as new model output becomes available. The SD values will be updated as knowledge on nominal depth improves.

The Labrador Current transport along the NL shelf break was out of phase with that of the Scotian shelf break current for most of the years over 1993–2023 (Figure 45). The transport over the NL shelf break was strong in the early- and mid-1990s, weak in the mid-2000s and early-2010s, and became strong again in late 2010s. In contrast, the transport over the Scotian shelf break fluctuated in a nearly opposite way. The Labrador Current transport index was positively and negatively correlated with the winter NAO index over the NL and Scotian shelves breaks, respectively.

In 2023 the annual-mean transport of the Labrador Current over the Labrador and northeastern Newfoundland Slope was above normal for an the eight consecutive year at +1.1 SD. The transport on the Scotian Slope in 2023 was above normal for the first time in 10 years at +1.4 SD. The last time the transport in both regions was more than 1 SD above normal was in 1996. A positive transport on the Scotian slope indicates that fresher and colder Labrador Slope water may reach the Scotian shelf and the mouth of the Laurentian Channel.

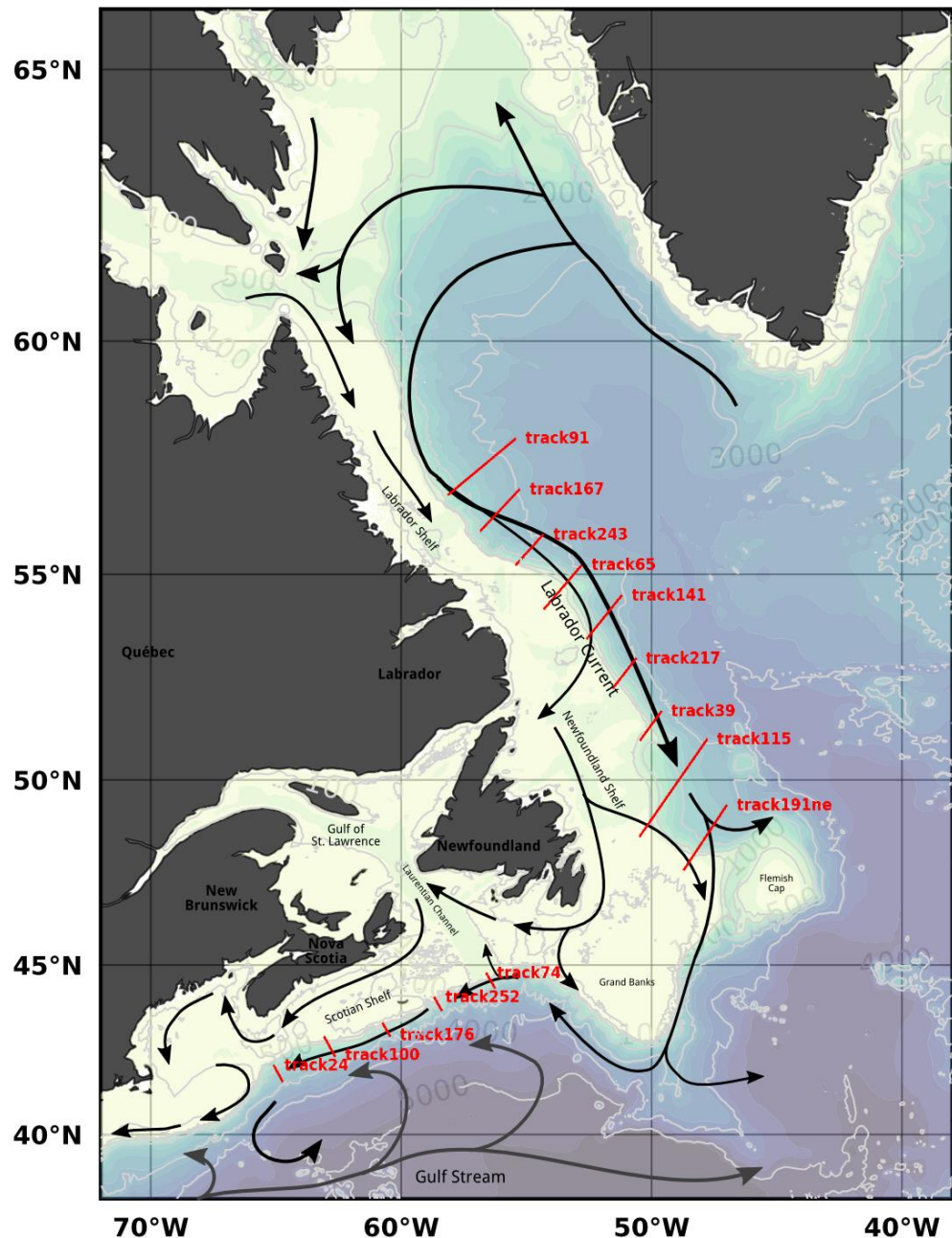


**Figure 44.** Map showing the Northwest Atlantic bottom topography (depth contour values in light gray) and schematic flow patterns (arrows). The transport is calculated across the cross-slope sections (red lines) identified by their satellite ground tracks numbers. The series of northern tracks are used for the Labrador Current calculation on the Newfoundland and Labrador slope, while the series of tracks in the south are used for the Shelf Break Current transport on the Scotian Shelf slope.

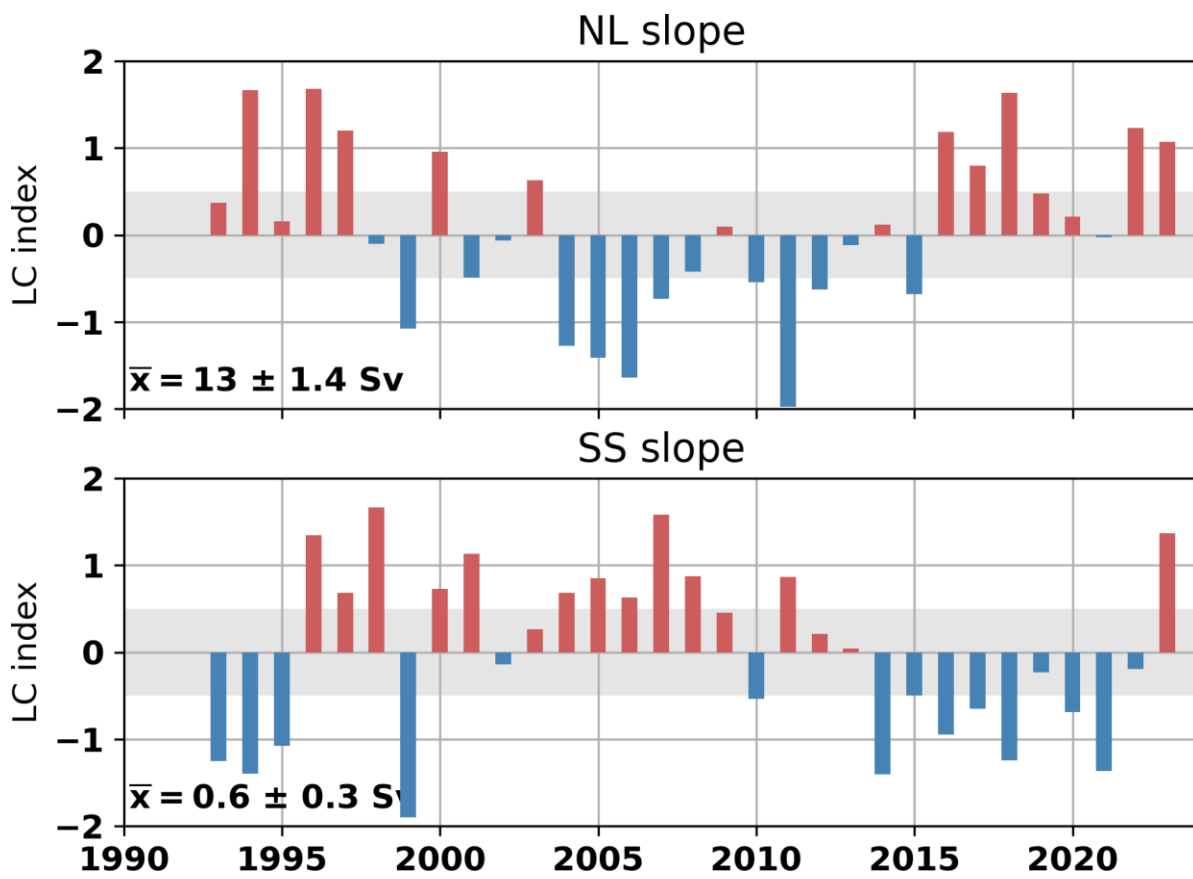


**Figure 45.** Normalized index of the annual-mean transport of the Labrador Current on the NL shelf break (top) and Scotian shelf break (bottom). Long-term averages over 1993–2023 (with standard deviation) are  $13.0 \pm 1.4 \text{ Sv}$  for the Labrador Current and  $0.6 \pm 0.3 \text{ Sv}$  for the Scotian shelf break current. Shaded gray areas represent the  $\pm 0.5 \text{ SD}$  range considered “normal”.

## Summary

An overview of physical environmental conditions for NAFO Divisions 2, 3 & 4 were presented. The highlights of 2023 can be summarized as follows:

- The winter North Atlantic Oscillation (NAO) index, a key indicator of the direction and intensity of the winter wind field patterns over the Northwest Atlantic was near neutral at +0.2.
- The annual air temperature was above normal across the zone.
- Sea ice conditions (season duration and maximum cover) were near normal (-0.5 SD).
- Sea surface temperatures averaged over the ice-free months were second highest of the time series.
- Observations from the summer AZMP oceanographic survey indicate that the CIL area along Seal Island, Bonavista Bay and Flemish Cap section were about normal.
- Spatially-averaged bottom temperatures in across the zones were between normal to slightly warm, but much colder than the last two years where several records were established across the zone.
- The transport on the Scotian Slope was positive (+1.4 SD) for the first time in 10 years.

A series of physical and biogeochemical indices in NAFO subareas 0-4 in support of the Standing Committee on Fisheries Science (STACFIS) that uses some information from this report is presented in Cyr & Bélanger (2024).

## Acknowledgments

We thank the many scientists and technicians at the Northwest Atlantic Fisheries Centre, Bedford Institute of Oceanography and St. Andrews Biological Station for collecting and providing much of the data contained in this analysis and to the Ocean Science Branch of Fisheries and Oceans in Ottawa for providing most of the historical data. Environment Canada provided the meteorological data. We also thank the captain and crew of the CCGS Sigma-t, CCGS Viola M. Davidson, CCGS Teleost, CCGS Captain Jacques Cartier, CCGS John Cabot and RSS Discovery for successful oceanographic survey during 2023. Finally, we thank the numerous technicians and scientists that contributed to the Atlantic Zone Monitoring Program for making this important work possible.

## References

- Colbourne, E., Holden, J., Craig, J., Senciall, D., Bailey, W., Stead, P., & Fitzpatrick, C. (2015). Physical Oceanographic Conditions on the Newfoundland and Labrador Shelf During 2014. *DFO Can. Sci. Advis. Sec. Res. Doc.*, 2015/053, v + 37 p.
- Colbourne, E., Narayanan, S., & Prinsenberg, S. (1994). Climatic changes and environmental conditions in the Northwest Atlantic, 1970-1993. *ICES Journal of Marine Science Symposia*, 198, 311-322.
- Coyne, J., & Cyr, F. (2024). Canadian Atlantic Bottom Observations of Temperature and Salinity (CABOTS). *Federated Research Data Repository*. <https://doi.org/10.20383/103.0969>
- Coyne, J., Cyr, F., Donnet, S., Galbraith, P. S., Geoffroy, M., Hebert, D., Layton, C., Ratsimandresy, A., Snook, S., Soontiens, N., & Walkusz, W. (2023). Canadian Atlantic Shelf Temperature-Salinity (CASTS). *Federated Research Data Repository*. <https://doi.org/10.20383/102.0739>
- Cyr, F., & Bélanger, D. (2024). Environmental indices for NAFO subareas 0 to 4 in support of the Standing Committee on Fisheries Science (STACFIS) – 2023 update. *NAFO SCR Doc*, 24/012, 18 p.
- Cyr, F., Colbourne, E., Holden, J., Snook, S., Han, G., Chen, N., Bailey, W., Higdon, J., Lewis, S., Pye, B., & Senciall, D. (2019). Physical Oceanographic Conditions on the Newfoundland and Labrador Shelf during 2017. *DFO Can. Sci. Advis. Sec. Res. Doc.*, 2019/051, iv + 58 pp. <http://waves-vagues.dfo-mpo.gc.ca/Library/362068.pdf>
- Cyr, F., Coyne, J., Snook, S., Bishop, C., Galbraith, P. S., Chen, N., & Han, G. (2024). Physical Oceanographic Conditions on the Newfoundland and Labrador Shelf during 2022. *Canadian Technical Report of Hydrography and Ocean Sciences*, 377, iv + 53 p.
- Cyr, F., & Galbraith, P. S. (2022). Newfoundland-Labrador Shelf. Ch. 4.3. In C. González-Pola, K. M. H. Larsen, P. Fratantoni, & A. Beszczynska-Möller (Eds.), *ICES Report on Ocean Climate 2020* (p. 121 pp.). ICES Cooperative Research Reports No. 356.
- Cyr, F., Galbraith, P. S., Layton, C., Hebert, D., Chen, N., & Han, G. (2022). Environmental and Physical Oceanographic Conditions on the Eastern Canadian shelves (NAFO Sub-areas 2, 3 and 4) during 2021. *NAFO SCR Doc*, 22/020.
- Cyr, F., Snook, S., Bishop, C., Galbraith, P. S., Chen, N., & Han, G. (2022). Physical Oceanographic Conditions on the Newfoundland and Labrador Shelf during 2021. *DFO Can. Sci. Advis. Sec. Res. Doc*, 2022/040, iv + 48 p. [http://www.dfo-mpo.gc.ca/csas-sccs/Publications/ResDocs-DocRech/2016/2016\\_079-eng.html](http://www.dfo-mpo.gc.ca/csas-sccs/Publications/ResDocs-DocRech/2016/2016_079-eng.html)
- Dever, M., Hebert, D., Greenan, B. J. W., Sheng, J., & Smith, P. C. (2016). Hydrography and Coastal Circulation along the Halifax Line and the Connections with the Gulf of St. Lawrence. *Atmosphere - Ocean*, 54(3), 199–217. <https://doi.org/10.1080/07055900.2016.1189397>
- Doubleday, W. G. (1981). Manual on groundfish surveys in the Northwest Atlantic. In *NAFC Soc. Coun. Studies 2* (p. 56 p.).
- Drinkwater, K. F. (1996). Atmospheric and oceanic variability in the northwest Atlantic during the 1980s and early 1990s. *Journal of Northwest Atlantic Fishery Science*, 18, 77–97. <https://doi.org/10.2960/J.v18.a6>
- Drinkwater, K. F., & Trites, R. W. (1987). Monthly means of temperature and salinity in the Scotian Shelf region. *Canadian Technical Report of Fisheries and Aquatic Sciences*, 1539, iv + 101 p.
- Florindo-López, C., Bacon, S., Aksenen, Y., Chafik, L., Colbourne, E., & Penny Holliday, N. (2020). Arctic ocean and hudson bay freshwater exports: New estimates from seven decades of hydrographic surveys on the Labrador shelf. *Journal of Climate*, 33(20), 8849–8868. <https://doi.org/10.1175/JCLI-D-19-0083.1>
- Galbraith, P. S., Chassé, J., Shaw, J., Dumas, J., Lefavre, D., & Bourassa, M. (2023). Physical Oceanographic Conditions in the Gulf of St. Lawrence during 2022. *Canadian Technical Report of Hydrography and Ocean Sciences*, 354, v+88p.
- Galbraith, P. S., Larouche, P., Caverhill, C., Galbraith, P. S., Larouche, P., & Sea-surface, C. C. A. (2021).

- A Sea-Surface Temperature Homogenization Blend for the Northwest Atlantic A Sea-Surface Temperature Homogenization Blend for the. *Canadian Journal of Remote Sensing*, 47(4), 554-568. <https://doi.org/10.1080/07038992.2021.1924645>
- GEBCO Compilation Group. (2023). *GEBCO 2023 Grid*. <https://doi.org/10.5285/f98b053b-0cbc-6c23-e053-6c86abc0af7b>
- Gilbert, D., Sundby, B., Gobeil, C., Mucci, A., & Tremblay, G.-H. (2005). A seventy-two-year record of diminishing deep-water oxygen in the St. Lawrence estuary: The northwest Atlantic connection. *Limnology and Oceanography*, 50(5), 1654–1666. <https://doi.org/10.4319/lo.2005.50.5.1654>
- Han, G., Chen, N., & Ma, Z. (2014). Is there a north-south phase shift in the surface Labrador Current transport on the interannual-to-decadal scale? *Journal of Geophysical Research: Oceans*, 119(1), 276–287. <https://doi.org/10.1002/2013JC009102>
- Han, G., Hannah, C. G., Loder, J. W., & Smith, P. C. (1997). Seasonal variation of the three-dimensional mean circulation over the Scotian Shelf. *Journal of Geophysical Research: Oceans*, 102(1), 1011–1025. <https://doi.org/10.1029/96jc03285>
- Han, G., Lu, Z., Wang, Z., Helbig, J., Chen, N., & de Young, B. (2008). Seasonal variability of the Labrador Current and shelf circulation off Newfoundland. *Journal of Geophysical Research*, 113(C10), C10013. <https://doi.org/10.1029/2007JC004376>
- ICNAF. (1978). List of ICNAF Standard Oceanographic Sections and Stations. *ICNAF Selected Papers Number 3*, 109–117. <https://doi.org/10.1111/j.1949-8594.1914.tb16026.x>
- Kerr, R. A. (2000). A North Atlantic Climate Pacemaker for the Centuries. *Science*, 288(5473), 1984–1985.
- Lu, G. Y., & Wong, D. W. (2008). An adaptive inverse-distance weighting spatial interpolation technique. *Computers and Geosciences*, 34(9), 1044–1055. <https://doi.org/10.1016/j.cageo.2007.07.010>
- McDougall, T. J., & Barker, P. M. (2011). *Getting started with TEOS-10 and the Gibbs Seawater (GSW) Oceanographic Toolbox* (Issue May). SCOR/IAPSO WG127.
- NOAA/STAR. (2021). GHRSST NOAA/STAR ACSPO v2.80 0.02 degree L3S Dataset from Afternoon LEO Satellites (GDS v2). Ver. v2.80. PO.DAAC, CA, USA. <https://doi.org/10.5067/GHLP-3SS28>
- Petrie, B., Akenhead, S. A., Lazier, S. A., & Loder, J. (1988). The cold intermediate layer on the Labrador and Northeast Newfoundland Shelves, 1978–86. *NAFO Science Council Studies*, 12, 57–69.
- Petrie, B., Drinkwater, K. F., Sandström, A., Pettipas, R., Gregory, D., Gilbert, D., & Sekhon, P. (1996). *Temperature, salinity and sigma-T atlas for the Gulf of St. Lawrence*.
- Petrie, B., Pettipas, R. G., Petrie, W. M., & Soukhovtsev, V. V. (2007). Physical Oceanographic Conditions on the Scotian Shelf and in the Gulf of Maine during 2006. *DFO Can. Sci. Advis. Sec. Res. Doc.*, 2007/023, iv + 41 p.
- Therriault, J. C., Petrie, B., Pepin, P., Gagnon, J., Gregory, D., Helbig, J., Herman, A., Lefavre, D., Mitchell, M., Pelchat, B., Runge, J., & Sameoto, D. (1998). Proposal for a northwest zonal monitoring program. *Canadian Technical Report of Hydrographic and Ocean Sciences*, 194, vii + 57 p.
- Thyng, K. M., Greene, C. A., Hetland, R. D., Zimmerle, H. M., & DiMarco, S. F. (2016). True colors of oceanography: Guidelines for effective and accurate colormap selection. *Oceanography*, 29(3), 9–13. <https://doi.org/10.5670/oceanog.2016.66>
- Vincent, L. A., Wang, X. L., Milewska, E. J., Wan, H., Yang, F., & Swail, V. (2012). A second generation of homogenized Canadian monthly surface air temperature for climate trend analysis. *Journal of Geophysical Research*, 117(D18110). <https://doi.org/10.1029/2012JD017859>
- World Meteorological Organization. (2017). WMO guidelines on the calculation of climate normals. In *WMO-No. 1203*. [https://library.wmo.int/doc\\_num.php?explnum\\_id=4166](https://library.wmo.int/doc_num.php?explnum_id=4166)